

**THE ROLE OF WNTS IN ADULT MURINE
HEMATOPOIESIS AND INTESTINAL
HOMEOSTASIS**

ZAHRA KABIRI

(MD, *IUMS*; M.Sc., *NUS*)

**A THESIS SUBMITTED FOR THE DEGREE OF
DOCTOR OF PHILOSOPHY (PhD)**

DEPARTMENT OF BIOCHEMISTRY

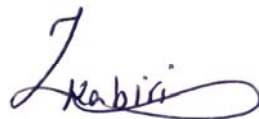
NATIONAL UNIVERSITY OF SINGAPORE (NUS)

2014

DECLARATION

I hereby declare that this thesis is my original work and it has been written by me in its entirety. I have duly acknowledged all the sources of information which have been used in the thesis.

This thesis has also not been submitted for any degree in any university previously.

A handwritten signature in blue ink, reading 'Zahra Kabiri', with a horizontal line underneath it.

Zahra Kabiri

6 June 2014

Acknowledgements

I would like to thank my supervisor, Prof. David M. Virshup. He has been the most reliable and supportive mentor any student could hope to have. I am incredibly grateful for his guidance, advice, and expertise.

I thank Dr. Gediminas Gričius for his great mentorship as well as friendship. I am very fortunate to have had the opportunity to work with him during my PhD.

I am extremely thankful to Prof. Daniel G. Tenen and thesis advisory committee members: A/P Alexandra Pietersen, Nicholas Barker, and Prof. Kanaga Sabapathy for their immense support and advice.

I thank Dr. Akira Kawasaki, Dr. Kyle D. Proffitt, Dr. Tracy M. Covery, Dr. Yunhua Zhu, Dr. Ralph M. Bunte, Ms. Simran Kaur, Mr. Edison, Mr. Jamal Alivey, and all of my friends at CSCB program and CSI. I learnt a lot working with them. They helped me troubleshoot and always kindly support me. I'm indebted to them.

I thank Dr. Amber Sawyer for her great help in English proofreading of my thesis.

And last but not least, I am incredibly grateful to my husband Hamed for his staunch support, love, and patience and to my parents Naser and Manijeh for their love and encouragement.

Table of Contents

Acknowledgements.....	I
Summary.....	V
List of Tables.....	VII
List of Figures.....	VIII
List of Abbreviations.....	XIV
1. Introduction.....	1
1.1 Wnt.....	2
1.2 Wnt/ β -catenin pathway (canonical pathway).....	2
1.3 Non-canonical or alternative Wnt pathways.....	5
1.3.1 PCP pathway.....	6
1.3.2 Wnt/ Ca^{2+} pathway.....	6
1.4 Wnt secretion.....	8
1.4.1 Wntless.....	8
1.4.2 PORCN.....	9
1.5 Extracellular Wnt modulators.....	12
1.6 Wnt signaling in development.....	14
1.7 Role of Wnts in adult stem cell self-renewal.....	15
1.7.1 Skin.....	16
1.7.2 Small intestine and large intestine.....	17
1.7.3 Hematopoiesis.....	20
1.8 Wnt high-diseases and potential therapeutic approaches.....	23

1.9 Hypothesis.....	25
2. Role of Wnt Signaling in Murine Intestinal Homeostasis	26
2.1 Introduction.....	27
2.2 Results.....	31
2.2.1 Normal intestine homeostasis after complete inhibition of epithelial Wnt secretion.....	31
2.2.2 Stroma expresses Wnts and <i>Rspo3</i> forms a niche for epithelial stem cells	45
2.2.3 <i>Wls</i> knockout resembles the <i>Porcn</i> knockout.....	50
2.2.4 The role of stromal Wnts in vivo.....	52
2.2.5 High-dose PORCN inhibition impaired intestinal homeostasis.....	65
2.3 Discussion.....	68
2.4 Materials and methods.....	73
2.4.1 Mouse strains and drug administration.....	73
2.4.3 Crypt isolation and culture	75
2.4.6 Stromal Isolation for culture.....	76
2.4.7 Tissue preparation for staining.....	77
2.4.8 Antibodies and staining condition.....	78
2.4.9 Cell proliferation assay.....	79
3.1 Introduction.....	81
3.2 Results.....	83
3.2.1 Total body knock out of <i>Porcn</i> in adult mice.....	83
3.2.2 Increase of granulopoiesis after <i>Porcn</i> inactivation in the total body of adult mice.	87

3.2.3 Normal hematopoiesis following <i>Porcn</i> inactivation in hematopoietic cells.....	102
3.2.4 Murine hematopoietic Wnts are dispensable for adult hematopoiesis.....	111
3.4 Materials and methods.....	119
4. Discussion and Conclusions	124
4.1 Wnts in intestinal homeostasis	125
4.1.1 Conclusion.....	125
4.1.2 Discussion	131
4.1.3 Future plans	134
4.2 Role of Wnt signaling in hematopoiesis	135
4.2.1 Conclusions.....	135
4.2.2 Discussion	138
4.2.3 Future plans	139
Bibliography	141

Summary

Wnt proteins belong to a family of secreted autocrine and paracrine hormones that regulate cell proliferation and migration, embryonic development, and adult tissue homeostasis. Aberrant regulation of Wnt pathways is involved in various diseases. Thus, inhibition of Wnt pathways will probably benefit patients with high Wnt disease such as cancer and fibrosis. However, if Wnt pathways are required for self-renewal of adult stem cells, inhibition of Wnts might have adverse effects on normal tissue homeostasis. To address the role and source of Wnt pathways in adult tissue homeostasis, we used pharmacological and genetic approaches to inhibit Wnt secretions in mice by targeting PORCN, an enzyme required for secretion and normal activity of all Wnts.

Wnt/ β -catenin signaling supports intestinal homeostasis by regulating proliferation in the crypt. Multiple Wnts are expressed in Paneth as well as other intestinal epithelial and stromal cells. *Ex vivo*, Wnts secreted by Paneth cells can support intestinal stem cells when Wnt signaling is enhanced with supplemental R-Spondin 1 (RSPO1). However, *in vivo*, the source of Wnts in the stem cell niche is less clear. Genetic ablation of *Porcn* confirmed the role of intestinal epithelial Wnts in *ex vivo* culture. Unexpectedly, mice lacking epithelial Wnt activity (*Villin-Cre/Porcn^{Del}* mice) had normal intestinal proliferation and differentiation, as well as successful regeneration after radiation injury, indicating epithelial Wnts are dispensable for these processes. Consistent with a key role for stroma in the crypt niche, intestinal stromal cells endogenously expressing Wnts and *Rspo3* support the growth of *Porcn^{Del}* organoids *ex vivo* without RSPO1 supplementation. Conversely, increasing

pharmacologic PORCN inhibition, affecting both stroma and epithelium, reduced *Lgr5* intestinal stem cells, inhibited recovery from radiation injury, and at the highest dose fully blocked intestinal proliferation. We conclude that epithelial Wnts are dispensable, and that stromal production of Wnts can fully support normal murine intestinal homeostasis.

We also investigated the role of Wnt signaling in hematopoiesis by targeting *Porcn* in hematopoietic tissues. Deletion of *Porcn* or inhibition of Wnt secretion in *Rosa-CreER^{T2}/Porcn^{Del}*, *MX1-Cre/Porcn^{Del}*, and *Vav-Cre/Porcn^{Del}* mice had minimal effects on proliferation, differentiation, or self-renewal of adult hematopoietic stem cells. Additionally, *Porcn* was not completely inhibited in hematopoietic stem cell niche in these three animal models; therefore, we could not address the role of Wnt signaling in hematopoiesis without blocking Wnt secretion in both hematopoietic cells and their niche. However, this study clearly excludes hematopoietic Wnts as an essential source of Wnts in adult murine hematopoiesis.

In conclusion, we confirmed the role of Wnt signaling in hair regeneration and intestinal homeostasis but not hematopoiesis.

List of Tables

Table 2.1 RT-PCR primer sequences.....	74
Table 3.1 Frequency of HSCs and progenitors in total live BM cells from primary BMT recipients of <i>Mx1-Cre/Porcn^{WT}</i> and <i>Porcn^{Del}</i> mice.....	109
Table 3.2 Frequency of HSCs and progenitors in total live BM cells from secondary BMT recipients of <i>Mx1-Cre/Porcn^{WT}</i> and <i>Porcn^{Del}</i> mice.....	110

List of Figures

Figure 1.1 A schematic diagram for a novel regulatory model of canonical Wnt signaling.....	5
Figure 1.2 A schematic figure of the Wnt/Ca ²⁺ pathway.....	7
Figure 1.3 A schematic picture of PORCN and its isoforms.....	10
Figure 1.4 Predicted topology map of PORCN and its active sites.....	10
Figure 1.5 A schematic representation of the core Wnt secretory pathway....	13
Figure 1.6 A schematic model for R-spondin–WNT signaling.....	14
Figure 1.7 Overview of the hematopoietic hierarchy.....	21
Figure 1.8 A model for members of the Wnt signaling pathway in the BM niche.....	22
Figure 2.1 Complete deletion of Porcn in intestinal epithelial cells of <i>Villin-Cre/Porcn^{Del}</i> mice.....	32
Figure 2.2 PORCN inactivated epithelial cells could not form organoids <i>in vitro</i>	33
Figure 2.3 Organoid formation from <i>Porcn^{Del}</i> crypts is rescued by Wnt-secreting cells.....	34
Figure 2.4 PORCN inactivated epithelial cells could not form organoid unless co-cultured with Wnt producing cells.....	35
Figure 2.5 MEF cells highly express endogenous Wnt3.....	35
Figure 2.6 Epithelial Wnt secretion is dispensable for intestinal homeostasis in mice.....	37
Figure 2.7 Normal epithelial differentiation in <i>Villin-Cre/Porcn^{WT}</i> and <i>Villin-Cre/Porcn^{Del}</i> mice.....	38

Figure 2.8 Normal proliferation and nuclear β -catenin in <i>Villin-Cre/Porc^{WT}</i> and <i>Villin-Cre/Porc^{Del}</i>	39
Figure 2.9 No significant changes in expression of Wnt/ β -catenin target genes in jejunum of <i>Villin-Cre/Porc^{Del}</i> mice.....	40
Figure 2.10 No major compensatory changes in gene expression were observed after epithelial <i>Porcn</i> inactivation.....	41
Figure 2.11 No changes in gene expression of Wnt/ β -catenin pathway was observed after epithelial <i>Porcn</i> inactivation.....	42
Figure 2.12 No changes in gene expression of Notch pathway was observed after epithelial <i>Porcn</i> inactivation.....	43
Figure 2.13 No changes in gene expression of EGF pathway was observed after epithelial <i>Porcn</i> inactivation.....	44
Figure 2.14 Stroma could support intestinal epithelia growth in absence of Epithelial Wnts <i>ex vivo</i>	46
Figure 2.15 Cultured stroma is enriched in myofibroblasts.....	48
Figure 2.16 Cultured stroma expresses multiple Wnts.....	48
Figure 2.17 R-spondin 3 (<i>Rspo3</i>) is highly expressed in intestinal stroma....	49
Figure 2.18 Cultured stromal cells from <i>Vav-cre//Villin-Cre/Porc^{Del}</i> mice support organoids in <i>Porcn^{Del}</i> epithelial cell culture.....	50
Figure 2.19 Normal intestinal structure in <i>Villin-Cre/Wls^{Del}</i> mice.....	51
Figure 2.20 Pharmacologic Porcn inhibitors block organoid formation.....	52
Figure 2.21 Expression of CBC markers were blocked after C59 treatment...	53
Figure 2.22 Moderate PORCN inhibition did not alter intestinal structure....	54

Figure 2.23 Suppression of Wnt/ β -catenin target genes including <i>Lgr5</i> did not affect short-term proliferation.....	55
Figure 2.24 Systemic PORCN inhibition leads to decreased expression of intestinal stem cell markers.....	56
Figure 2.25 Systemic PORCN inhibition leads to decreased expression of intestinal stem cell markers.....	57
Figure 2.26 Wnt target genes and stem cell markers were down-regulated in crypts prepared from C59-treated mice.....	58
Figure 2.27 Inhibition of Paneth cell differentiation in C59 treated mice.....	59
Figure 2.28 Gross changes in length and diameter of small intestine after irradiation in C59 pretreated mice.....	61
Figure 2.29 Stromal Wnts support a cell population required for epithelial regeneration in response to radiation-induced injury.....	62
Figure 2.30 Proliferation was decreased in intestine of C59 pretreated mice..	63
Figure 2.31 Epithelial Wnt secretion is not required for epithelial regeneration after radiation injury.....	64
Figure 2.32 Normal β -catenin in C59 treated mice.....	65
Figure 2.33 Systemic inhibition of Wnt signaling leads to impaired intestinal homeostasis.....	66
Figure 2.34 High dose C59 treatment for 6 days blocks proliferation in all regions of the small intestine.....	67
Figure 2.35 C59 treatment did not lead to increased apoptosis.....	68
Figure 2.36 Long term treatment with intermediate dose C59 affects gut homeostasis.....	71
Figure 3.1 Hair loss phenotype in <i>Rosa-CreER^{T2}/Porcn^{Del}</i> mice.....	85

Figure 3.2 Loss of hair follicles in skin after <i>Porcn</i> inactivation.....	85
Figure 3.3 Inactivation of <i>Porcn</i> caused down-regulation of Wnt/ β -catenin target genes (<i>Axin2</i>) in the skin samples of <i>Rosa-CreER^{T2}/Porcn^{Del}</i> mice.....	86
Figure 3.4 Weight loss phenotype in <i>Rosa-CreER^{T2}/Porcn^{Del}</i> mice.....	87
Figure 3.5 <i>Porcn</i> deletion in blood samples of <i>Rosa-CreER^{T2}/Porcn^{Del}</i> mice.....	87
Figure 3.6 Complete blood count test showed granulocytosis after deletion of <i>Porcn</i>	88
Figure 3.7 Normal Hb, RBC, and PLT in <i>Rosa-CreER^{T2}/Porcn^{Del}</i> mice.....	89
Figure 3.8 <i>Porcn</i> and <i>c-myc</i> (Wnt/ β -catenin target gene) were down-regulated in bone marrow samples of <i>Porcn</i> inactivated mice.....	89
Figure 3.9 The frequency of LSK, ST-HSC, and LT-HSC in <i>Rosa-CreER^{T2}/Porcn^{Del}</i> mice were similar to <i>Rosa-CreER^{T2}/Porcn^{WT}</i> mice.....	91
Figure 3.10 Frequency of myeloid progenitors were similar in both <i>Rosa-CreER^{T2}/Porcn^{WT}</i> and <i>Porcn^{Del}</i> mice.....	92
Figure 3.11 Increased granulopoiesis in <i>Rosa-CreER^{T2}/Porcn^{Del}</i> mice.....	92
Figure 3.12 Inhibition of Wnt signaling caused reduction of Common Lymphoid progenitors (CLP) in <i>Rosa-CreER^{T2}/Porcn^{Del}</i> mice.....	93
Figure 3.13 Higher granulocyte colonies from <i>Rosa-CreER^{T2}/Porcn^{Del}</i> BM samples.....	94
Figure 3.14 Donor <i>Porcn^{Del}</i> BM cells were able to reconstitute in primary BMT recipient mice.....	95
Figure 3.15 Successful reconstitution of donor <i>Rosa-CreER^{T2}/Porcn^{Del}</i> BM cells in sub-lethally irradiated recipient mice.....	97
Figure 3.16 Comparable LSK and progenitors frequencies in both <i>Rosa-CreER^{T2}/Porcn^{Del}</i> and <i>Rosa-CreER^{T2}/Porcn^{Del}</i> recipient mice.....	97

Figure 3.17 Normal LT-HSC and ST-HSC frequency in primary recipient of <i>Rosa-CreER^{T2}/Porcn^{Del}</i> mice.....	98
Figure 3.18 Normal myeloid progenitors frequency in primary recipient of <i>Rosa-CreER^{T2}/Porcn^{Del}</i> mice.....	99
Figure 3.19 Normal CLP frequency in primary recipient of <i>Rosa-CreER^{T2}/Porcn^{Del}</i> mice.....	99
Figure 3.20 Normal HSCs frequency in Secondary BMT recipient mice.....	100
Figure 3.21 Normal frequency of Myeloid progenitors in Secondary BMT recipient mice.....	101
Figure 3.22 Normal WBC frequency in Secondary BMT recipient mice of <i>Rosa-CreER^{T2}/Porcn^{Del}</i>	101
Figure 3.23 Normal WBC counts in <i>MXI-Cre/Porcn^{Del}</i> mice.....	102
Figure 3.24 <i>Porcn</i> deletion in blood samples of <i>MXI-Cre/Porcn^{Del}</i> mice.....	103
Figure 3.25 Wnt/ β -catenin target genes were not down-regulated in blood samples of <i>MxI-Cre/Porcn^{Del}</i> mice.....	103
Figure 3.26 Neutrophils and Lymphocytes present at the normal ratio in <i>MxI-Cre/Porcn^{Del}</i> mice.....	104
Figure 3.27 The frequency of LSK, LT-HSC, and ST-HSC did not change between <i>MXI-Cre/Porcn^{WT}</i> and <i>Porcn^{Del}</i> mice.....	105
Figure 3.28 The frequency of myeloid progenitors did not change between <i>MXI-Cre/Porcn^{WT}</i> and <i>Porcn^{Del}</i> mice.....	106
Figure 3.29 Normal differentiation ability of <i>Porcn</i> deleted HSC in colony forming assay.....	106
Figure 3.30 Successful BM reconstitution of <i>Porcn</i> inactivated donor HSCs in recipient mice.....	107

Figure 3.31 Donor <i>Mx1-Cre/Porc^{Del}</i> BM cells were able to reconstitute in primary BMT recipient mice.....	108
Figure 3.32. Complete deletion of <i>Porcn</i> in blood samples of <i>Vav-Cre/Porc^{Del}</i> mice.....	112
Figure 3.33 Normal CBC in <i>Vav-Cre/Porc^{Del}</i> mice.....	113
Figure 3.34 Normal lymphocyte and neutrophil frequency in BM samples of <i>Vav-Cre/Porc^{Del}</i> mice.....	114
Figure 3.35 Normal myeloid progenitors numbers in <i>Vav-Cre/Porc^{Del}</i> mice.....	115
Figure 3.36 Normal lymphoid progenitor numbers in <i>Vav-Cre/Porc^{Del}</i> mice.....	115
Figure 3.37 Normal differentiation of T-lymphocytes in thymus of <i>Vav-Cre/Porc^{Del}</i> mice.....	116
Figure 4.1 Normal small intestine histology and β -catenin distribution in <i>Porcn</i> -inactivated mice.....	126
Figure 4.2 Preferential inactivation of <i>Porcn</i> in epithelium rather than stroma of <i>CreER^{T2}/Porcn^{Del}</i> intestine.....	127
Figure 4.3 <i>Rosa-CreER^{T2}/Porcn^{Del}</i> crypts form less organoid than <i>Rosa-CreER^{T2}/Porcn^{WT}</i> crypts.....	128

List of Abbreviations

AGM	Aorta-gonad meonephros
APC	Adenomatous polyposis coli
ASCL2	Achaete-Scute Complex Homolog 2
BM	Bone marrow
BMP	Bone morphogenic protein
BMT	Bone marrow transplantation
CBC	Crypt base columnar cell
CK1	Casein kinase 1
CLP	Common lymphoid progenitor
CMP	Common myeloid progenitor
DAG	Diacylglycerol
DKK	Dickkopf
Dvl	Dishevelled
EC	Convergent extension
EGFR	Epithelial growth factor receptor pathway
FAP	Familial adenomatous polyposis
FDH	Focal dermal hypoplasia
Fz	Frizzled
GMP	Granulocyte/Macrophage progenitor
GPRC	G protein couple receptors
Gr	Granulocyte
GSK3	Glycogen synthase kinase 3
Gy	Gray

Hb	Hemoglobin
HDAC	Histone deacetylase
HSC	Hematopoietic stem cell
HSPG	Heparan sulfate proteoglycan
IWP	Inhibitor of Wnt production
LEF	Lymphocyte enhancer factor
Lgr	Leucine-rich repeat-containing G-protein coupled receptor
LRC	Label-retaining cell
LRP	Low-density lipoprotein receptor-related protein
LSK	Lin ⁻ , Sca-1 ⁺ , c-Kit ⁺ cells
LT-HSC	Long term hematopoietic stem cell
Lym	Lymphocyte
MEF	Mouse embryonic fibroblast
MEP	Megakaryocyte/Erythrocyte progenitor
MMP	Multipotent progenitor
Olfm4	Olfactomedin 4
PCP	Planar cell polarity
PCR	polymerase chain reaction
PKC	Protein kinase C
PLC	Phospholipase C
Plt	Platelet
PORCN	Porcupine
qRT-PCR	Real Time quantitative Reverse Transcription PCR
RBC	Red Blood counts

RSPO	R-spondin
sFRP	secreted Fz related protein
ST-HSC	Short term hematopoietic stem cell
TA	Transit amplifying
TCF	T cell factor
TGFβ	Transforming growth factor beta
VEGF	Vascular endothelial growth factor
WBC	White blood counts
WIF1	Wnt inhibitory factor-1
Wls	Wntless

1. Introduction

1.1 Wnt

Wnt proteins belong to a family of secreted autocrine and paracrine hormones that regulate cell proliferation and migration, embryonic development and adult tissue homeostasis. Wnts are a conserved family of proteins in many species, from cnidarian Hydra to human (Kusserow et al., 2005). In 1982, the Wnt-1 gene was identified as Int1, a gene activated by insertion of MMTV viral DNA into mouse breast cancer (Nusse and Varmus, 1982). Following, *Drosophila* wingless gene was shown to be a ortholog of Wnt1 (Rijsewijk et al., 1987). There are at least 19 Wnt genes in mice and humans that are categorized into 12 Wnt subfamilies, all of which consist of approximately 40 KD and have conserved cysteine rich domains (Tanaka et al., 2002). Wnts have several receptors including 10 Frizzleds (Fz), 2 LRPs, Ror and Ryk. Based on the cell type and expression of certain receptors, Wnts can activate different downstream pathways, including the Wnt/ β -catenin (canonical), planar cell polarity (PCP) and Wnt/Ca²⁺ (non-canonical) pathways.

1.2 Wnt/ β -catenin pathway (canonical pathway)

The Wnt/ β -catenin pathway is involved in cell differentiation, proliferation by stabilization of β -catenin, and modification of cell transcription programs. Wnt ligands can bind to heterodimeric receptor complexes of LRP5/6 proteins and Fz. All Fz receptors have large extracellular N-terminal cysteine rich domains (CRDs), which provide binding sites for Wnts (Bhanot et al., 1996; Dann et al., 2001; Janda et al., 2012). Based on the structure of the CRDs, there are several potential binding sites between Fz and Wnts (Janda et al.,

2012). The cooperation of Fz and low-density lipoprotein receptor-related proteins (LRPs) are required to activate the canonical Wnt pathway. Recently, it has been shown that LRP6 has separate binding sites for different Wnts, which can add more complexity to Wnt-receptor interactions (Gong et al., 2010).

In the absence of Wnt ligands, Axin and adenomatous polyposis (APC) bring β -catenin to GSK3 and CK1 to allow phosphorylation at specific serine/threonine residues. Phosphorylated β -catenin is then predominantly targeted by E3 ligase β -TrCP for polyubiquitination and proteosomal destruction (Baron and Kneissel, 2013). Consequently, the amounts of cytoplasmic β -catenin are lowered, thus reducing their translocation to the nucleus as a transcription factor for the expression of thousands of genes.

In the presence of Wnt ligands, the canonical Wnt pathway is activated by the binding of Wnt to complexes of Fz and LRP5/6 receptors, resulting in the inactivation of β -catenin destruction complex, as well as cytoplasmic stabilization of β -catenin and its translocation into the nucleus. Upon binding of canonical Wnt to its receptors, Fz undergoes conformational changes, which then allow interaction between Fz and disheveled (DVL or DSH). This complex can then recruit Axin to bind to LRP5/6 in the membrane. As such, Axin binds to the cytoplasmic tail of LRP6 through the phosphorylation of LRP6 by GSK3 and CK1. Following, both the destruction complex released from β -catenin and cytoplasmic β -catenin translocate to the nucleus in order to interact with the TCF/LEF complex (Clevers and Nusse, 2012).

The mechanisms by which β -catenin translocates to the nucleus following

Wnt activation are not entirely clear. However, it is known that β -catenin interacts with the TCF/LEF-1 family of transcription factors including TCF-1, TCF-3, TCF-4 and LEF-1 once inside the nucleus. In the absence of Wnt, TCF/LEF-1 acts as a repressor of gene expression by making a complex with Groucho, a chromatin repressor, and histone deacetylases (HDACs). This repressor complex facilitates chromatin compression and inhibits transcription of Wnt target genes (Baarsma et al., 2013). In the presence of Wnt, active β -catenin binds to TCF/LEF-1 and dissociates Groucho and the HDACs. The β -catenin/TCF/LEF-1 complex then recruits other factors, such as CBP, p300, Bcl-9 or pygo, and turns on the gene transcription of Wnt target genes within the nucleus (Nusse, 2012). There is a growing list of Wnt/ β -catenin target genes in the literature involving a broad range of cellular processes, such as cell-cycle (cyclin D1), proliferation (e.g. c-myc, n-myc), cell growth (e.g. TGF- β and VEGF) and inflammation (e.g. COX2, IL-8) (The Wnt homepage: www.stanford.edu/group/nusselab/cgi-bin/wnt/target_genes).

In addition to the current Wnt/ β -catenin pathway model, Lie et al. proposed a new model for β -catenin pathway activation based on the β -catenin destruction complex. In the previous model, Wnt induces Axin binding to LRP6 and dissociation of β -catenin from the destruction complex, thus stabilizing β -catenin in the cytoplasm. Based on the new model, and in the absence of Wnts, the destruction complex associates with β -catenin in the cytoplasm, where it can phosphorylate and ubiquitinate β -catenin with the assistance of β -TRCP. After which, proteasomes can then degrade β -catenin. In the new model, Wnt induces association of the entire destruction complex to LRPs, where it can still bind and phosphorylate β -catenin, but it is not able

to ubiquitinate β -catenin, therefore blocking the degradation of the newly synthesized β -catenin. This interaction then results in the accumulation of β -catenin in the cytoplasm (Figure 1.1) (Li et al., 2012).

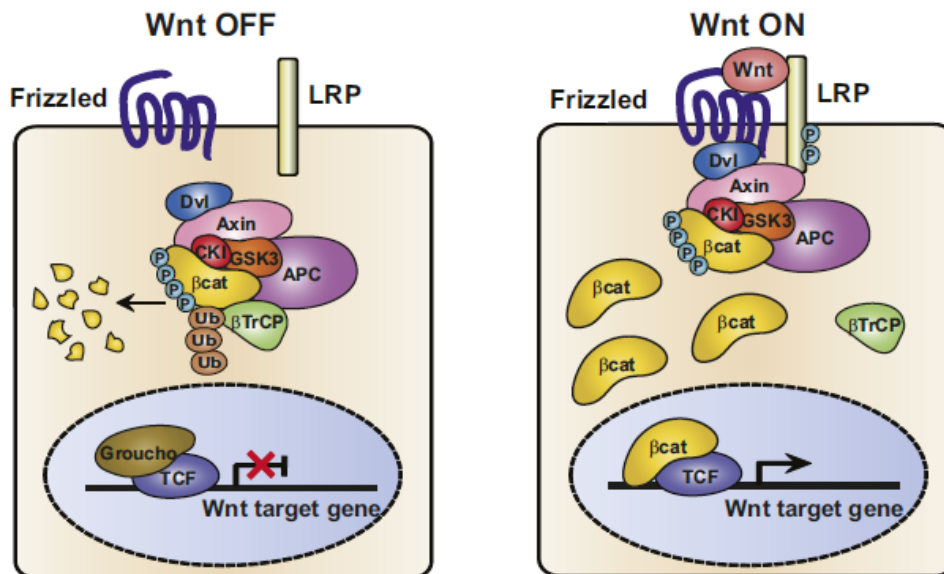


Figure 1.1 A schematic diagram for a novel regulatory model of canonical **Wnt signaling**. This figure was adapted from Li et al with permission. (Li et al., 2012).

1.3 Non-canonical or alternative Wnt pathways

Besides the canonical Wnt pathway, there are several other downstream pathways that can be activated by Wnt ligands, known as non-canonical or alternative Wnt pathways. The Planar Cell Polarity (PCP) and Wnt/ Ca^{2+} pathways are considered as two major non-canonical Wnt pathways. These pathways control many of the cellular processes and play major developmental roles in many species. For instance, deregulation of alternative Wnt pathways during development can cause deficits in branching morphogenesis, left and right patterning, cardiac output tract formation, limb outgrowth, intestinal elongation and neural tube closures (van Amerongen, 2012). Here is a brief summary of PCP and Wnt/ Ca^{2+} pathways:

1.3.1 PCP pathway

PCP is a process by which cells align themselves in tissue, such as mammalian inner hair cells or hair cells in the fly wing. PCP can also affect large structures in addition to cells in tissue, such as the alignment of entire hair follicles within the skin. The core components of PCP are Fzs and Dvls. There are several shared components between PCP and convergent extension (CE), the process that controls morphogenetic events such as neural tube closure or extension of the primary body axis (Keller et al., 1985). The mechanism of connection between PCP/CE receptors (including Fzs, Dvls, Ror and Ryk) and its downstream effectors remains largely unknown. It has been suggested that Dvl can activate two separate Rho GTPases (such as Rho, Cdc42 or Rac) and can regulate two individual branches of signaling. It is further known that the full length of Dvl is required to activate Rho (which may repress activation of Rac). However, the DEP domain of Dvl is sufficient to activate Rac and JNK.

1.3.2 Wnt/Ca²⁺ pathway

The Wnt/Ca²⁺ pathway was first shown in zebrafish, where co-injections of extopic Wnt5a and Fz2 caused an increase in intracellular Ca²⁺ transient (Slusarski et al., 1997). The Wnt/Ca²⁺ pathway, through G protein couple receptors (GPCRs), Fz and Dvl, can activate phospholipase C (PLC) and release Ca²⁺ from the ER. Calcium fluxes stimulate activation of several proteins, including calcineurin and CamKII, which in turn activate NF- κ B and NFAT. Additionally, release of Ca²⁺ from the ER can activate diacylglycerol

(DAG) and protein kinase C (PKC). PKC can then trigger CERB and NFκB. Subsequently, NFAT, CERB and NFκB can translocate to the nucleus and regulate transcription of several genes (Figure 1.2) (De, 2011; van Amerongen, 2012).

Wnt5a can also bind to Ror1/2 and stimulate alternative Wnt pathways by production of Caplain, Siah and CDX2. The Wnt5a/Ror pathway can inhibit the Wnt/β-catenin pathway through the down-regulation of β-catenin by Siah, and CDX2 can also act as a transcription factor (De, 2011).

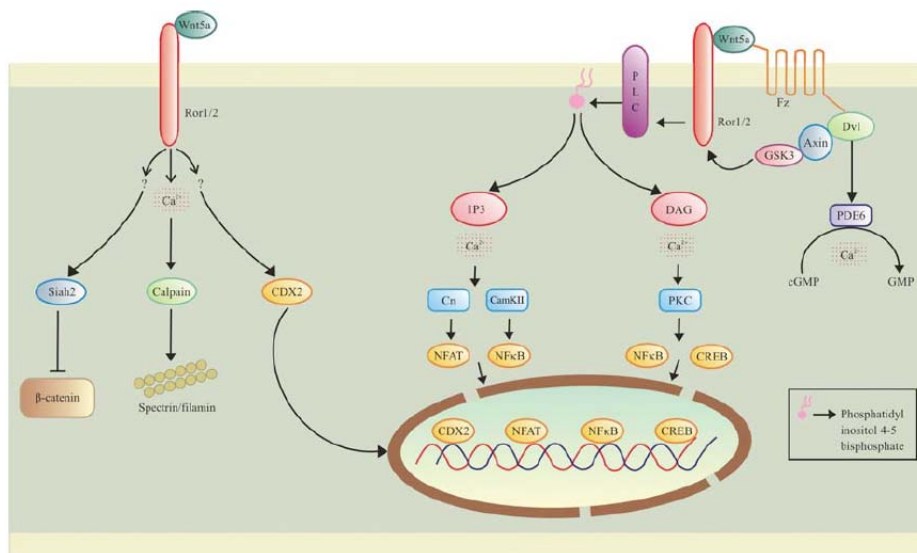


Figure 1.2 A schematic figure of the Wnt/Ca²⁺ pathway. This figure was adapted from De et al. with permission (De, 2011).

Although some studies have classified Wnts into two categories including canonical Wnts (Wnt1, Wnt3A, Wnt3, Wnt8, Wnt8b) and non-canonical Wnts (Wnt4 and Wnt5a), this may be too simplistic a view. Specifically, individual Wnt ligands can activate both canonical and non-canonical pathways based on cell types or on the existence of specific receptors (Najdi et al., 2012).

1.4 Wnt secretion

Wnt ligand secretion is a complex and tightly regulated process. This regulation is partially a consequence of the post-translational modifications of Wnts, of which there are two types including glycosylation and acylation. Interestingly, all Wnts carry at least one N-linked glycan; however, the precise role of glycosylation remains unknown (Tang et al., 2012). Additionally, Wnts are lipid-modified on two conserved residues, e.g., cysteine 77 and serine 209 in mouse Wnt3a (Harterink and Korswagen, 2012). These sites are conserved between the Wnt family members in all animal species, except *Drosophila* WntD (Herr and Basler, 2012). Lipid-modifications of Wnts are essential for activity and secretion of all Wnts, based on several independent studies (Coombs et al., 2010; Herr and Basler, 2012; Janda et al., 2012; Proffitt and Virshup, 2012; Takada et al., 2006). The two core proteins in the Wnt secretion pathway are Wntless and Porcupine (PORCN):

1.4.1 Wntless

Wntless (also known as Evi, Wls or GPR177) is a highly conserved multipass transmembrane protein, which acts as a cargo receptor that transports Wnts from the ER to the plasma membrane (Yu et al., 2014). Wls is widely expressed in a variety of adult and embryonic tissues in rat, mouse, zebrafish and human, confirming its global role in Wnt pathways. Acylation of Wnts by Porcn enzyme has been shown to be required for the interaction of Wls and palmitoleated Wnts (Coombs et al., 2010; Najdi et al., 2012; Proffitt and Virshup, 2012). Because Wls assists the transportation of Wnts to the plasma membrane, it is necessary for the secretion of all canonical and non-

canonical Wnts, with the exception of the *Drosophila* WntD (Herr et al., 2012; Najdi et al., 2012; Proffitt and Virshup, 2012). Furthermore, analysis of Wls null mice revealed similar phenotypes as Wnt3 null and β -catenin knockout mice, the earliest described Wnt phenotype (Carpenter et al., 2010; Fu et al., 2009; Huelsken et al., 2000; Liu et al., 1999). Thus, these data confirm the importance of Wls in the secretion of all vertebrate Wnts.

1.4.2 PORCN

PORCN was first discovered in *Drosophila* as a segment polarity gene involved in the normal processing of Wingless (Wg), the *Drosophila* homolog of Wnt (Kadowaki et al., 1996). *Porcn* gene is located in the X chromosome and contains 15 exons (exon 2-15) and 460 amino acids. The Porcn enzyme resides in the ER and has 8 transmembrane domains with a carboxy-terminal tail ending in the ER membrane (Figure 1.3 and 1.4). The catalytic active site of PORCN is within the third loop towards the ER lumen (Galli et al., 2007). There are 4 isoforms of PORCN in mice and human resulting from 4 splice variants of the single *Porcn* gene, which differs by a few amino acids within the cytoplasmic loop of the protein (Figure 1.3). The isoform expression is tissue specific with an unknown significance (Tanaka et al., 2003); however, the isoforms can compensate for each other because any of the four can rescue Wnt secretion from the *Porcn* mutant cells.

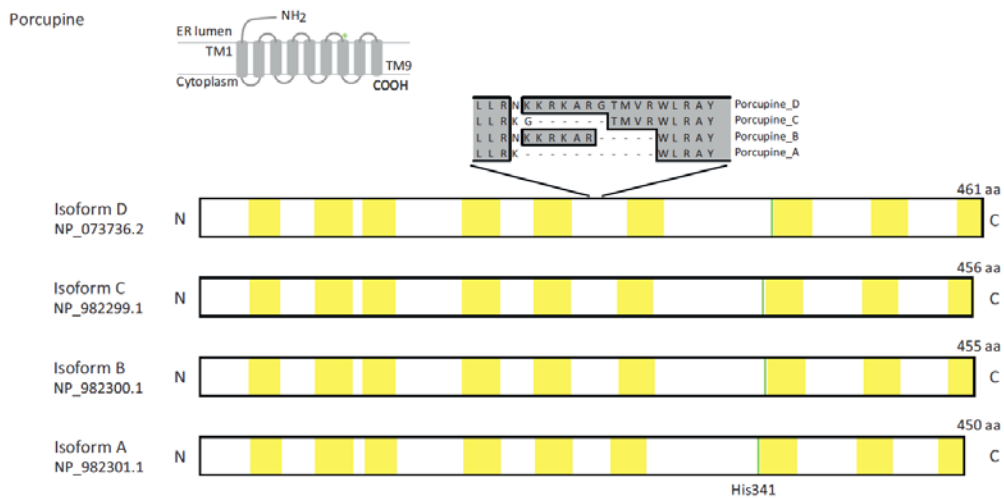


Figure 1.3 A schematic picture of PORCN and its isoforms. Adapted from Herr et al with permission. (Herr et al., 2012).

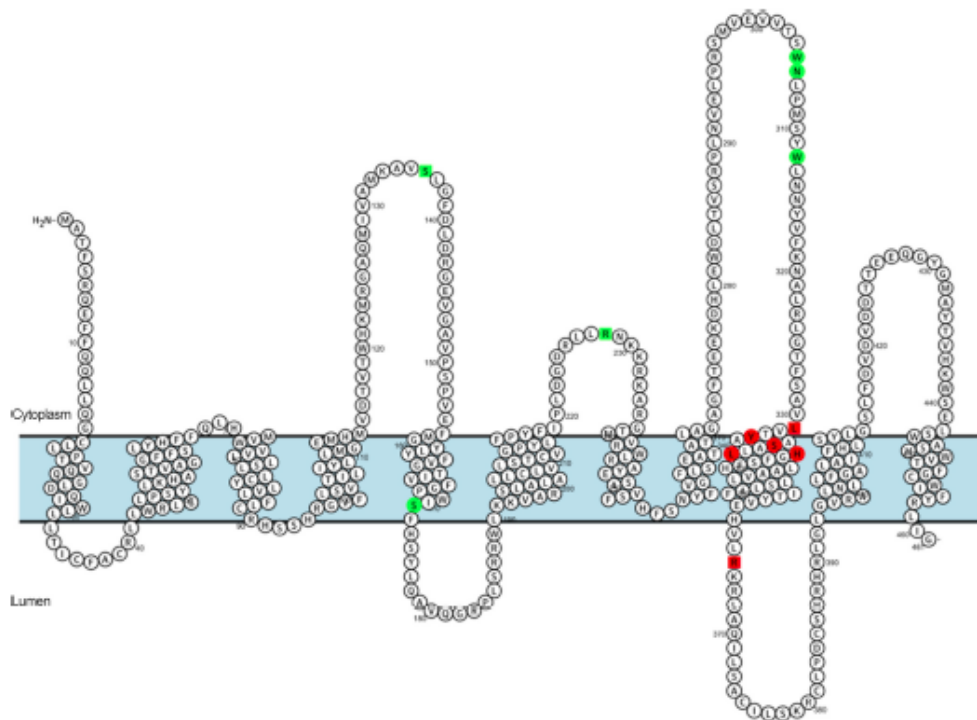


Figure 1.4 Predicted topology map of PORCN and its active sites. The enzymatic active site of Porcn is highlighted in red color. This figure was adapted from Rios J et al. with permission. (Rios-Esteves et al., 2014)

PORCN, as a member of the MBOAT family, is conserved among species with no indication of functional redundancy (Kadowaki et al., 1996). This gene lipid-modifies Wnt ligands (Biechele et al., 2011; Chen et al., 2012;

Tanaka et al., 2000). Acylation of Wnts by PORCN enzyme is required for the interaction of Wnts with Wls, thus indicating the necessity of PORCN for the secretion and activity of all Wnts in diverse organisms, except *Drosophila* WntD (Buechling et al., 2011; Coombs et al., 2010; Najdi et al., 2012; Proffitt and Virshup, 2012). Furthermore, palmitoleation is necessary for the ability of Wnt ligands to interact with Fz receptors at the cell membrane (Coombs et al., 2010; Herr et al., 2012; Janda et al., 2012). Hence, PORCN is a unique protein in the Wnt biogenesis pathway.

Consistent with the critical role of PORCN in Wnt signaling, the germ line mutations of *Porcn* is associated with focal dermal hypoplasia (FDH; OMIM 305600), an X-linked dominant genetic disease known as Goltz syndrome (Grzeschik et al., 2007; Wang et al., 2007). Mutation of the *Porcn* gene is fatal during embryogenesis (Cox et al., 2010); however, heterozygous mutations of *Porcn* primarily occurs in females and leads to FDH in human and mice (Barrott et al., 2011; Grzeschik et al., 2007; Liu et al., 2012; Wang et al., 2007). FDH rarely affects males, due to postzygotic mutations of *Porcn*, but not germ line mutation, which cause fatal phenotype during embryogenesis in male. The phenotypical manifestation of FDH syndrome varies due to random X-inactivation in different tissues and is associated with defects in tissues originating from the ectoderm and mesoderm during development. Individual FDH patients may have the following birth defects: skin malformation, such as fat herniation, superficial skin striation or atrophy, limb shortening and syndactyly, papillomas in the mucosal membrane, eye abnormality, distinctive facial features, mental retardation, and gastrointestinal and kidney abnormalities (Murakami et al., 2011). Regarding PORCN functions in Wnt

biogenesis, it has been presumed that FDH is ultimately a Wnt disease, but it is not yet proven.

Recently, two groups were able to produce models of FDH by making conditional knockouts of *Porcn* in mice (Barrott et al., 2011; Liu et al., 2012). Additionally, Biechele et al. generated *Porcn*^{fllox} mice and investigated the role of Wnt secretion during the implantation and gastrulation stages (Biechele et al., 2013). Thus, generation of *Porcn* conditional knockout mice by three independent groups has confirmed the role of *Porcn* during mouse embryonic development and demonstrated that *Porcn* deletion caused FDH in mice (Barrott et al., 2011; Biechele et al., 2013; Cox et al., 2010; Liu et al., 2012).

1.5 Extracellular Wnt modulators

Wnts are hydrophobic and need special mechanisms to move within tissues and to act as morphogenes. Wnts can travel from secreting cells and affect receiving cells by several proposed mechanisms, such as those associated with heparan sulfate proteoglycans (HSPGs), lipoprotein particles, Swim and exosomes (Kleinschmit et al., 2010; Mulligan et al., 2012; Neumann et al., 2009; Panáková et al., 2005; Savina et al., 2002). Each mechanism requires a way to protect the palmitoleated Wnts and move them into the surrounding cells.

There are also several extracellular secreted inhibitors of the Wnt pathways that add layers of complexity for a tight regulation of Wnt signaling. These include the Dickkopf family of proteins (DKK1-4), the secreted Fz related protein family (sFRP1-5), Wnt inhibitory factor-1 (WIF1) and the cysteine knot family, including WISE and SOST (Bovolenta et al., 2008; Lintern et al., 2009; Niehrs, 2006; Semenov et al., 2005). These soluble

inhibitors bind to Wnts, Fz and LRP5/6 to block Wnt/receptor complex formation and to inhibit Wnt signaling. Many of these inhibitors are non-specific, because they can interact with other proteins and signaling pathways beyond the Wnt pathway (Bovolenta et al., 2008; Mii and Taira, 2011).

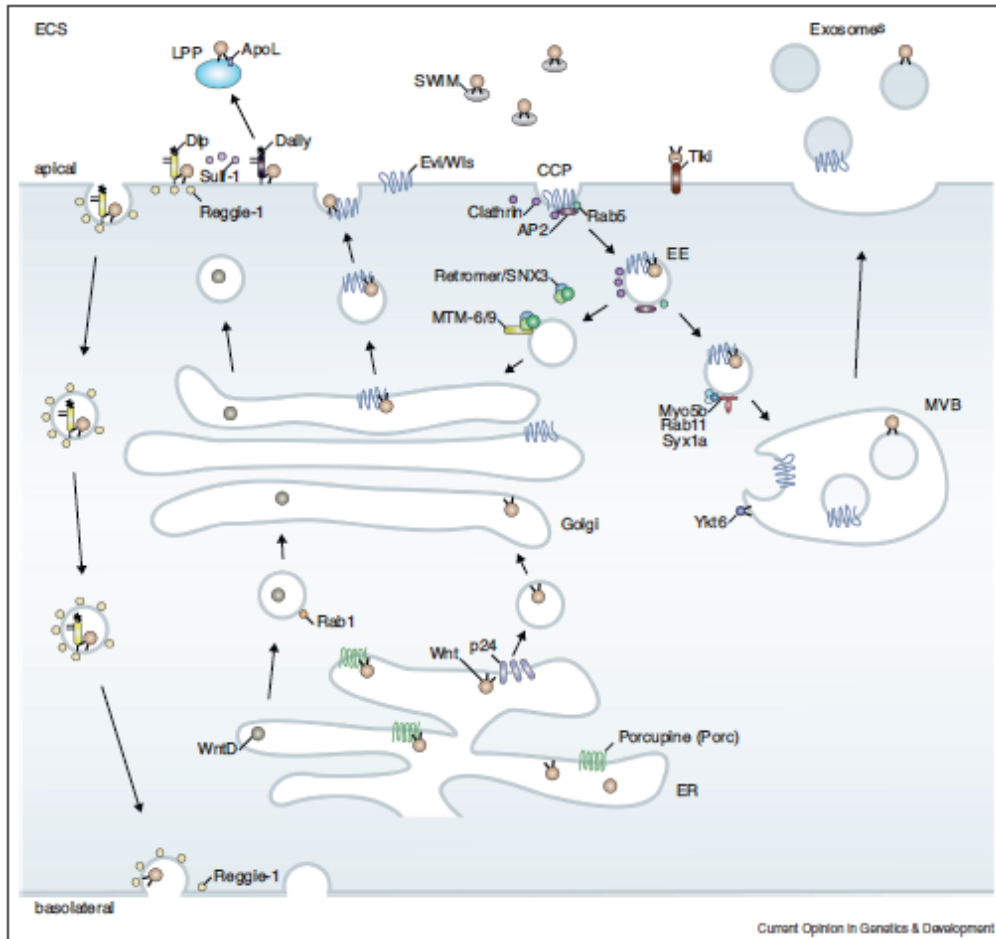


Figure 1.5 A schematic representation of the core Wnt secretory pathway. Wnt proteins are palmitoleated in the ER by Porcn, then transported to the plasma membrane with the help of Wls. Wls can recycle to the Golgi by an SNX3-retromer-dependent step involving MTM-6/9. Otherwise, Wls and Wnts reach multivesicular bodies, where they are secreted onto exosomes into the extracellular space (ECS). Wnts also can attach to lipophorin (ApoL) on lipoprotein particles (LPPs) and can solubilize by binding to SWIM or HSPGs, such as Sulf-1, Dally and Dlp. WntD in *Drosophila* is secreted independent of the core Wnt secretion pathway. This figure was adapted from Gross et al. with permission. (Gross and Boutros, 2013).

In contrast to Wnts inhibitors, there are also secreted factors including the R-spondin family of proteins (4 members, RSPO1-4) that can promote Wnt

signaling. R-spondin can enhance the Wnt canonical and PCP pathways by binding to Lgr receptors and forming a complex that causes internalization of ZNRF3, and RNF43 (Figure 1.6). ZNRF3 and RNF43 are negative regulators of Wnt signaling that induce ubiquitination of Fz receptors and remove Fzs and possibly Lrp6 from the plasma membrane. Therefore, R-spondins can only enhance Wnt signaling in the presence of the Wnt ligands, and they are indirectly dependent on intact Wnt secretion machinery (Niehrs, 2012; Ong et al., 2012).

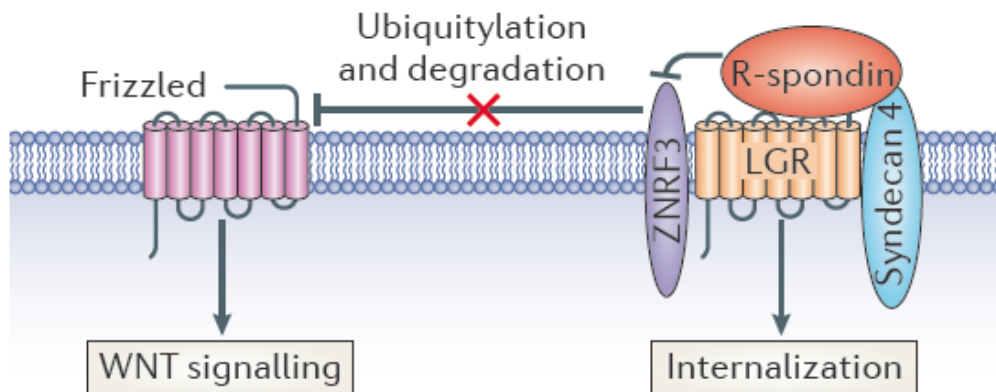


Figure 1.6 A schematic model for R-spondin–WNT signaling. ZNRF3 ubiquitinates Fz and targets it for degradation. In the presence of RSPO, ZNRF3 binds to Lgr receptors (4-6) and forms a complex with Syndecan 4, where it is internalized by endocytosis. Additionally, RSPO can bind to Syndecan 4 and enhance the PCP pathway. This figure was adapted from Niehrs et al. with permission. (Niehrs, 2012).

1.6 Wnt signaling in development

Wnt/ β -catenin signaling is critical for gastrulation and axis development. Loss of function studies in activating components of the Wnt pathway inhibit primitive streak formation, indicating that Wnt/ β -catenin is absolutely essential for this process (Hsieh et al., 2003; Huelsken et al., 2000; Kelly et al., 2004; Liu et al., 1999). Gain of function studies in activators of this pathway have led to two distinctive phenotypes, including posterior axis duplication

and anterior truncation in mice (Fossat et al., 2011; Hikasa and Sokol, 2013; Merrill et al., 2004). Notably, the commonly used assay to identify any new component of Wnt signaling is the induction and inhibition of axis duplication (Zhang et al., 2012).

In addition to Wnt/ β -catenin signaling, the non-canonical Wnt pathways play important roles in CE movement, development of dorsoventral polarity and various organ formations (De, 2011).

Regarding Wnt signaling, the earliest phenotype occurs in Wnt3 and β -catenin knockout mice. Recent studies with Porcn and Wls knockout mice have also shown similar phenotypes with Wnt3 knockout mice (Barrott et al., 2011; Fu et al., 2009; Liu et al., 2012). Furthermore, targeting different Wnt ligands or other components of the Wnt signaling pathway specifies the importance of different Wnt ligands, as well as other Wnt signaling components in different stages of development. Thus, genetic studies have confirmed the critical role of Wnt signaling in development (van Amerongen and Berns, 2006).

1.7 Role of Wnts in adult stem cell self-renewal

Wnt signaling not only plays important roles in development, it has also been proposed to be involved in tissue homeostasis of mammals by maintaining the self-renewal of adult stem cells in the brain, skin, gut, bone, bone marrow, adipose tissue and pancreas (Miller and McCrea, 2010). The role of Wnts in adult stem cell self-renewal will be discussed in details below for skin, gut and hematopoietic tissues, which are the primary focus of this thesis.

1.7.1 Skin

Wnts are involved in the early stage of skin development when embryonic cells differentiate from mesoderm and ectoderm to form dermis and epidermis, respectively (Fuchs, 2007). The ectoderm is able to form either the skin epithelium or the nervous system, and Wnt signaling strongly influences the fate of ectoderm differentiation towards epidermis (Wilson and Hemmati-Brivanlou, 1995). The mesoderm segments into somites and eventually gives rise to dermis in the influence of Wnt signaling (Atit et al., 2006). The cross talk between dermis and epidermis is critical for hair follicle formation.

The skin is a composite of multiple miniorgans. The outer layer is a stratified epidermis containing keratinocytes that differentiate and migrate from the basal layer to the suprabasal and ultimately form dead squames. The epidermis has several different appendages including hair follicles, sweat glands and sebaceous glands. The second layer is dermis, which surrounds the hair follicles and is composed of fibroblasts and other mesenchymal cells. Melanocytes are scattered among the keratinocytes and hair follicles to pigment the skin and hair. The subcutaneous layer resides under dermis and consists of adipocytes to protect the skin.

Epidermal stem cells can be found in the bulge of hair follicles, where they can generate all hair lineages, sebocytes and inter-follicular epidermis (Alonso and Fuchs, 2003). Bulge stem cells (Lgr5 expressing cells) can migrate downwards in the outer root sheath and reside in the dermal papilloma to generate hair. Additionally, bulge stem cells (Lgr6 expressing cells) can migrate upwards and form the sebaceous gland. They can potentially generate

epidermis, as well as the hair. The requirement of Wnt signaling in hair formation has been established based on several mouse models. Inhibition of Lef1, as well as conditional deletion of β -catenin in skin, reportedly disrupts hair formation (Huelsenken et al., 2001). Conversely, overexpression of Lef1 or β -catenin in skin can lead to excessive hair formation in the epidermis (Alonso and Fuchs, 2003).

Recently, several groups targeted Wls in skin epidermis and showed that epithelial Wnt secretion was required for hair follicle formation and skin homeostasis (Augustin et al., 2013; Myung et al., 2013). Conditional deletion of Wls (with K14-Cre) showed an arrest in the hair cycle, as well as inflammation in the epidermis, a condition similar to human psoriasis. Thus, Wls knockout skin phenotypes have confirmed the important role of epithelial Wnt secretion in skin homeostasis (Augustin et al., 2013; Myung et al., 2013).

1.7. 2 Small intestine and large intestine

The gastrointestinal epithelium is derived from endoderm, whereas hematopoietic elements, smooth muscle and connective tissue are formed from mesoderm.

The gastrointestinal tract is shaped by the folding of the endoderm and is accompanied by gene expression changes in the anterior–posterior axis, leading to anterior–posterior patterning and the development of foregut (duodenum, pancreas and liver), midgut and hindgut. Thereafter, rapid proliferation of the endoderm and mesenchyme layers results in elongation of the gut tube and formation of the lumen and crypt–villus axis. The stratified epithelium becomes a single epithelial layer overlying the lamina propria.

However, this mature intestinal epithelium displays morphological and functional differences from the duodenum to the ileum and colon.

The development and homeostasis of the small intestine are dependent on several signaling pathways conserved from metazoan to mammals. These pathways include the Notch, Wnt (wingless), hedgehog and bone morphogenic protein (BMP) pathways. The role of Wnt in intestinal homeostasis was first proposed following the discovery of a mutation in the APC gene as a main cause of the familial adenomatous polyposis (FAP) disease. Furthermore, growing body of studies have supported the role of Wnt signaling in intestinal development by using different transgenic mouse models including epithelial deletion of TCF4, double knockout of Lrp5/6 and epithelial overexpression of DKK1 (Korinek et al., 1998; Pinto et al., 2003; Zhang et al., 2012). Both TCF4 and LRP5/6 knockout epithelial mice reportedly died shortly after birth due to the lack of proliferation in the inter-villus area of the small intestine where neonatal intestinal stem cells reside. These results indicate the important role of Wnt/ β -catenin signaling in the late embryonic phase of intestinal development, but not in the early phase.

The importance of Wnt signaling in adult intestinal homeostasis was also investigated by utilizing different transgenic mouse models including β -catenin and TCF4 epithelial knockouts (Fevr et al., 2007; van Es et al., 2012b). Small intestine proliferation was blocked shortly after deletion of these genes, and crypts disappeared within 5 to 6 days in all parts of the small intestine. The mice died due to impaired intestinal homeostasis. Moreover, transient adenoviral overexpression of DKK1 (canonical Wnt inhibitor) in the adult

mice showed a lack of proliferation in the small and large intestines, as well as a shortening of villi in all parts of the small intestine (Kuhnert et al., 2004).

The small intestinal epithelial layer renews every 3 to 5 days. Maintaining such a high rate of proliferation depends on intestinal stem cells residing at the base of the crypt (Buckley et al., 2011; Buczacki et al., 2011; Scoville et al., 2008). Stem cells can give rise to progenitor cells or transit amplifying (TA) cells, which are rapidly dividing cells, and can differentiate into all mature cell types of the epithelium. Two distinctive intestinal stem cell populations exist within the small intestine. One is the label-retaining cells (LRCs) or quiescent stem cells, which reside at position 4 and are marked with *Bmi1*, *Hopx*, *mTert* and *Lrig1* (Montgomery et al., 2011; Sangiorgi and Capecchi, 2008; Takeda et al., 2011; Wong et al., 2012). The second population of stem cells are fast cycling stem cells and labeled as *Lgr5*, *Olfm4* and *ASCL2* stem cells (Barker et al., 2007; Jubb et al., 2006; van der Flier et al., 2009a). Interestingly, LRCs can interact and interconvert to *Lgr5* stem cells upon stress or injury to maintain intestinal homeostasis (Takeda et al., 2011; Yan et al., 2012). Indeed, a bidirectional relationship exists between quiescent and active stem cells of the intestine, but the hierarchical connection between these two populations of stem cells remains unknown (Tian et al., 2011).

Lgr5 and *Ascl2* are Wnt/ β -catenin target genes that support the connection between Wnt signaling and intestinal stem cells. The Paneth cells and their progenies are involved in the response to tissue injury and maintenance of intestinal homeostasis (Buczacki et al., 2013; Roth et al., 2012). Wnt signaling has been shown to be required for differentiation of Paneth cells and goblet cells (Roth et al., 2012; Scoville et al., 2008). Thus, Wnt signaling may control

several aspects of intestinal homeostasis, including intestinal stem cell proliferation, differentiation and response to injury.

1.7.3 Hematopoiesis

The formation of blood components by hematopoietic stem cells (HSCs) is called hematopoiesis. HSCs are the most studied stem cells in mammals and are known to give rise to all blood cell types. Additionally, HSCs also have an ability to produce stem cells through asymmetrical cell division in the BM niche, as well as maintain certain numbers of HSCs as a reservoir pool of stem cells within the BM. At the top hierarchy of the mammalian blood system are long-term HSCs (LT-HSCs). These cells are quiescent stem cells, and they are capable of a rapid response to proliferative stimuli generated by the external macroenvironment or BM niche. Downstream of LT-HSCs are short term HSCs (ST-HSCs), which can produce all blood cell types with limited self-renewal capacity compared to LT-HSCs. The ST-HSCs can produce multipotent progenitors (MMPs) or lineage restricted progenitors, including common myeloid progenitors (CMPs), granulocyte/macrophage progenitors (GMPs), megakaryocyte/ erythrocyte progenitors (MEPs) and common lymphoid progenitors (CLPs). The progenitors rapidly divide and differentiate into a pool of mature cells that eventually exit the BM (Figure 1.7)(Rossi et al., 2012).

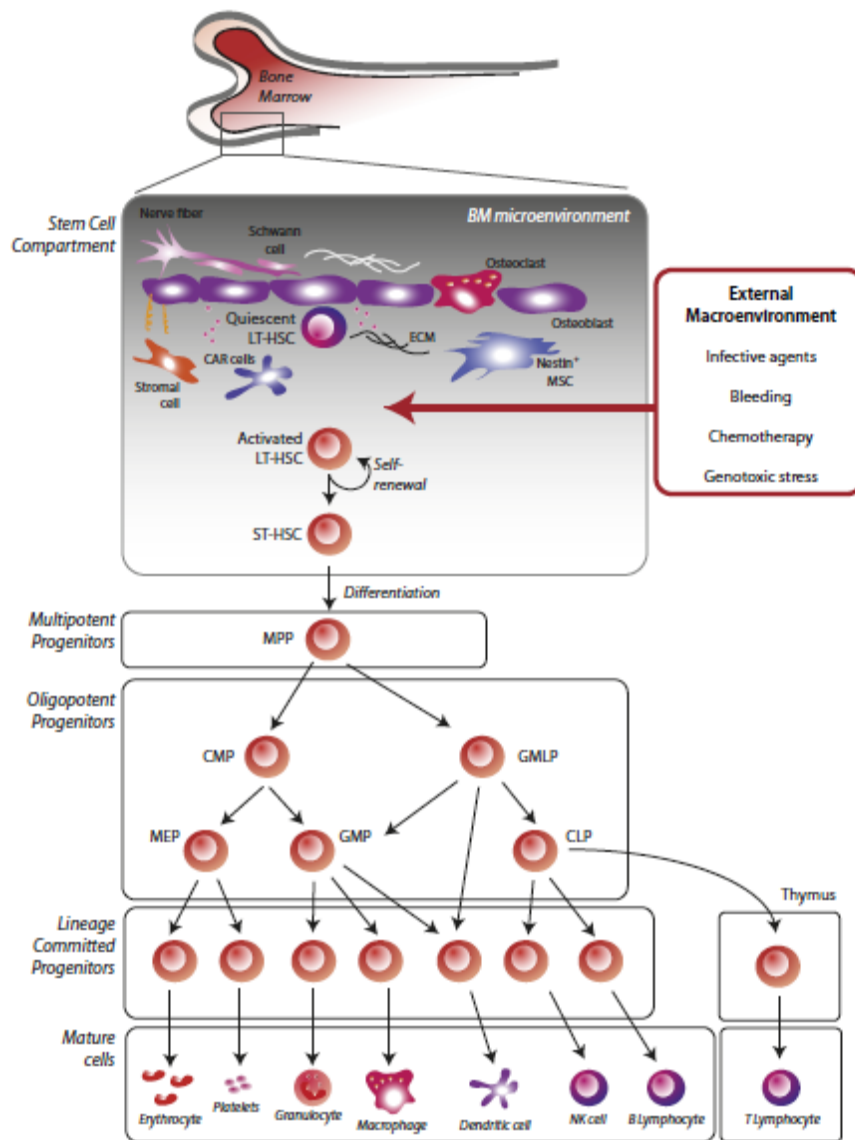


Figure 1.7 Overview of the hematopoietic hierarchy. This figure was adapted from Rossi et al. with permission (Rossi et al., 2012).

Many studies have implicated a role for Wnt signaling in embryonic or adult hematopoiesis; however, to date, there is no direct evidence for the importance of Wnt signaling in adult hematopoiesis. It is known that the emergence of mouse embryonic HSCs is dependent on the transient activation of β -catenin in endothelial-like cells residing in the aorta-gonad meonephros (AGM). However, the maintenance of HSCs is independent of β -catenin during late embryonic development and in adult mice (Cobas et al., 2004;

Ruiz-Herguido et al., 2012). More direct evidence for the role of Wnt signaling in embryonic hematopoiesis was demonstrated by transplantation of fetal $Wnt3a^{-/-}$ HSCs into $WNT3a^{+/+}$ recipient mice, which resulted in bone marrow failure in the secondary bone marrow transplanted recipient mice due to an impaired self-renewal capacity of the fetal $Wnt3^{-/-}$ HSCs (Luis et al., 2009).

Both adult HSCs and their niche express different Wnt ligands and inhibitors, indicating a possible role of Wnts in adult hematopoiesis (Figure 1.8). Studies that support the role of Wnt signaling in adult hematopoiesis mostly target downstream of Wnt receptors or target Wnt inhibitors that can alter the BM niche and indirectly affect hematopoiesis (Fleming et al., 2008; Luis et al., 2011). Conversely, some studies have revealed a limited role for Wnt signaling in adult hematopoiesis (Cobas et al., 2004; Jeannet et al., 2008). Thus, the role of Wnt in adult hematopoiesis remains controversial.

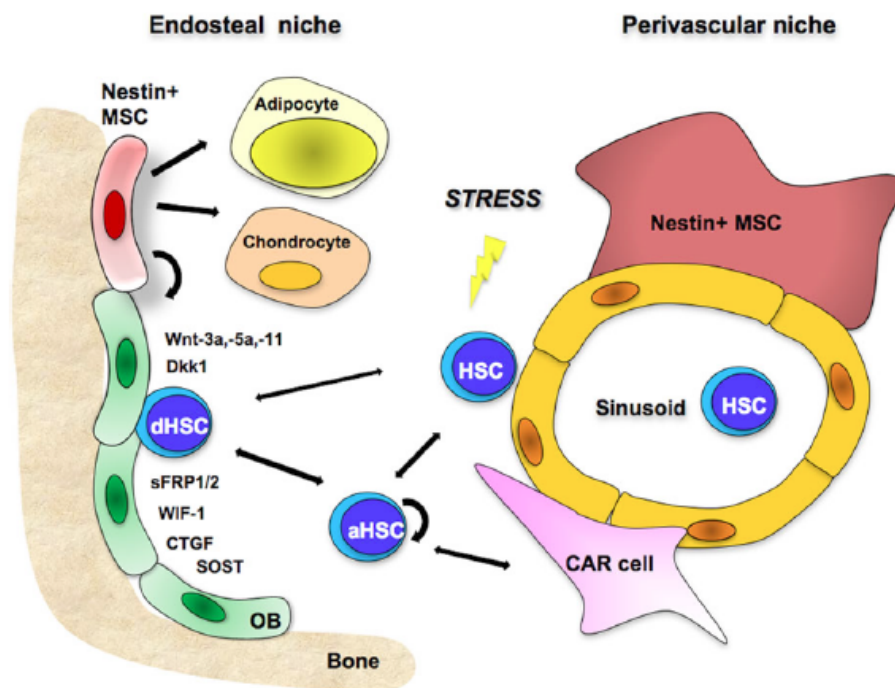


Figure 1.8 A model for members of the Wnt signaling pathway in the BM niche. Factors of Wnt signaling (including the Wnt proteins Wnt-3A, Wnt-11

and Wnt-5A and the Wnt inhibitors CTGF, SOST, Dkk-1, sFRP-1, sFRP-2 and WIF-1) express in the BM and can regulate HSC quiescence. Osteoblasts and nestin⁺ mesenchymal stem cells (endosteal niche), as well as CAR cells (perivascular niche) secrete essential factors required for HSC self-renewal and control hematopoiesis in normal and stress conditions within the BM microenvironment. This figure was adapted from Schreck et al. with permission (Schreck et al., 2014).

1.8 Wnt high-diseases and potential therapeutic approaches

Dysregulation of Wnt signaling results in several developmental defects (van Amerongen and Nusse, 2009). The list of Wnt diseases that affect adult patients is growing, of which more details can be found in several review papers (Clevers and Nusse, 2012; Herr and Basler, 2012). Colon carcinoma is the most intensely studied disease of Wnt signaling, which is characterized by mutation in APC and β -catenin. Other disorders associated with abnormal Wnt signaling include inflammatory bowel disease (linked to Wnt4), lung cancer, diabetes type II (linked to Wnt5B) and kidney disease (Hughes et al., 2011; Kanazawa et al., 2004; Mazieres et al., 2005; Pulkkinen et al., 2008).

Besides mutation in downstream canonical and non-canonical Wnt signaling, there are several human diseases associated with a high level of Wnt expression and production. These diseases include kidney and bone disorders, pathological fibrosis and several types of cancers, such as colon cancer, non-small cell lung carcinomas, breast cancers, ovarian cancers and head and neck cancers (Bafico et al., 2004; Hughes et al., 2011; Mazieres et al., 2005). Wls, as a key protein in the Wnt secretion pathway, has also been shown to promote tumor progression in glioma cell lines by enhancing Wnt/ β -catenin signaling (Augustin et al., 2012). As mentioned, Wnt signaling is tightly regulated, and small changes in Wnt expression levels can have significant impacts on the onset, progression and outcome of Wnt high diseases.

The strategy for the treatment of Wnt diseases will be determined by the nature of the disease. A promising approach in cancer treatment includes neutralizing antibodies against specific Wnts. This approach has been tested successfully in colon carcinoma, sarcoma, non-small lung carcinoma and breast cancer (He et al., 2005; He et al., 2004). Blocking Wnt signaling at the level of the Wnt ligand may occur by several extracellular Wnt inhibitors such as DKK1 or sFRP; however, these inhibitors may also affect other proteins beside Wnts (Lavergne et al., 2011).

Targeting the components of the destruction complex of β -catenin is another therapeutic approach, but it is only useful for inhibiting canonical Wnt signaling. These drugs could be inhibitors of GSK3, APC or Axin. There are several GSK3 inhibitors available clinically, but should be used with caution, because GSK3 has other substrates alongside β -catenin (Taelman et al., 2010). More specific inhibition of β -catenin may be achieved by blocking AXIN with IWR compounds (Chen et al., 2009).

There are several redundancies between Wnt ligands in Wnt high-diseases; therefore targeting Wnt secretion may offer an alternative approach to inhibit canonical and non-canonical Wnts. Two known possible methods to block Wnt secretion are by inhibiting either PORCN or WLS function.

Indeed PORCN inhibitor (IWP) has been commonly used in basic research for years. IWP can bind to the active site of the PORCN enzyme and block lipid modification of Wnts, consequently affecting Wnt secretion (Chen et al., 2009). Novartis has recently developed several PORCN inhibitors for *in vivo* use, including C59 and LGK974, that are now in clinical trials (Liu et al., 2013). Our group was among the first laboratories to use C59 for the treatment

of mice mammary tumors. This drug successfully suppressed MMTV-Wnt1 mammary tumors in mice at a low dosage without general toxicity (Proffitt et al., 2013). Importantly, if Wnt signaling is required for adult tissue proliferation and homeostasis, PORCN inhibition may have severe side effects in proliferative tissues including intestine, skin and bone marrow. Therefore, more studies need to identify the role of PORCN and Wnt secretion in the maintenance of tissue homeostasis.

1.9 Hypothesis

The role of Wnt secretion in adult stem cell self-renewal and tissue homeostasis has not been clearly tested yet. To address the importance of Wnt signaling in adult tissue homeostasis, most studies have focused on knockout or knock-in mouse models of inhibitors, receptors and downstream components of Wnt/ β -catenin signaling. Although these approaches are interesting, none of these methods can directly demonstrate the role of Wnt ligands in the self-renewal of adult intestinal stem cells and HSCs. In this study, we used the advantages of the *Porcn* conditional knockout mouse model and potent PORCN inhibitor, C59, to address the role of Wnt signaling in adult intestinal homeostasis and hematopoiesis. Additionally, targeting *Porcn* may help to identify critical Wnt producing cells within tissue, as well as help to elucidate specific cell types as the adult stem cell niche.

2. Role of Wnt Signaling in Murine Intestinal Homeostasis*

* This chapter is reproduced from my paper “Stroma provides an intestinal stem cell niche in the absence of epithelial Wnts” which was published in *Development*, 2014, 141:11, 2206-2215.

2.1 Introduction

The epithelial lining of the intestine continuously renews itself every 3 to 5 days. In the crypts of the murine small intestine, long-lived, label-retaining stem cells in the +4 position marked by *Bmi1*, *mTert* and *Hopx* interact with and interconvert with more rapidly proliferating, radiation resistant, crypt base columnar cells that express markers including *Lgr5*, *Olfm4*, *Lrig1* and *Ascl2* (Barker et al., 2007; Buczacki et al., 2013; Takeda et al., 2011; van der Flier et al., 2009b; Wong et al., 2012; Yan et al., 2012). This stem cell compartment gives rise to committed progenitor cells that proliferate rapidly and produce the diverse differentiated progeny that migrate up the villi before being shed into the lumen.

Wnt/ β -catenin signaling plays a critical role in maintaining normal proliferation in the intestinal crypt of the adult mouse. Secreted Wnts bind to LRP5/6 and Frizzled co-receptors present on epithelial crypt cells, leading to an increase in β -catenin protein (Clevers and Nusse, 2012). Activated β -catenin binds to the nuclear transcription factor TCF4 to drive a gene expression program that supports stem cell maintenance, proliferation and differentiation. Disruption of the Wnt/ β -catenin pathway blocks intestinal proliferation. Embryonic knockout of *TCF4* in intestinal epithelial cells leads to lack of proliferation in the inter-villus region of the neonatal small intestine, while inducible knockout of *TCF4* and β -catenin in adults blocks proliferation in the crypt compartment (Fevr et al., 2007; Korinek et al., 1998; van Es et al., 2012b). Conversely, stabilization of β -catenin by expression of constitutive active β -catenin or mutation of *APC* stimulates proliferation. Surprisingly, the evidence that secreted Wnt ligands regulate intestinal homeostasis in adult

mice remains indirect. The strongest evidence comes from studies inhibiting or knocking out the Wnt ligand co-receptors *Lrp5* and *Lrp6*, leading to a near total loss of epithelial proliferation (Kuhnert et al., 2004; Zhang et al., 2012).

The identity and cellular source of the Wnts that regulate the intestinal stem cell niche is not clear. Many of the 19 different Wnt genes are expressed in the small intestine, each with a distinct pattern of expression in diverse cell types of the epithelium and stroma (Gregorieff et al., 2005). These multiple Wnts may regulate diverse processes beyond the stem cell niche, including innate and adaptive immunity, injury repair, and intermediary metabolism (Cervantes et al., 2009; Davies et al., 2008; Zeve et al., 2012). The limited number of studies knocking out Wnts in mouse intestine have not identified defects in *in vivo* crypt stem cell proliferation (Cervantes et al., 2009; Farin et al., 2012). Paneth cells in the crypt base are a potential source of the Wnts that regulate stem cell proliferation. They express several Wnts, including *Wnt3*. In purified epithelial cell preparations, WNT3 from Paneth cells is required for the growth in culture of organoids derived from *Lgr5*-expressing intestine stem cells, although supplementation with R-Spondin 1 (RSPO1) is also required (Farin et al., 2012; Ootani et al., 2009; Sato et al., 2011; Sato et al., 2009). Based on this data, it has been proposed that Paneth cells form the niche for the isolated intestinal stem cells (Sato et al., 2011). However, depletion of Paneth cells or knock out of *Wnt3* in the epithelial cells of the intestine did not show an obvious *in vivo* phenotype (Durand et al., 2012; Farin et al., 2012), indicating that other functionally important Wnts are made by epithelial or stromal niche cells. Several groups have demonstrated that stromal cells can support the growth of intestinal epithelium in culture (Farin

et al., 2012; Lahar et al., 2011). Intestinal stromal cells express multiple Wnts (Farin et al., 2012; Gregorieff et al., 2005). Farin et al. demonstrated that purified stromal cells could support organoid formation from *Wnt3* knockout epithelial cells, but the question of whether other epithelial-produced Wnts are essential *ex vivo* and more importantly, *in vivo*, remains unanswered.

One approach to address the functionally relevant source of Wnts in the small intestine is to globally target their secretion. This can be achieved by knockout or inhibition of either of two genes, *Porcn* and *Wls*, that are indispensable parts of the core Wnt secretion machinery (Najdi et al., 2012; Proffitt and Virshup, 2012). The PORCN protein is a membrane bound O-acyl transferase that resides in the endoplasmic reticulum. PORCN palmitoleates all Wnts as they are synthesized (Biechele et al., 2011; Kadowaki et al., 1996; Tanaka et al., 2000). Palmitoleation is required for Wnts to bind to WLS, an integral membrane carrier protein that is essential for the secretion of all known vertebrate Wnts (Coombs et al., 2012; Najdi et al., 2012). Wnt palmitoleation is also required for secreted Wnt ligands to interact with Frizzled receptors at the cell membrane (Janda et al., 2012). *Porcn* is encoded by a single copy gene on the X chromosome and has no closely related homologues in the genome. *Zygotic Porcn* mutants exhibit gastrulation failure leading to early embryonic lethality (Barrott et al., 2011; Biechele et al., 2013; Biechele et al., 2011). Several potent small molecule inhibitors of PORCN have been developed that phenocopy the biochemical effects of *Porcn* knockout, and may be of value in the treatment of Wnt-high diseases including cancer and fibrotic disorders (Chen et al., 2009; Proffitt et al., 2013). Indeed, one PORCN inhibitor, LGK974, is currently in phase 1 trials in humans (Liu

et al., 2013). However, due to potential detrimental effects on adult stem cell self-renewal, the role of pharmacologic inhibition of PORCN remains to be determined.

To dissect the role of epithelial and stromal Wnts in intestinal homeostasis and assess the potential toxicity of PORCN inhibition, we used genetic and pharmacological approaches to block Wnt production in the gut. We find that epithelial Wnts are dispensable for normal proliferation in the mouse intestine. In contrast, pharmacologic inhibition of Wnt production produces a graded decrease in proliferation. At intermediate doses, Wnt-responsive *Lgr5* expression is markedly reduced, accompanied by impaired recovery from radiation injury, but without a decrease in the proliferation of transit amplifying cells. At higher doses of the PORCN inhibitor, global intestinal proliferation ceases. A stromal fraction enriched for myofibroblasts that endogenously expresses both Wnts and *Rspo3* supports *Porcn^{Del}* organoid proliferation in the absence of supplemental RSPO1. These studies suggest that a stromal Wnt/RSPO3-producing niche is sufficient for normal and stressed intestinal homeostasis and support the role of the *Lgr5* cell population in recovery from radiation injury.

2.2 Results

2.2.1 Normal intestine homeostasis after complete inhibition of epithelial Wnt secretion

Multiple studies have demonstrated a role for Wnt/ β -catenin signaling in intestinal homeostasis, but whether intestinal epithelial cells provide any Wnts important in the niche remains an open question. To assess the role of the epithelial Wnts in intestinal homeostasis, we used a floxed allele of *Porcn* that is null for Wnt secretion after Cre-mediated excision (Biechele et al., 2013; Proffitt and Virshup, 2012). *Porcn*^{lox} and *Porcn*^{WT} mice were crossed with *Villin-Cre* mice to generate *Villin-Cre/Porcn*^{Del} or *Villin-Cre/Porcn*^{WT} mice, respectively. *Villin* expression begins in late embryogenesis in all epithelial cells of the intestine. Our hypothesis was that embryonic inactivation of *Porcn* in the intestinal epithelium would be lethal in the neonatal period, similar to what was observed in the *Tcf4* or *Lrp5/Lrp6* double knockout (Korinek et al., 1998; Zhang et al., 2012). Unexpectedly, *Villin-Cre/Porcn*^{Del} pups were viable, appeared phenotypically normal, and suckled and weaned without difficulty. We confirmed by genomic PCR and RT-qPCR that purified intestinal epithelial cells from *Villin-Cre/Porcn*^{Del} mice had complete excision of the *Porcn* gene (Figure 2.1 A and B).

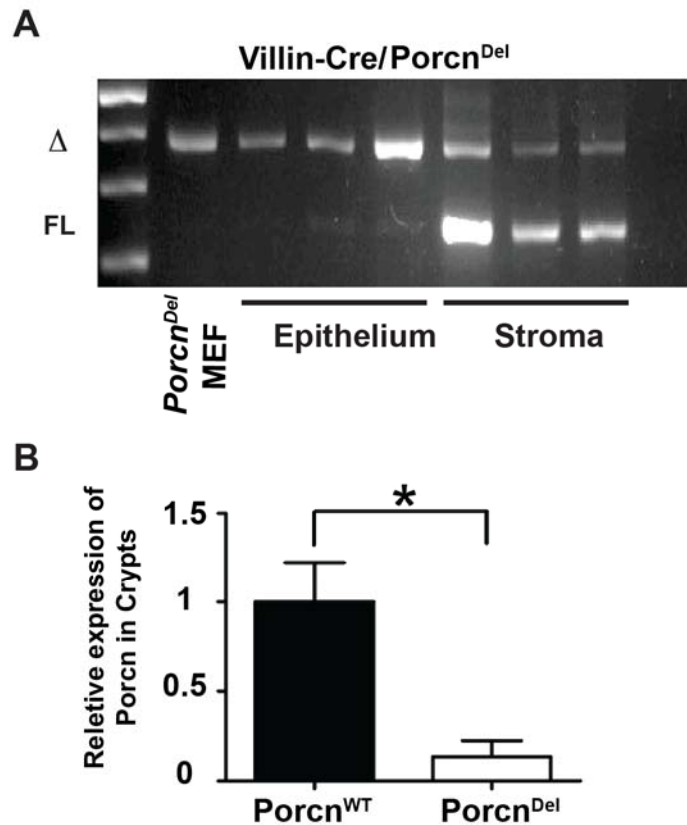


Figure 2.1 Complete deletion of *Porcn* in intestinal epithelial cells of *Villin-Cre/Porcn^{Del}* mice. **A)** *Porcn* deletion in purified intestinal epithelial cells from *Villin-Cre/Porcn^{Del}* mice is efficient. PCR was performed using gDNA from the epithelial or stromal fractions of individual mice or knockout MEFs (Δ : excised *Porcn* allele, FL: floxed allele). The small amount of unexcised *PORCN* allele present in two of the epithelial fractions most likely represents residual stromal contamination visible after 40 PCR cycles. **B)** Purified crypt cells were analyzed for *Porcn* mRNA expression using RT-qPCR. Samples were normalized for housekeeping genes (*Pgk* and *β -actin*). Data represent different epithelial preps from age and gender matched mice (n = 5 in each group). Error bars indicate SD.

To confirm functional excision of *Porcn*, we took advantage of the observation that Wnt secretion from Paneth cells or other epithelial cells is required for purified crypts to form organoids in culture (Ootani et al., 2009; Sato et al., 2009). Indeed, purified isolated crypts from *Villin-Cre/Porcn^{Del}* mice did not form organoids *in vitro* (Figure 2.2 and 2.4). This result phenocopies both knockout of *Wnt3* (Farin et al., 2012) and the effect of small molecule PORCN inhibition (Sato et al., 2011), confirming the functional

inactivation of epithelial *Porcn* in *Villin-Cre/Porcn^{Del}* mice and supporting the central role of epithelial Wnts in *ex vivo* culture of purified intestinal stem cells.

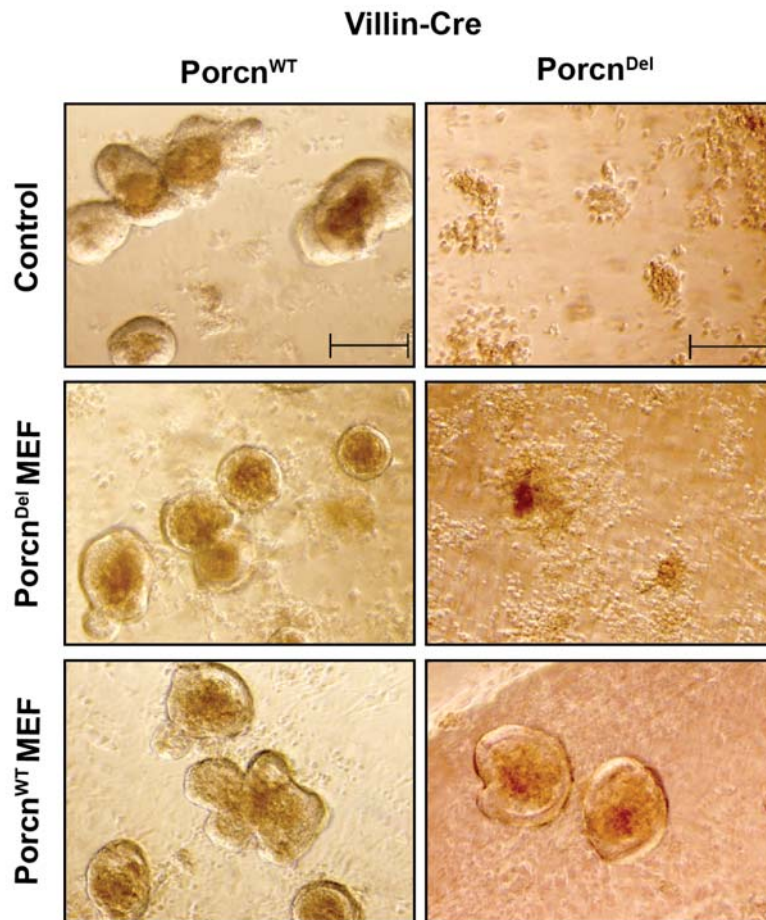


Figure 2.2 PORCN inactivated epithelial cells could not form organoids *in vitro*. Crypts from *Villin-Cre/Porcn^{Del}* mice, either alone or co-cultured with *Porcn^{Del}* MEFs, did not form organoids (top and middle panels, respectively). In contrast, co-culture with *Porcn^{Del}* MEFs stably expressing *Porcn^{WT}* (*Porcn^{WT}* MEFs) rescued organoid formation (bottom panels). 5000 MEFs were plated with 6000 crypts per well. The scale bar is 200 μ m.

To confirm that the defect in organoid formation was due to loss of secreted Wnts and not to a non-Wnt consequence of *Porcn* knockout (Covey et al., 2012), we employed two approaches. First organoid formation from *Villin-Cre/Porcn^{Del}* crypts was rescued by co-culture with WNT3A-secreting

mouse L (L3A) or human HEK293 (STF3A) cells (Figures 2.3 and 2.4). Second, organoid formation was also partially rescued by co-culture with MEFs that we found express endogenous WNT3 (Figures 2.2, 2.4 and 2.5). However, *Porcn*^{Del} MEFs failed to rescue (Proffitt and Virshup, 2012). These findings are consistent with existing data that intestinal epithelial stem cells require a source of palmitoleated Wnts to proliferate and form organoids, and that *ex vivo* the Wnts can be supplied by co-culture with WNT3A-secreting cells.

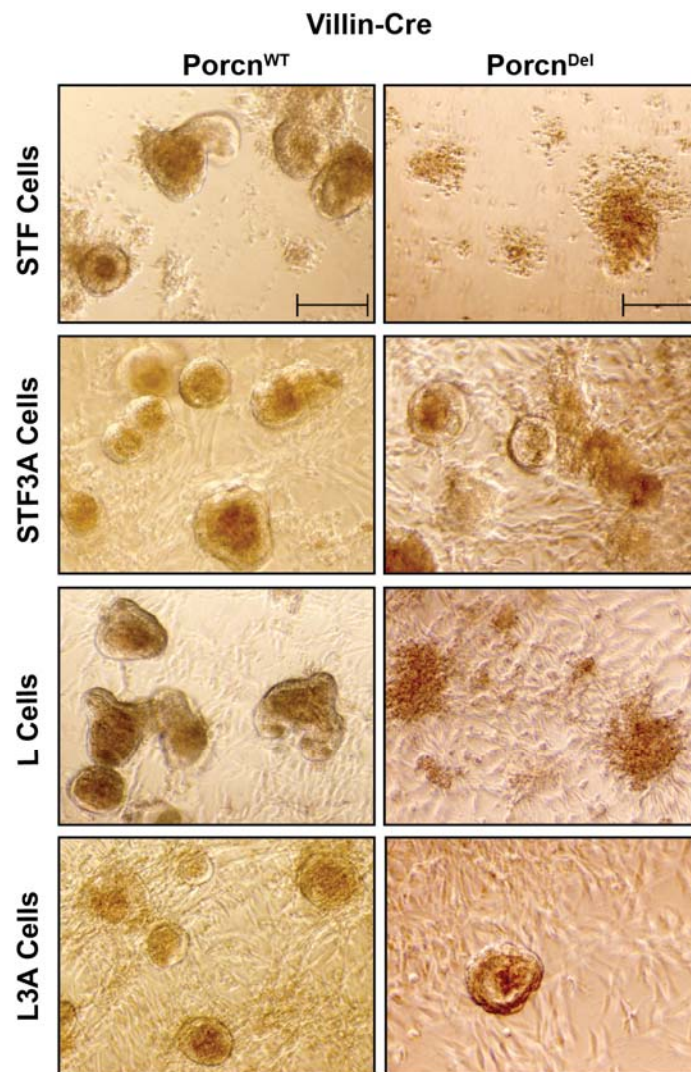


Figure 2.3 Organoid formation from *Porcn*^{Del} crypts is rescued by Wnt-secreting cells. No organoids form in co-cultures of crypt cells from *Villin*-

Cre/Porc^{Del} mice with L cells or STF cells, while the same cell lines expressing Wnt3A (L3A and STF3A cells, respectively) restore organoid formation. 5000 feeder cells were plated with 6000 crypts per well. The scale bar is 200 μ m.

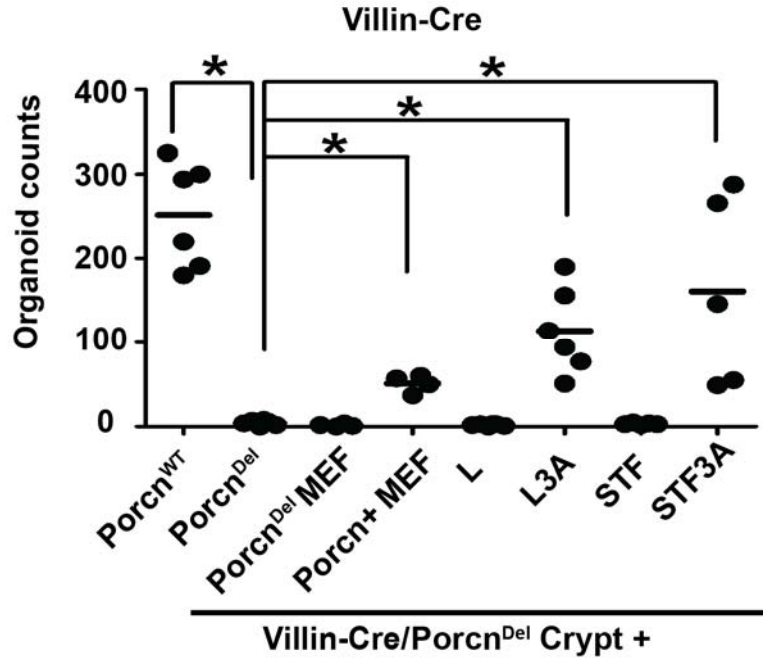


Figure 2.4 PORCN inactivated epithelial cells could not form organoid unless co-cultured with Wnt producing cells. Quantification of experiments in figure 2.2, and 2.3. Each point represents an independent biological replicate (* p < 0.001, two-tailed t-test).

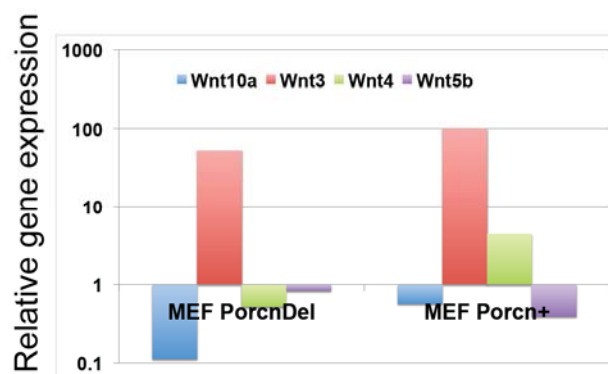


Figure 2.5 MEF cells highly express endogenous Wnt3. *Wnt* expression levels were measured by qPCR in mouse MEFs with *Porcn* knockout, without (*Del*) and with an *mPorcnD* transgene (+). Values of the 4 most highly expressed Wnts are shown as $2^{(-\Delta Ct)}$, with the highest expression level (WNT3, Ct 21.2) set to 100 and the reference gene *Pgk* with Ct of 20.3.

We assessed the phenotype of the intestine in the *Villin-Cre/Porcⁿ^{Del}* mice. The small and large intestines were grossly and microscopically normal (Figure 2.6). In addition, epithelial lineages including enteroendocrine, Paneth, and goblet cells were not detectably altered in the absence of epithelial Wnt secretion, and there was no increase in apoptotic cells (Figure 2.7). Loss of epithelial *Porcn* did not alter the committed progenitor (also called transit amplifying) compartment, as assessed by short term EdU incorporation (Figure 2.8 A and B). Importantly, β -catenin was observed in the nuclei of crypt cells of *Villin-Cre/Porcⁿ^{Del}* mice, indistinguishable from controls (Figure 2.8 A). Consistent with intact β -catenin signaling, the expression of *Axin2*, *Lgr5* and *Olfm4* did not differ significantly between jejunum samples of control and *Porcn*-inactivated mice (Figure 2.9). These data demonstrate that Wnt/ β -catenin/LGR5 signaling is ongoing in intestinal crypt cells in the absence of epithelial Wnt secretion. This strongly suggests that in *Villin-Cre/Porcⁿ^{Del}* mice the Wnts important in intestinal proliferation are adequately supplied from the stroma.

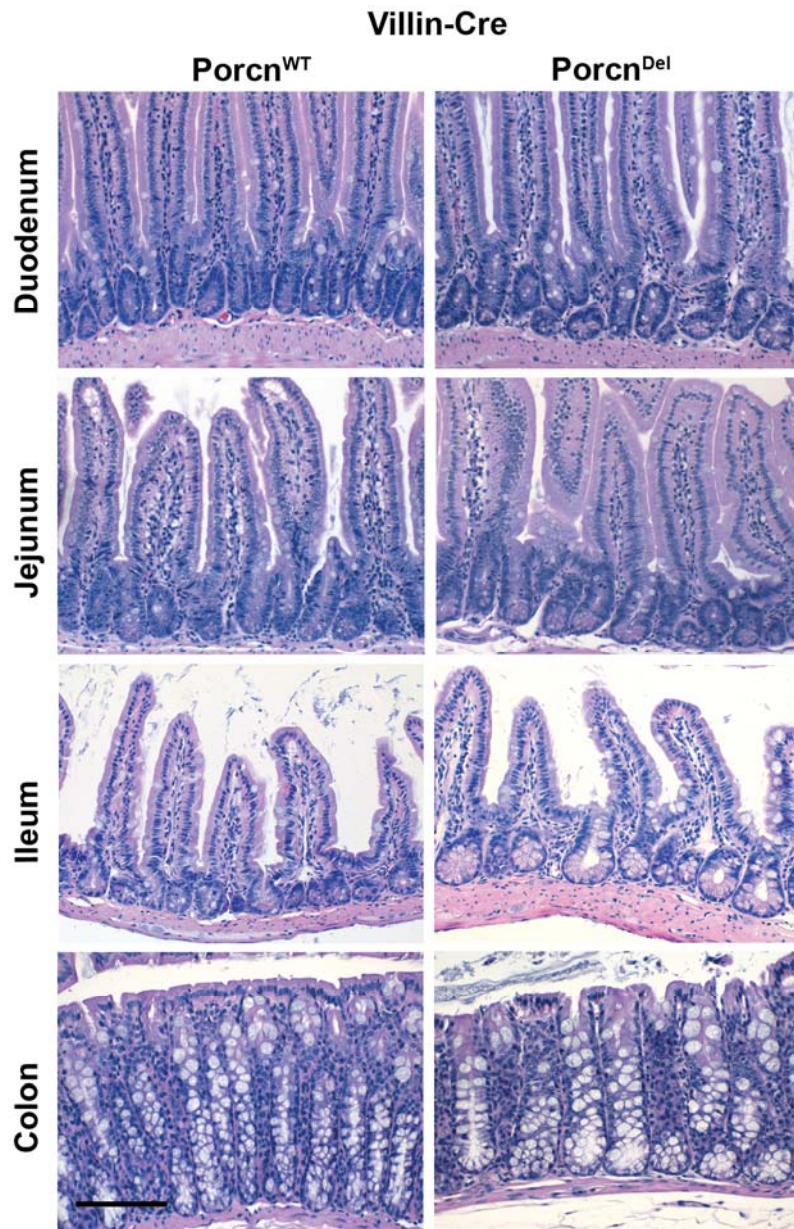


Figure 2.6 Epithelial Wnt secretion is dispensable for intestinal homeostasis in mice. Representative histology of small intestine and colon from *Villin-Cre/Porcn^{WT}* (n = 6) and *Villin-Cre/Porcn^{Del}* (n = 6). Mice were sacrificed between 3 to 12 months of age. The scale bar is 200 μ m.

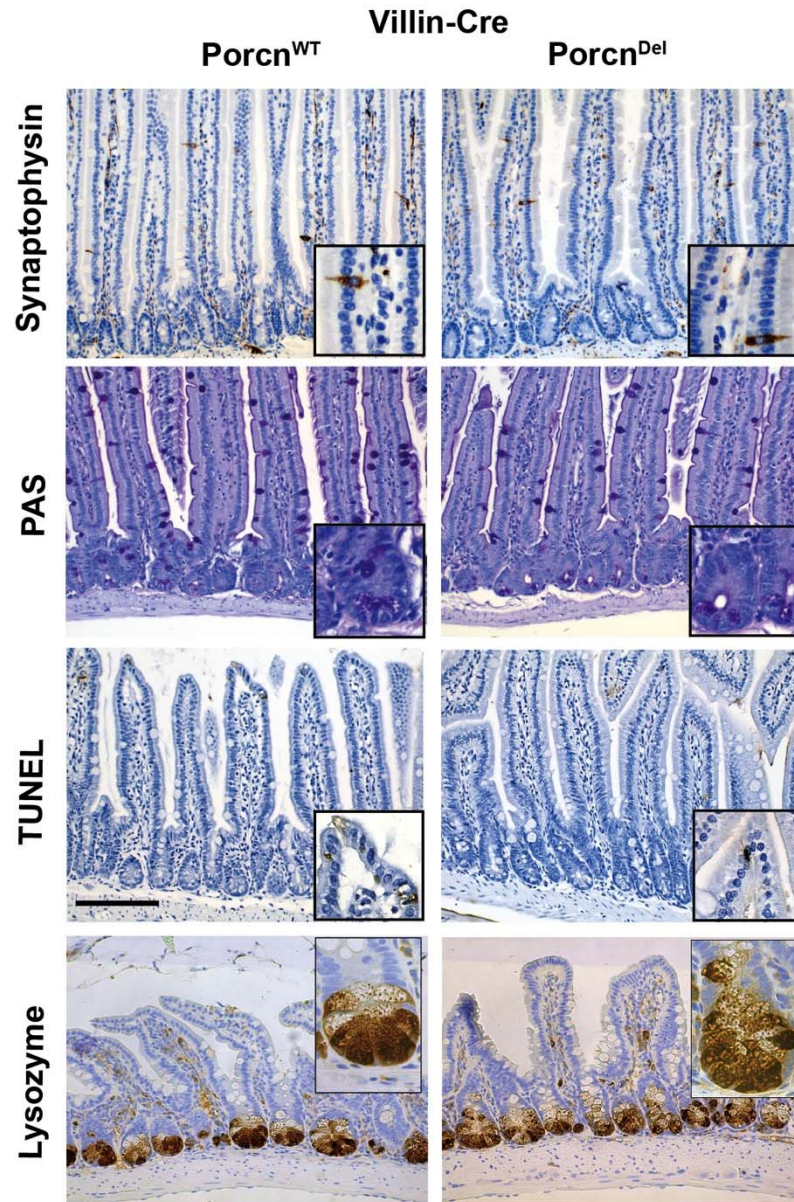


Figure 2.7 Normal epithelial differentiation in *Villin-Cre/Porcn^{WT}* and *Villin-Cre/Porcn^{Del}* mice. Enteroendocrine cells labeled by synaptophysin specific staining, goblet and Paneth cells labeled by PAS staining, apoptotic cells labeled by TUNEL staining and Paneth cell differentiation was assessed by lysozyme immunohistochemistry. Insets show higher magnification. (n = 3 mice per group) The scale bar is 200 μ m.

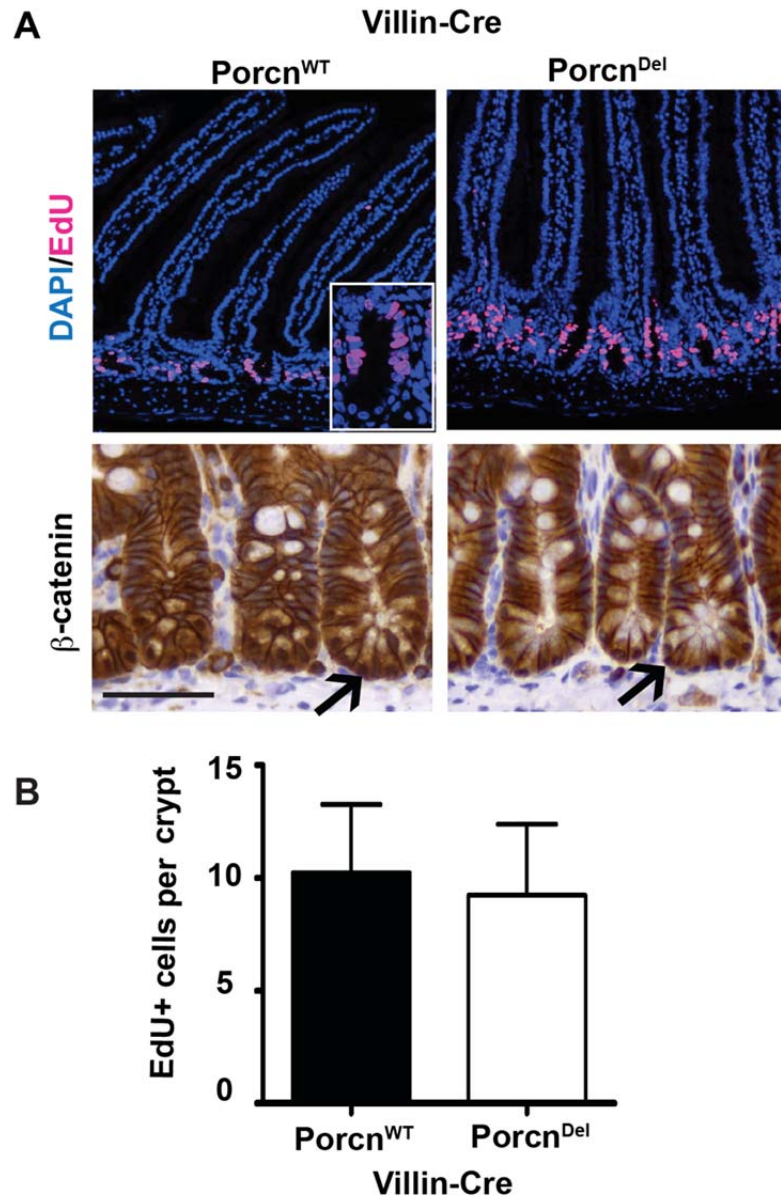


Figure 2.8 Normal proliferation and nuclear β -catenin in *Villin-Cre/Porcn^{WT}* and *Villin-Cre/Porcn^{Del}*. **A) Mice ($n = 3$ per group) were injected with EdU 2 hours prior to sacrifice. Arrows indicate nuclear β -catenin. The scale bar is 50 μ m. **B**) Quantitation of EdU positive cells per crypts (\pm SD) from *Villin-Cre/Porcn^{WT}* ($n = 3$) and *Villin-Cre/Porcn^{Del}* ($n = 3$). 63 crypts per genotype were counted.**

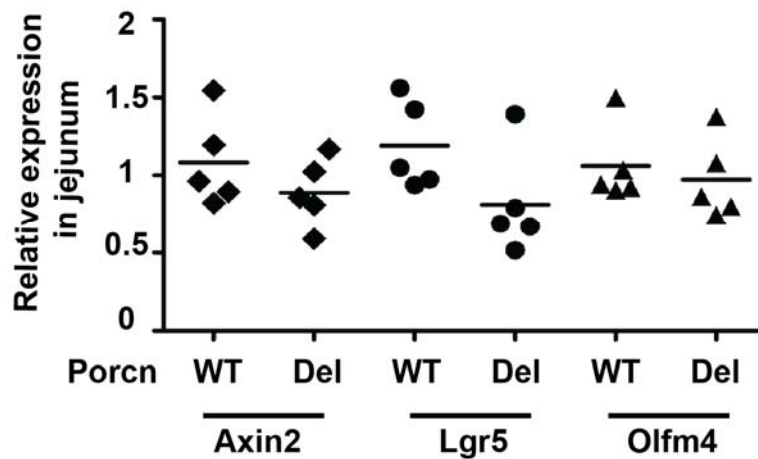


Figure 2.9 No significant changes in expression of Wnt/ β -catenin target genes in jejunum of *Villin-Cre/Porcn^{Del}* mice. No significant changes in expression of *Axin2*, *Lgr5* and *Olfm4* between jejunum of *Villin-Cre/Porcn^{WT}* and *Villin-Cre/Porcn^{Del}* mice. Expression levels were assessed by qPCR and normalized to *Pgk* and *β -actin* (n = 5 mice, p > 0.05, two-tailed t- test).

We tested if the unaltered proliferation and differentiation after epithelial loss of Wnt secretion resulted from compensatory changes in other signaling pathways regulating intestinal stem cell renewal. To assess this, gene expression profiling was performed on isolated epithelium and stroma from wildtype and *Porcn^{Del}* mouse intestine. As Figure 2.10 shows, there were only minimal changes in global gene expression detected, and there were no statistically significant alterations in known Wnt/ β -catenin pathway regulators (Figure 2.11). There were no significant changes in expression of genes associated with the Notch and EGF pathways (Figures 2.12 and 2.13). We conclude that epithelial Wnt secretion is not essential for normal murine small intestinal homeostasis *in vivo*, and its loss causes no readily detectable compensatory alterations in gene expression.

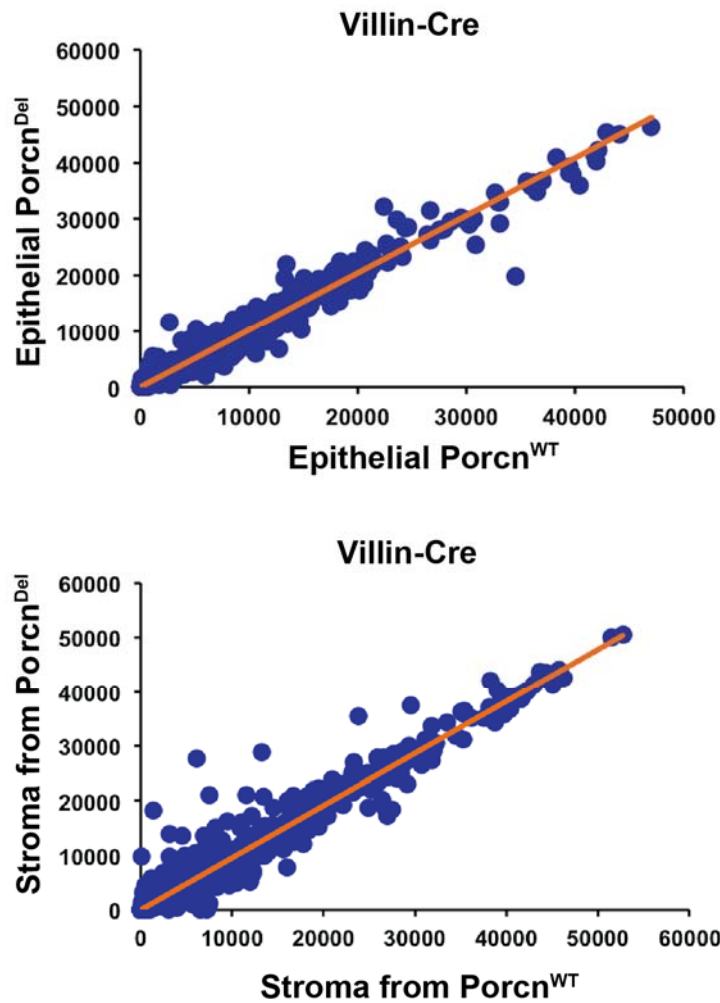


Figure 2.10 No major compensatory changes in gene expression were observed after epithelial *Porcn* inactivation. Normalized median-centered expression values from epithelial and stromal-enriched fractions from *Villin-Cre/Porcn^{WT}* and *Villin-Cre/Porcn^{Del}* mice are compared in scatter plots (n = 5 and 4 mice per group for epithelial and stromal samples, respectively). Only an increase of two genes in stroma, *Scd1* and *Atp7a* reached statistical significance.

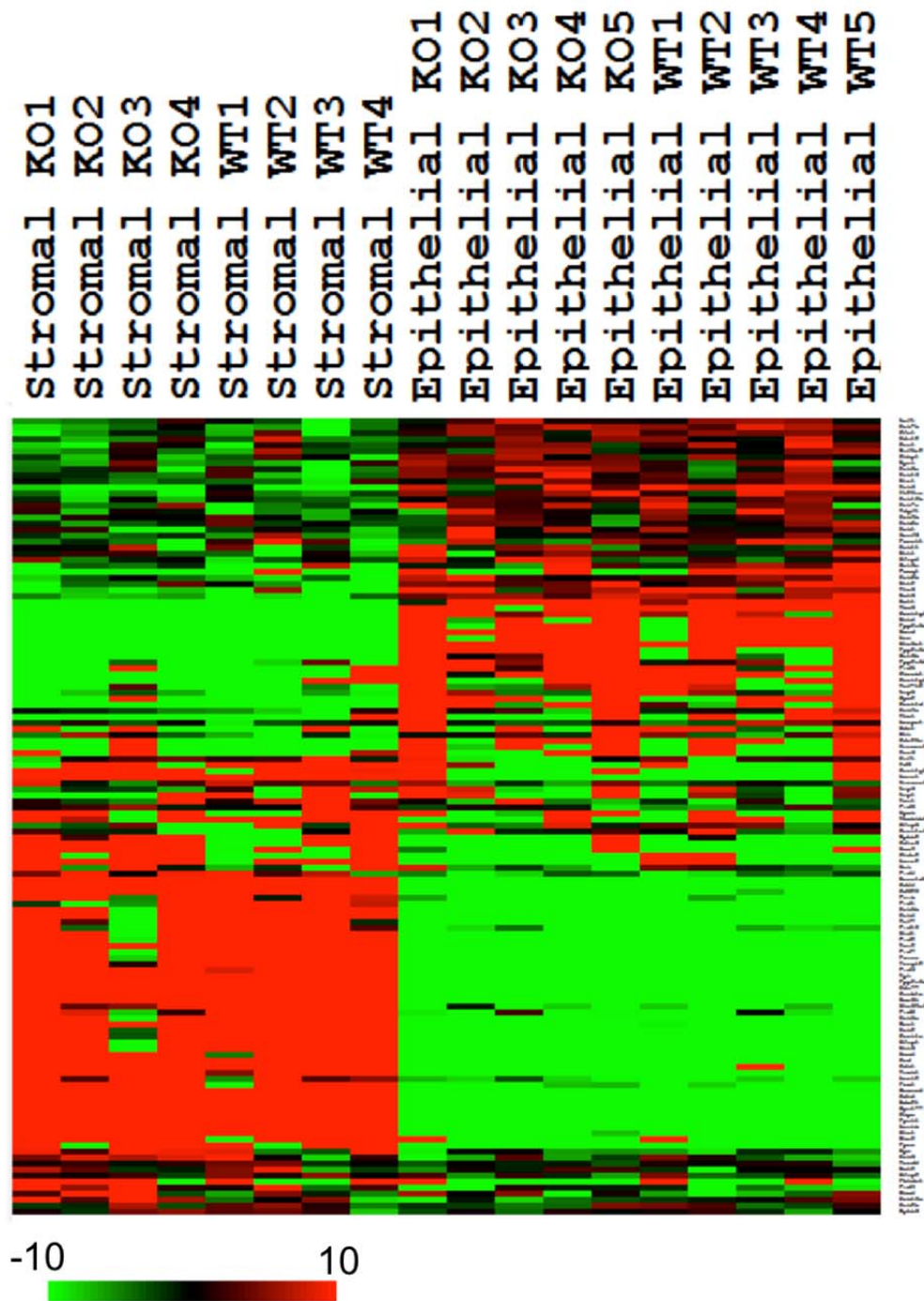


Figure 2.11 No changes in gene expression of Wnt/β-catenin pathway was observed after epithelial *Porcn* inactivation. Gene expression profile of Wnt/β-catenin pathway from Illumina arrays for epithelial and stromal cells from *Villin-Cre/Porcn^{WT}* and *Villin-Cre/Porcn^{Del}* mice is represented as a heatmap, where up- and down-regulation is indicated by red and green, respectively (n = 5 and 4 mice per group for epithelial and stromal samples, respectively).

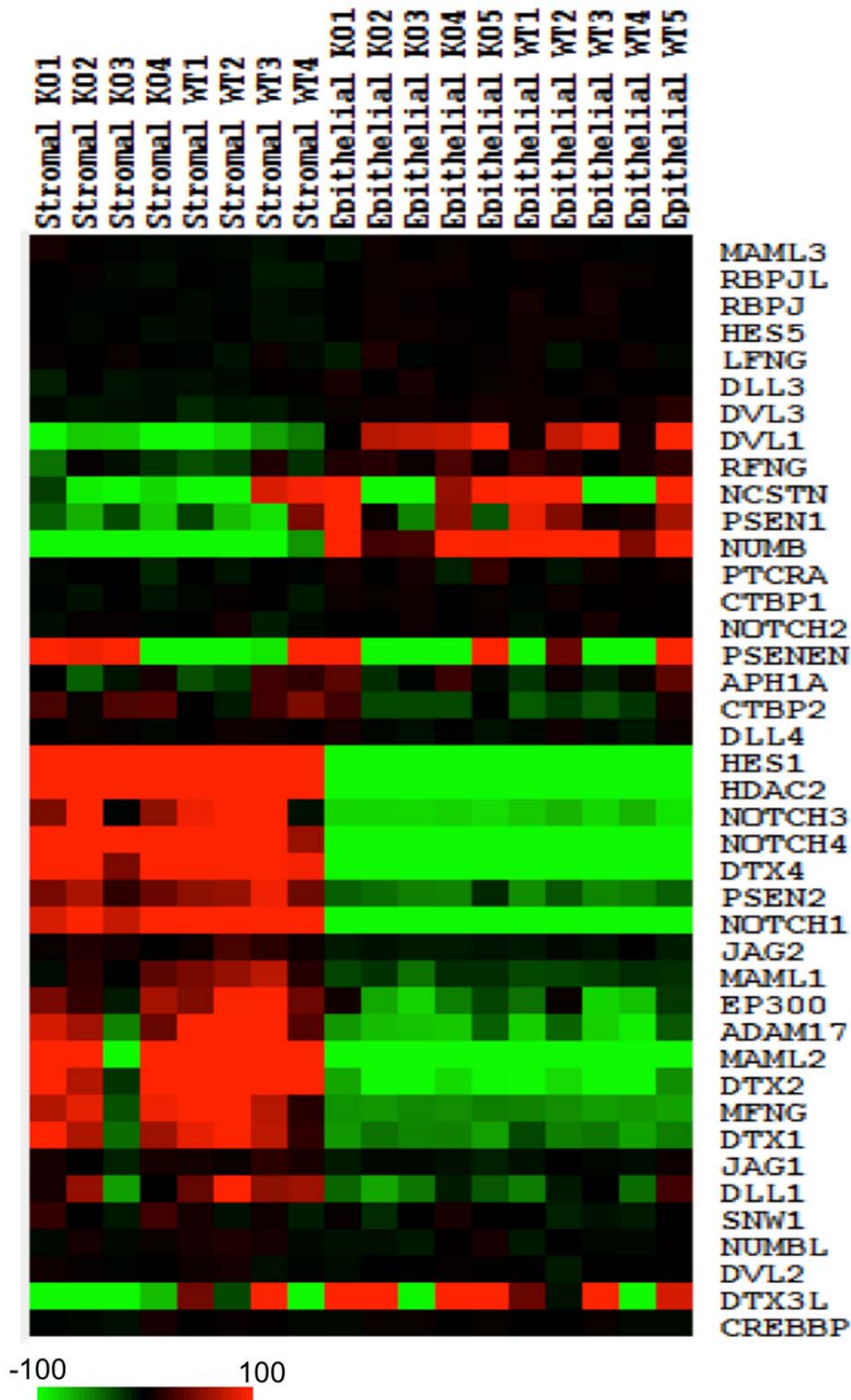


Figure 2.12 No changes in gene expression of Notch pathway was observed after epithelial *Porcn* inactivation. Gene expression profile of Notch pathway from Illumina arrays for epithelial and stroma-enriched samples from *Villin-Cre/Porcn^{WT}* and *Villin-Cre/Porcn^{Del}* mice is represented as a heat map where up- and down-regulation is indicated by red and green

respectively (n = 5 and 4 mice per group for epithelial and stromal samples, respectively).

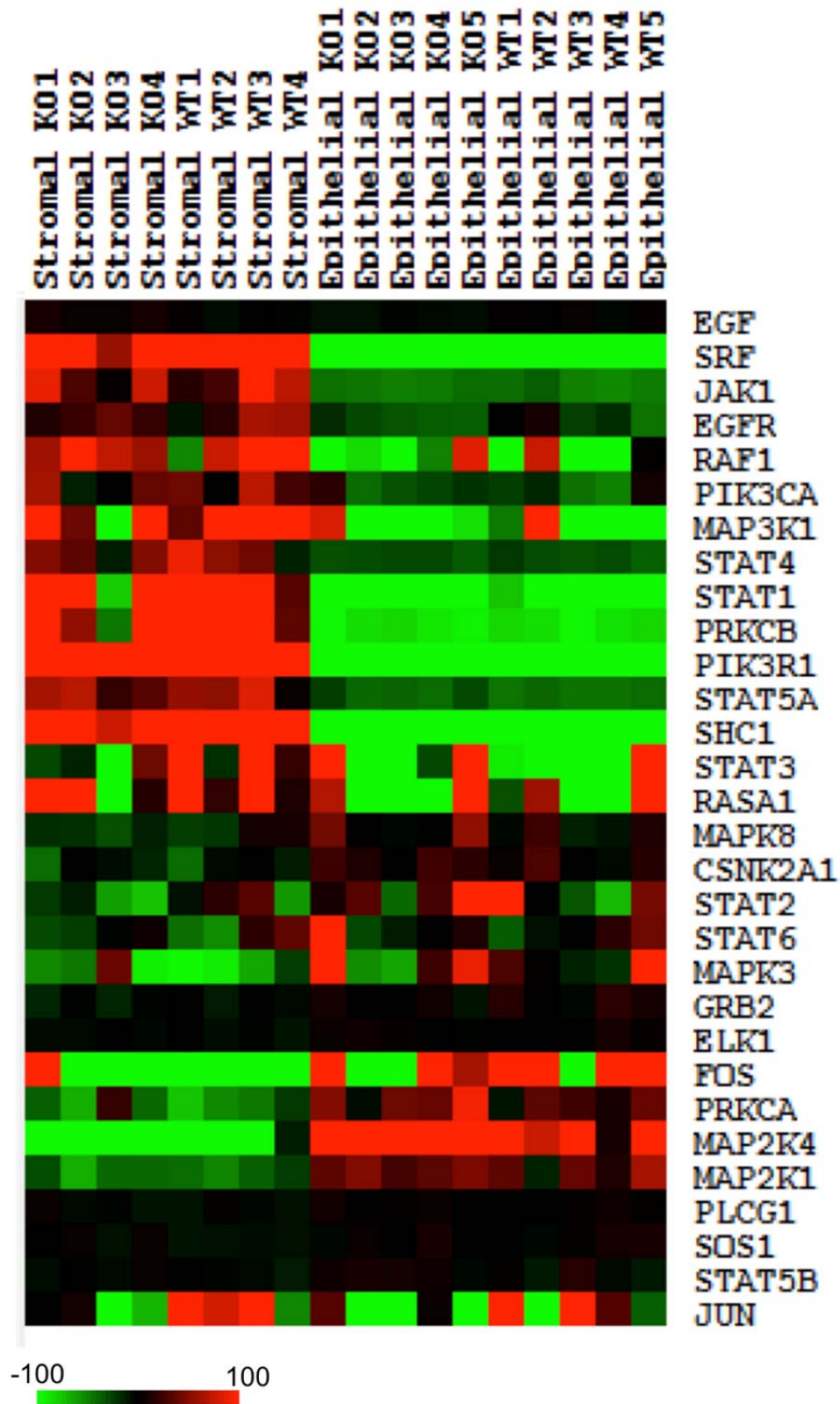


Figure 2.13 No changes in gene expression of EGF pathway was observed after epithelial *Porcn* inactivation. Gene expression profile of EGF pathway from Illumina arrays for epithelial and stromal cells from *Villin-Cre/Porcn^{WT}*

and *Villin-Cre/Porcn^{Del}* mice is represented as a heat map, where up- and down-regulation is indicated by red and green, respectively (n = 5 and 4 mice per group for epithelial and stromal samples, respectively).

2.2.2 Stroma expresses Wnts and *Rspo3* forms a niche for epithelial stem cells

A critical role for intestinal stroma in the self-renewal of epithelial stem cells has previously been suggested by Farin et al. (Farin et al., 2012). To test this, we isolated *Porcn^{Del}* crypts and *Porcn^{flox}* unfractionated stromal cells (“fresh stroma”) from *Villin-Cre/Porcn^{Del}* mice and cultured them separately or together. Stroma added to *Porcn^{Del}* crypts supported cystic organoid formation (Figure 2.14 A). Crypts depleted of stroma require supplementation with RSPO1 to form organoids in culture. We reasoned that the added RSPO1 might be required to amplify the WNT3 signal from the Paneth cells. Remarkably, we found that *Porcn^{Del}* crypts supplied with stroma did not require exogenous RSPO1 (Figure 2.14 A).

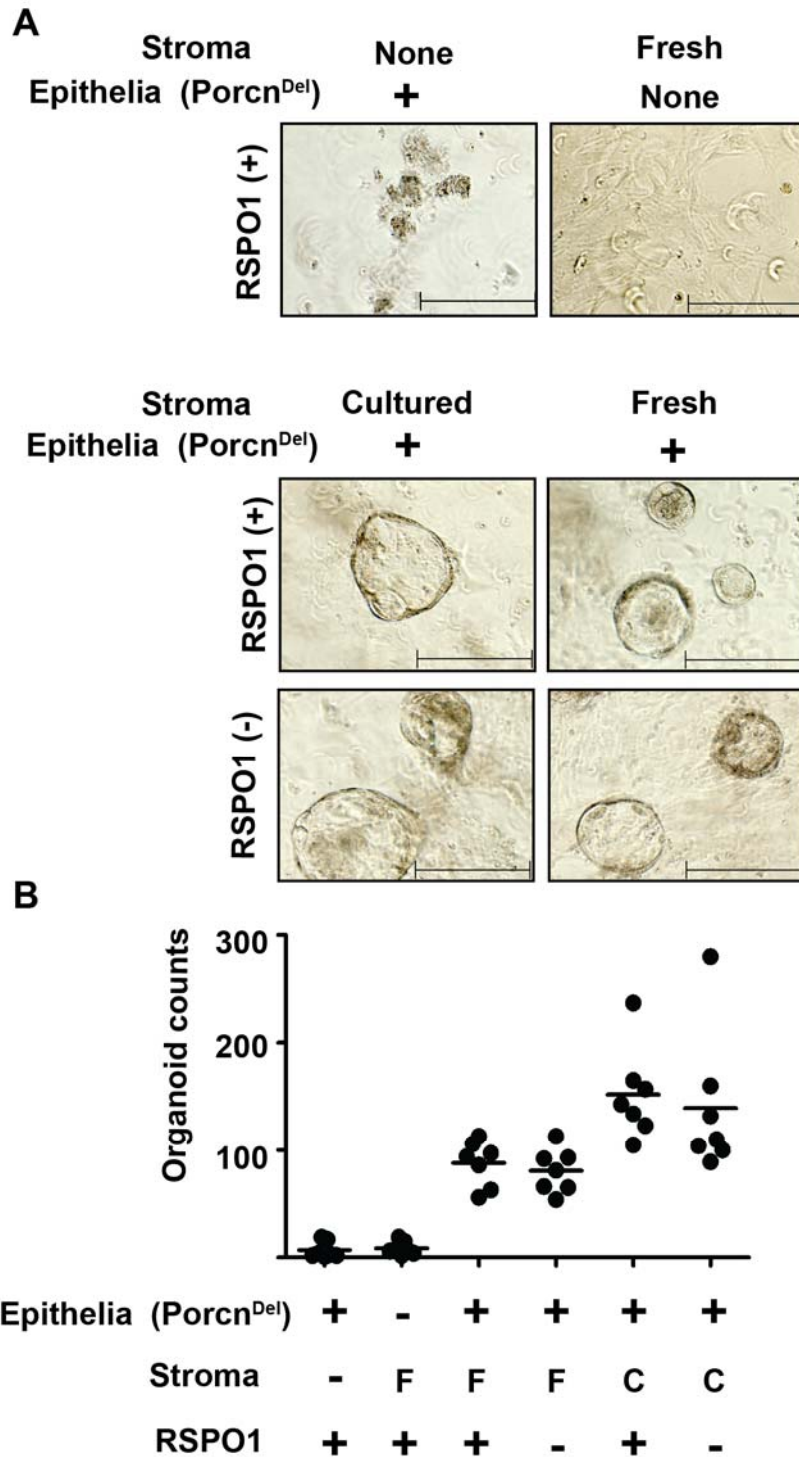


Figure 2.14 Stroma could support intestinal epithelia growth in absence of Epithelial Wnts *ex vivo*. **A)** *Villin-Cre/Porcn^{Del}* crypts (Epi (*Porcn^{Del}*)) do not form organoids (top left panel), unless supplemented with stromal cells (top right panel). Stromal and epithelial cells were prepared as described and cultured alone or in combination. Where indicated, 6000 crypts were combined with freshly prepared or cultured adherent stromal cells (5×10^4 and 2.5×10^4 , respectively) and then cultured for 5 days in the presence or absence

of supplemental RSPO1. The scale bar is 200 μm . **B)** Organoid counts from multiple wells from four mouse samples. All samples containing stromal cells had significantly higher organoid counts than group containing epithelial cells alone or stromal cells alone ($p < 0.005$, Mann Whitney test).

Wnts signal at short range, and myofibroblasts are anatomically adjacent to the epithelial crypt, making them a candidate source of stem cell supporting factors. We therefore prepared cultured adherent stromal cells highly enriched for myofibroblasts (vimentin positive (~100%), alpha-smooth muscle actin (α -SMA) positive (>50%), desmin positive (4%)) (Figure 2.15). Notably, these cells supported organoid formation better than unfractionated stromal cells even in the absence of supplemental RSPO1 (Figure 2.14 A and B). The myofibroblast-enriched population expresses multiple Wnts (Figure 2.16). In addition, these cells express abundant *Rspo3* (Figure 2.17 A and B). In contrast, the epithelium was a poor source of RSPOs, as assessed by both microarray and qPCR (Figure 2.17 A and B). Thus, the myofibroblast-enriched stromal fraction can provide both Wnts and R-Spondin and support intestinal stem cell proliferation.

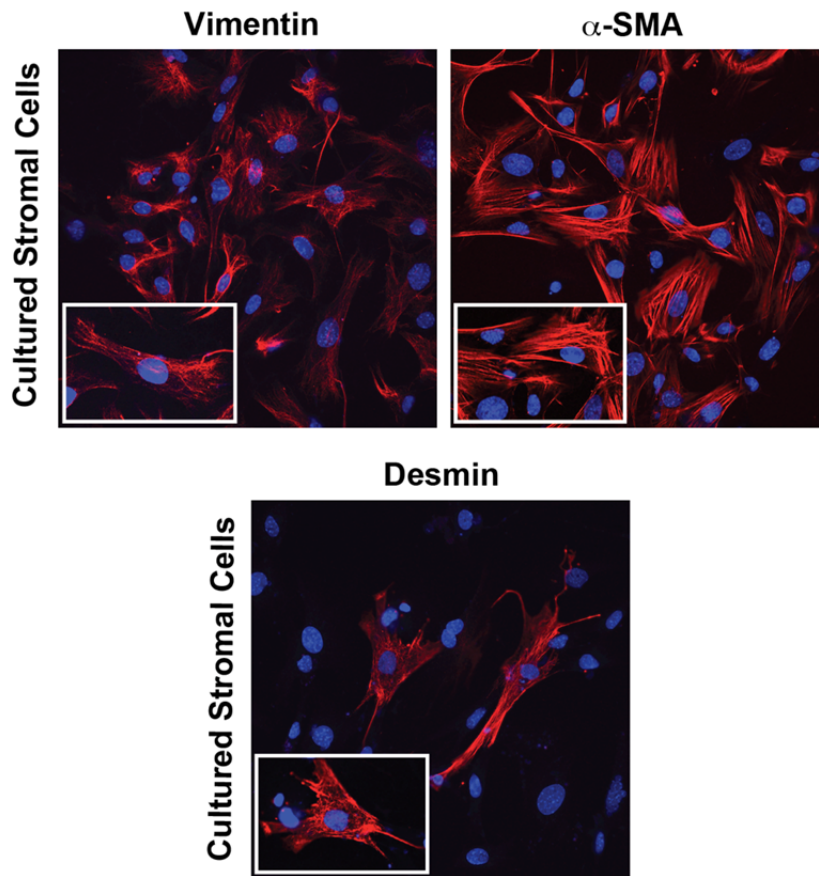


Figure 2.15 Cultured stroma is enriched in myofibroblasts. Stromal cells were cultured for 8 days and then assessed for vimentin, desmin or smooth muscle actin (α -SMA) by immunofluorescence confocal microscopy. Specific staining for indicated differentiation markers is shown in red. DAPI-labeled nuclei are shown in blue. Each picture is representative of three biological replicates.

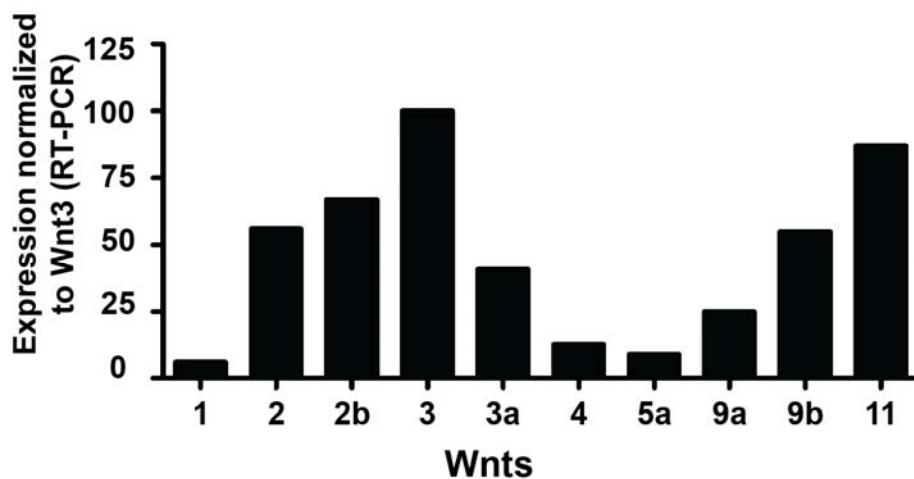


Figure 2.16 Cultured stroma expresses multiple Wnts. Cultured stroma was assessed for expression of different Wnts using RT-qPCR as indicated. Wnt RNA expression levels in adherent C57BL/6 stroma was assessed after one

week of culture. The selected Wnts had Ct values between 26 and 31. Expression levels were calculated as $2^{(-\Delta Ct)}$ and then graphed as a percentage of the Wnt3 expression level.

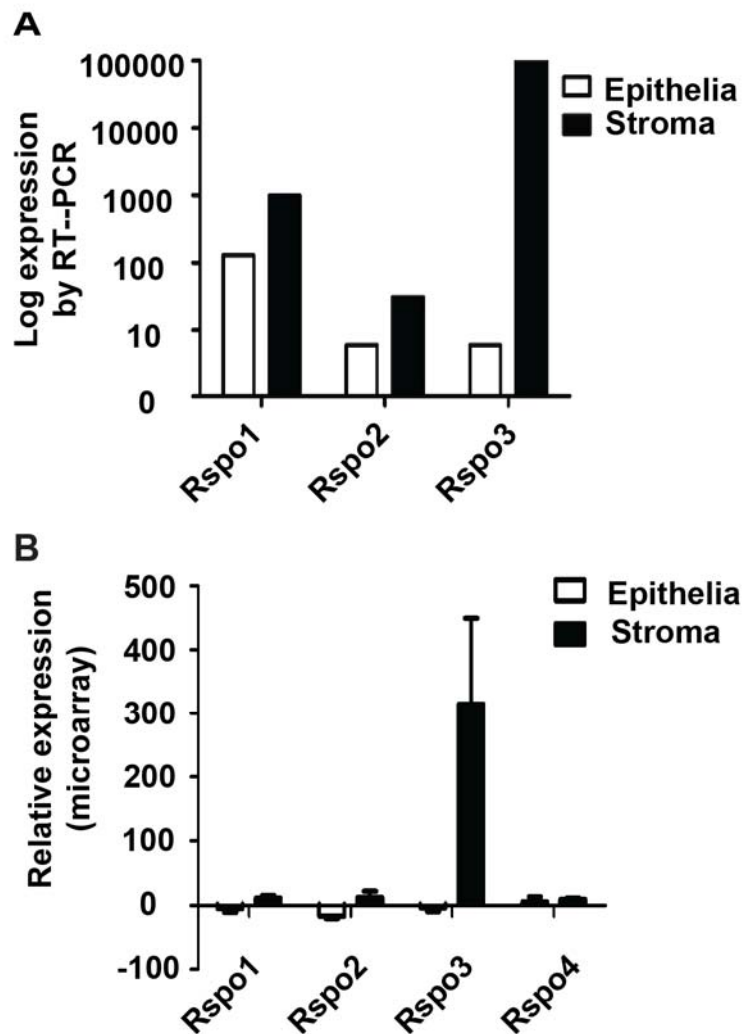


Figure 2.17 R-spondin 3 (*Rspo3*) is highly expressed in intestinal stroma. **A)** Epithelial crypts and cultured stromal cells were analyzed for *Rspo* expression using RT-qPCR. Relative expression of the various *Rspo* genes is calculated as $2^{(-\Delta Ct)}$ using *Pgk* expression level as a reference (n = 3). **B)** Expression levels of different RSPO isoforms were analyzed in Illumina arrays from epithelial and stromal-enriched fractions derived from *Villin-Cre/Porcⁿ^{WT}* and *Villin-Cre/Porcⁿ^{Del}* mice (n = 5 and 4 mice per group for epithelial and stromal samples, respectively).

To assess the contribution of immune and/or hematopoietic cells as a Wnt source for intestinal homeostasis, we crossed *Villin-Cre/Porcⁿ^{fllox}* mice to *Vav-Cre* mice to generate *Porcⁿ* knockout in intestinal epithelial cells as well as

hematopoietic and immune cells. These mice, which will be described in more detail elsewhere, were viable and their cultured adherent stroma also fully supported organoid formation from *Porcn*^{Del} epithelial cells (Figure 2.18). Taken together, the data are most consistent with stromal myofibroblasts as a significant source of Wnts and *Rspo3* both in vivo and in culture, although we cannot exclude the possibility that rare cell types form the niche.

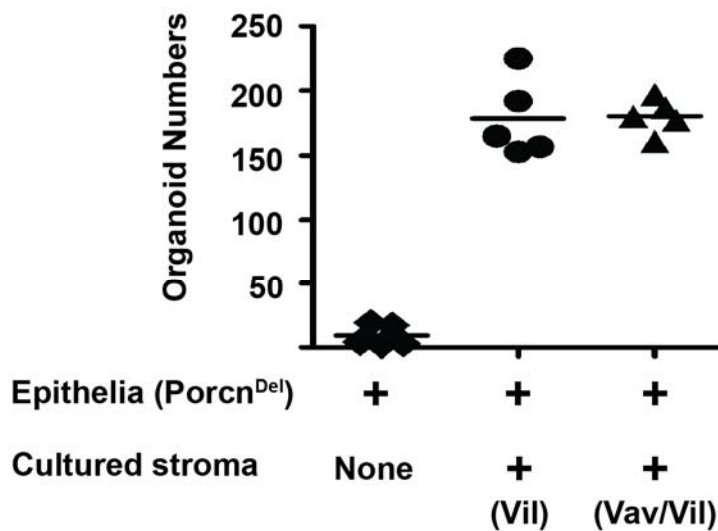


Figure 2.18 Cultured stromal cells from *Vav-cre//Villin-Cre/Porcn*^{Del} mice support organoids in *Porcn*^{Del} epithelial cell culture. *Porcn*^{Del} epithelial cells were cultured alone or in the presence of cultured stromal cells from *Villin-Cre/Porcn*^{Del} (*Vil*) or *Vav-Cre/Villin-Cre/Porcn*^{Del} (*Vav/Vil*) mice as indicated. Data represent four and two biological repeats for *Vil* and *Vav/Vil* stroma, respectively.

2.2.3 *Wls* knockout resembles the *Porcn* knockout

As loss of Wnt secretion in the intestinal epithelium was so strongly predicted to produce a phenotype, we asked if knockout of *Wls* phenocopied the *Porcn* knockout. *Wls* is a dedicated Wnt carrier that is required to transport palmitoleated Wnts to the cell membrane. *Wls*, like *Porcn*, is required for the activity of all human Wnts (Najdi et al., 2012). Similar to the *Porcn* deletion, *Villin-Cre/Wls*^{Del} pups were viable and had normal

development and growth. Histological appearance, proliferation, and β -catenin nuclear localization were identical in the intestines of one-year-old control (*Villin-Cre/Wls^{WT}*) and *Wls*-deleted (*Villin-Cre/Wls^{Del}*) mice (Figure 2.19). These data confirm that inhibition of epithelial Wnt secretion by targeting either *Porcn* or *Wls* does not significantly impact intestinal development and homeostasis.

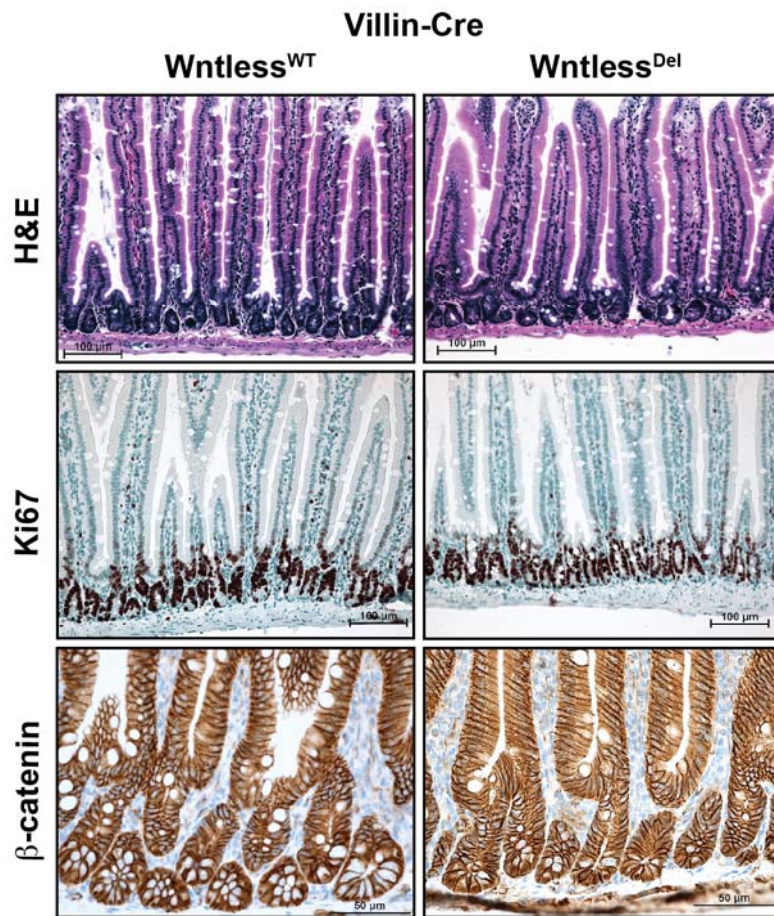


Figure 2.19 Normal intestinal structure in *Villin-Cre/Wls^{Del}* mice. Representative histology of different regions of the small intestine from *Villin-Cre/Wls^{WT}* (n = 3) and *Villin-Cre/Wls^{Del}* (n = 3) mice as indicated. Normal proliferation and intact Wnt/ β -catenin signaling were observed by Ki67 staining and nuclear β -catenin localization in bottom of crypts in *Villin-Cre/Wls^{WT}* and *Villin-Cre/Wls^{Del}* mice, respectively.

2.2.4 The role of stromal Wnts in vivo

Substantial data indicate that Wnt signaling is essential for intestinal stem cell regulation, but the targeted inhibition of Wnt secretion from the intestinal epithelium produced no phenotype. Either, against all expectations, Wnts are not required, or the intestinal stroma is sufficient as the niche providing the Wnts regulating stem cell proliferation. To differentiate between these possibilities, we took advantage of a recently validated pharmacological inhibitor of *Porcn*, C59. This drug is a readily absorbed, bioavailable inhibitor of *Porcn* with a sub-nanomolar IC50 that inhibits Wnt/ β -catenin signaling and blocks the growth of WNT1-dependent mammary tumors in mice (Proffitt et al., 2013). An added benefit of using a drug is the ability to titrate the dose to dissect intermediate phenotypes that are difficult to detect in gene deletion models. We reasoned that C59 should inhibit stromal as well as epithelial PORCN activity and, taken together with the results of epithelial *Porcn* knockout, be a good test of the role of stromal Wnt secretion.

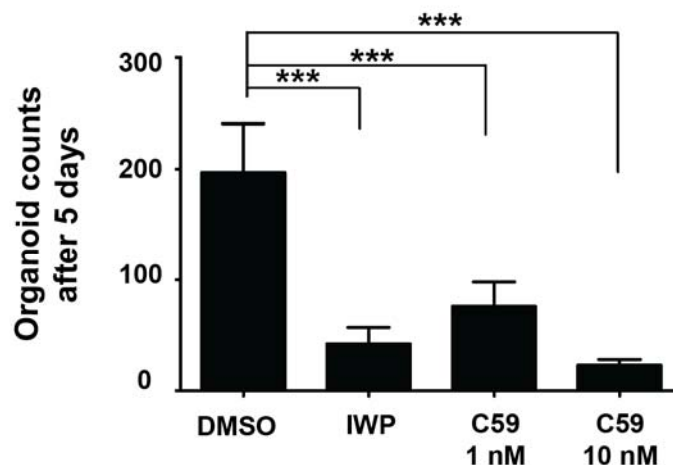


Figure 2.20 Pharmacologic Porcn inhibitors block organoid formation. Quantification of organoids formed from wildtype intestinal epithelium cultured in the presence or absence of C59 (1 or 10 nM) and IWP (1 μ M) for 5 days. Drugs were added to the culture medium on the first day. Error bars indicate standard deviation (***) $p < 0.001$, two-tailed t-test).

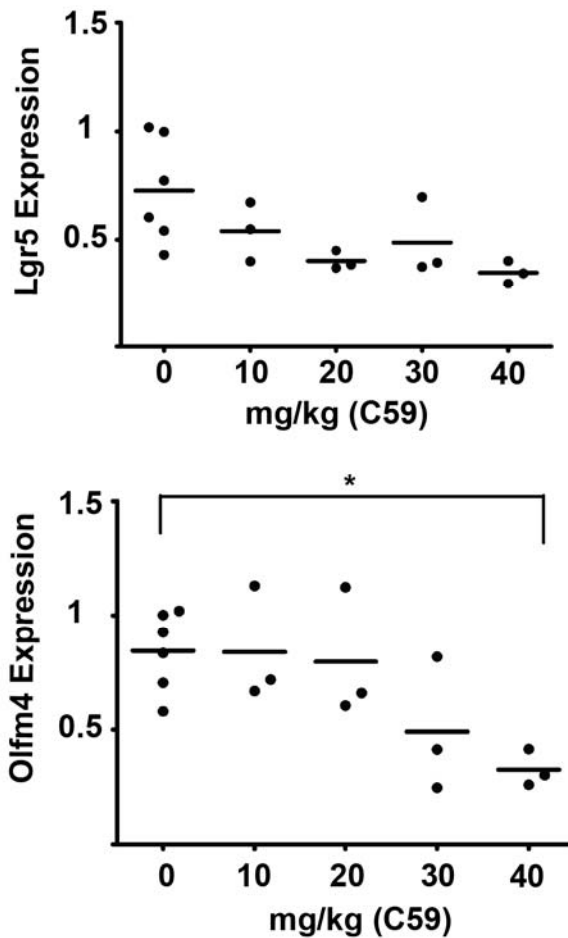


Figure 2.21 Expression of CBC markers were blocked after C59 treatment. To identify a C59 dose that inhibits Porcn function, increasing amounts of C59 were administered to mice for two days and then the expression level of *Lgr5* (upper panel) and *Olfm4* (stem cell marker, lower panel) were measured by RT-qPCR in jejunum samples. Expression levels were normalized to β -actin (* $p < 0.05$, two-tailed T-test).

We confirmed that C59 prevented the formation of intestinal organoids in culture, similar to the activity of IWP (Figure 2.20) (Sato et al., 2011). We previously reported that orally administered C59 at 5-10 mg/kg/day inhibited the growth of MMTV-Wnt1 mammary tumors without intestinal toxicity (Proffitt et al., 2013). To identify a C59 dose that inhibited Wnt/ β -catenin activity in the intestine, mice were administered various amounts of C59 daily for 2 days by gavage and their small intestines were harvested 20-24 hours

after the second dose. There was a dose-dependent reduction in the expression of the Wnt/ β -catenin target gene *Lgr5* and the crypt base columnar (CBC) cell marker *Olfm4* (Figure 2.21).

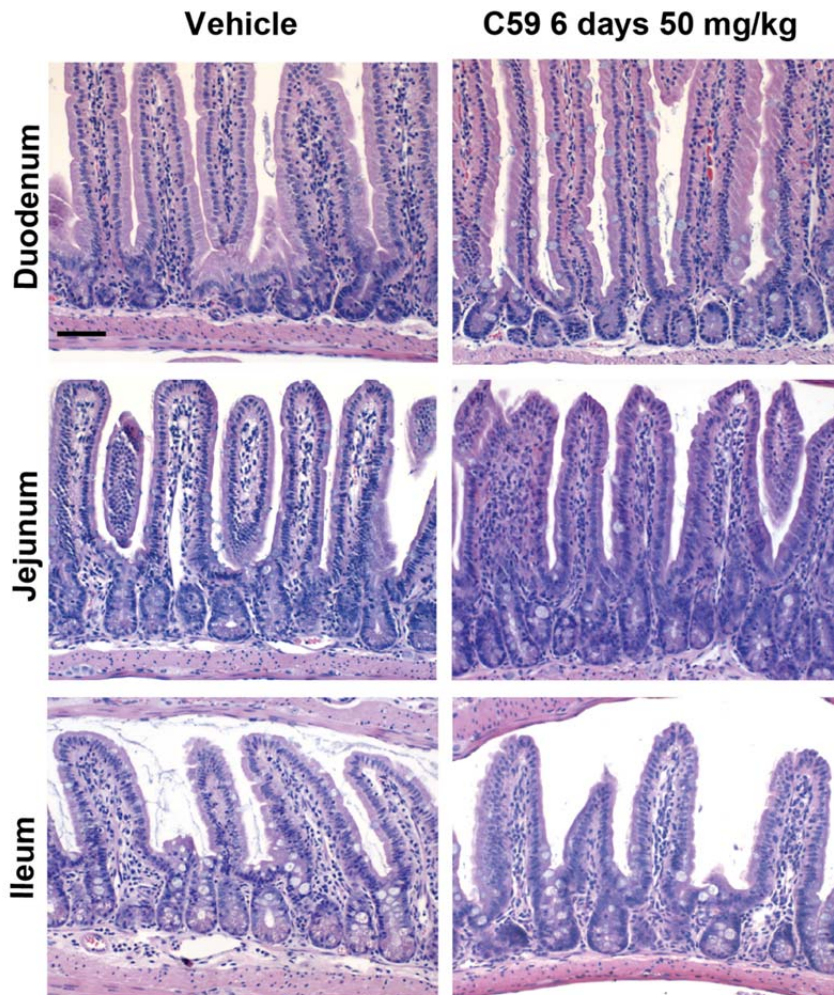


Figure 2.22 Moderate PORCN inhibition did not alter intestinal structure. Histology of different regions of small intestine following vehicle or C59 treatment (50 mg/kg/day) for 6 days (n = 5 in each group). The scale bar is 100 μ m.

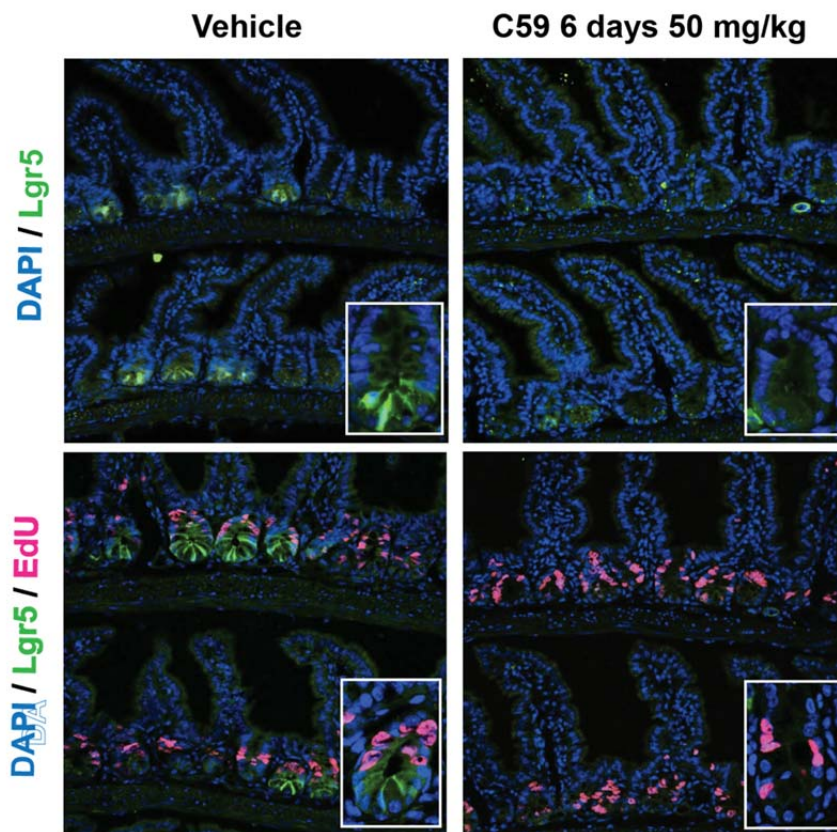


Figure 2.23 Suppression of Wnt/ β -catenin target genes including *Lgr5* did not affect short-term proliferation. *Lgr5-IRES-EGFP-CreER^{T2}* mice were treated with vehicle (n = 6) or C59 (50 mg/kg/day, for 6 days, n = 6). *Lgr5* expressing cells are labeled by EGFP. Nuclei of cells are labeled by DAPI. Proliferative cells were labeled with EdU given 2 hours prior to sacrifice (bottom panels). Insets show higher magnification of single crypt.

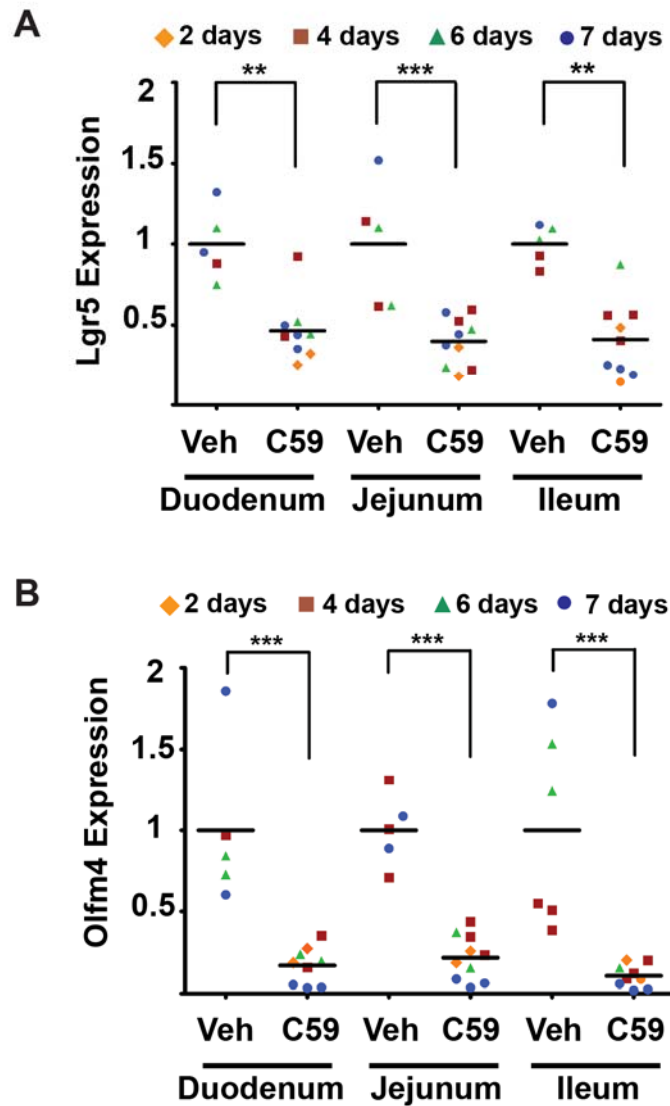


Figure 2.24 Systemic PORCN inhibition leads to decreased expression of intestinal stem cell markers. A and B) C59, 50 mg/kg/day, was administered for the indicated period and mice sacrificed 20-24 hours after the last dose. Expression levels of *Lgr5* and *Olfm4* were normalized to *Pgk* and β -*actin*. Mean values of respective vehicle-treated groups were set to 1 and compared to individual measurements within the same group ($p < 0.01$ and *** $p < 0.001$, Mann-Whitney test).**

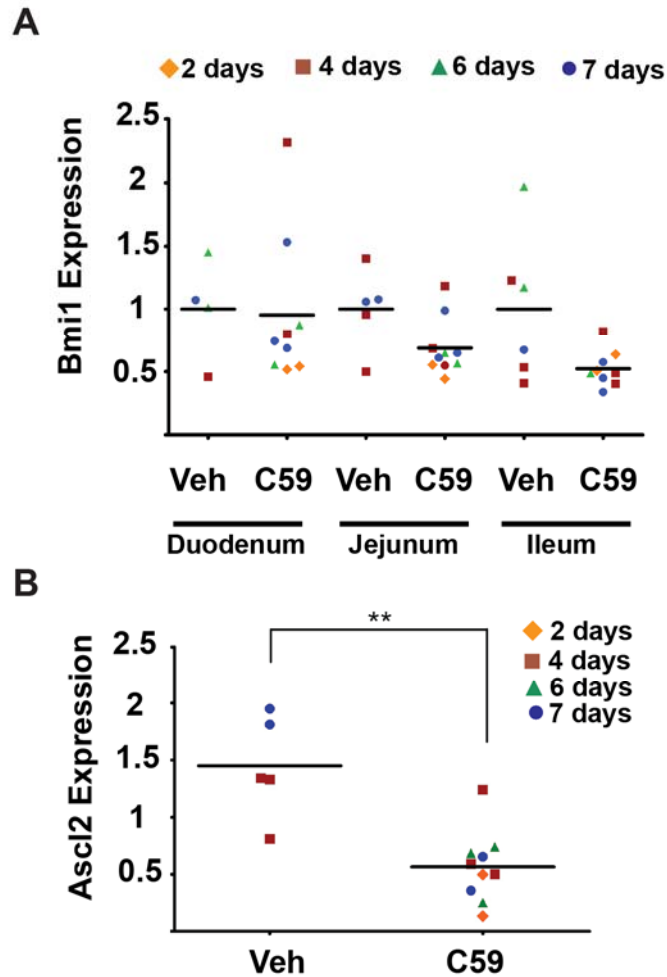


Figure 2.25 Systemic PORCN inhibition leads to decreased expression of intestinal stem cell markers. A) C59 administration did not alter expression of the *Bmi1* intestinal stem cell marker. **B)** Systemic Porcn inhibition by C59 treatment reduced *Ascl2* expression in jejunum samples. C59, 50 mg/kg/day by gavage, was given for the indicated time period. Quantitative RT-PCR was performed on intestinal samples after different duration of the treatment as indicated. Expression levels were normalized to *Pgk* and β -*actin*. Thereafter, mean values of respective vehicle groups were set to 1 and compared to individual measurements within the same group (** $p < 0.01$, Mann-Whitney test).

Mice receiving C59 50 mg/kg/day for 6 days maintained body weight and had normal intestinal structure and proliferation (Figure 2.22 and 2.23). This was despite the systemic C59 treatment causing a rapid, significant and persistent reduction in expression of the β -catenin target genes *Lgr5*, *Axin2* and *Ascl2*, as well as the crypt base columnar cell marker *Olfm4*, but not *Bmi1*

in the small intestine (Figure 2.24 A and B, 2.25 A and B). As an independent approach to confirm that *Lgr5* expression was reduced by C59 treatment, we treated *Lgr5-IRES-EGFP-CreERT2* mice that express EGFP from the endogenous *Lgr5* promoter with 50 mg/kg/day C59 for 6 days (Barker et al., 2007). We observed a marked decrease in EGFP expression in the C59 treated intestine (Figure 2.23). We confirmed that the C59-dependent decrease in Wnt/ β -catenin target gene expression was also seen in isolated intestinal crypts (Figure 2.26).

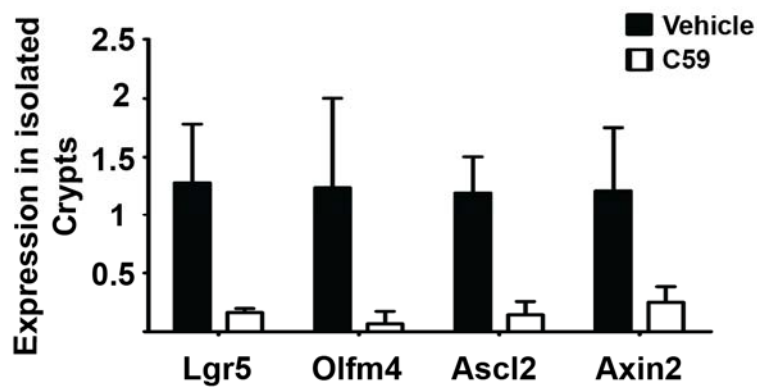


Figure 2.26 Wnt target genes and stem cell markers were down-regulated in crypts prepared from C59-treated mice. The mice were treated with 50 mg/kg/day of C59 for 6 days and crypts were isolated as described in materials and methods. Data represent three biological replicates. Error bars indicate standard deviation.

Wnt signaling can regulate Paneth cell differentiation, and we observed that the Paneth markers lysozyme and MMP7, but not cryptdin nor the goblet cell marker Muc2, were also decreased after one week of treatment (Figure 2.27 A and B). Thus, systemic, but not isolated epithelial inhibition of PORCN-dependent Wnt secretion suppresses Wnt/ β -catenin target gene expression in the intestine, consistent with an important role for stroma.

Unexpectedly, this suppression of Wnt/ β -catenin signaling was not essential for short term intestinal homeostasis.

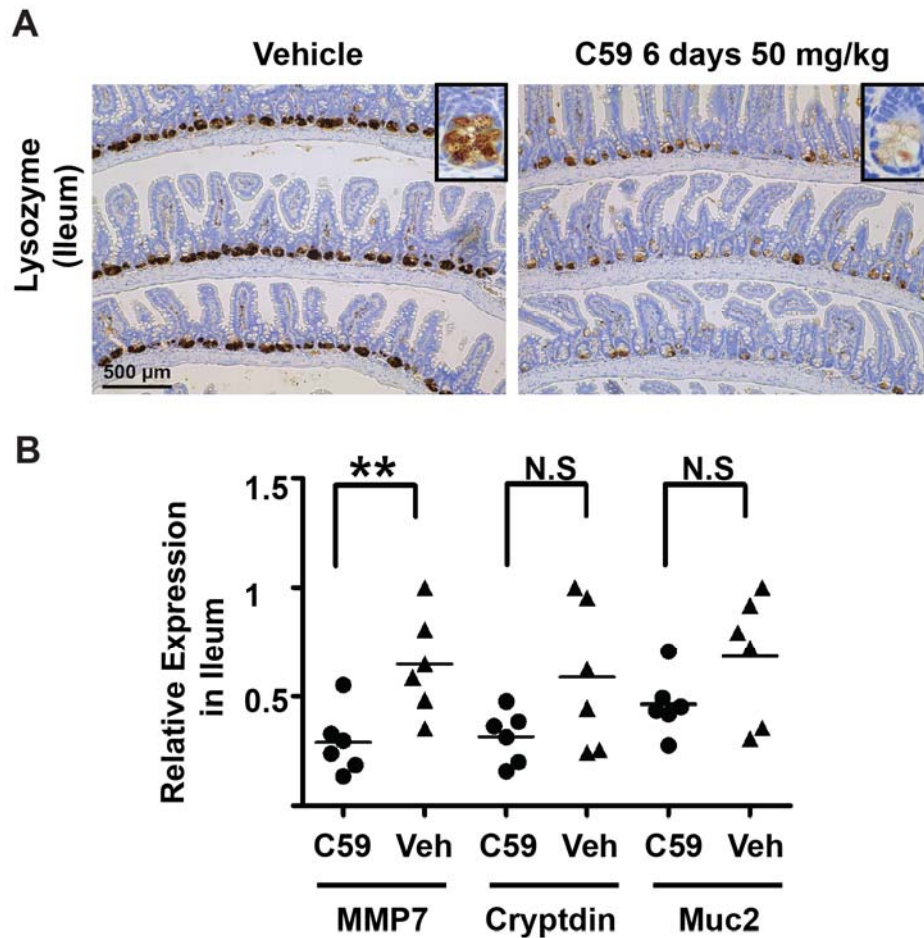


Figure 2.27 Inhibition of Paneth cell differentiation in C59 treated mice. **A)** Lysozyme expression as assessed by IHC is reduced in ileum of C59 treated mice (n = 3). Insets show Paneth cells in individual crypts. The scale bar indicates 500 μ m. **B)** Expression of Paneth and goblet cell markers. Mice were treated with 50 mg/kg of C59 for 6 days (n = 6 for each group). Ileum samples were collected and assessed for expression of indicated markers using RT-qPCR.

Lgr5-expressing CBC cells are relatively radiation resistant and proliferate after radiation injury (Hua et al., 2012). We reasoned that suppression of Wnt/ β -catenin signaling by PORCN inhibition might impair the response to injury. C57BL/6 mice were therefore treated with 50 mg/kg/day C59 for 6 days. 20 hours following the final dose of C59, mice were irradiated

with a single dose of 12 Gy, and sacrificed when they became ill 5 days later. In the C59 treated mice, the duodenum was dilated and the small intestine was markedly shortened (Figure 2.28). Histologic examination demonstrated a marked loss of crypts and villi throughout the small intestine in Wnt-suppressed compared to control mice (Figure 2.29). Proliferation of the epithelial layer was assessed by EdU incorporation 5 days after radiation. As expected, increased proliferation was observed in the epithelium of the control mice due to tissue regeneration. However, the C59 treated mice showed a marked reduction in EdU incorporation in the small intestine (Figure 2.30). Thus, intermediate inhibition of Wnt/ β -catenin signaling by C59 significantly reduced *Lgr5* expression in the CBC cells and impaired recovery from radiation injury. This is consistent with a recently proposed role for *Lgr5*-expressing cells in the response to radiation damage (Hua et al., 2012; Metcalfe et al., 2014).

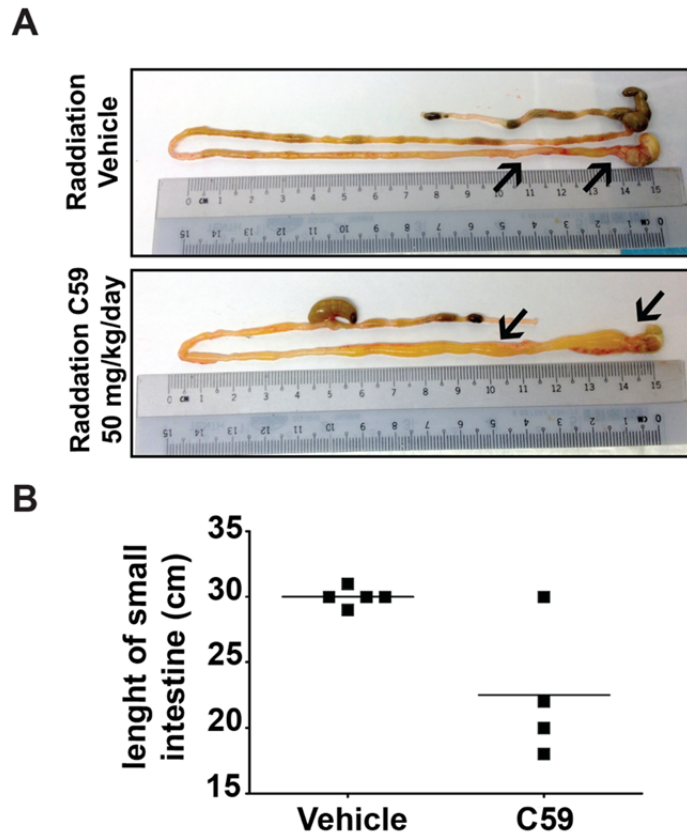


Figure 2.28 Gross changes in length and diameter of small intestine after irradiation in C59 pretreated mice. A) Intestinal length of C59 pretreated mice after irradiation. C57BL/6 mice were pretreated with vehicle or 50 mg/kg/day of C59 for 6 days and irradiated 20 hours after the last dose. The length of small intestine and width of duodenum (black arrows) were measured 5 days after irradiation (n = 5 and 4 for Vehicle and C59 groups, respectively. **B)** Intestinal length is plotted.

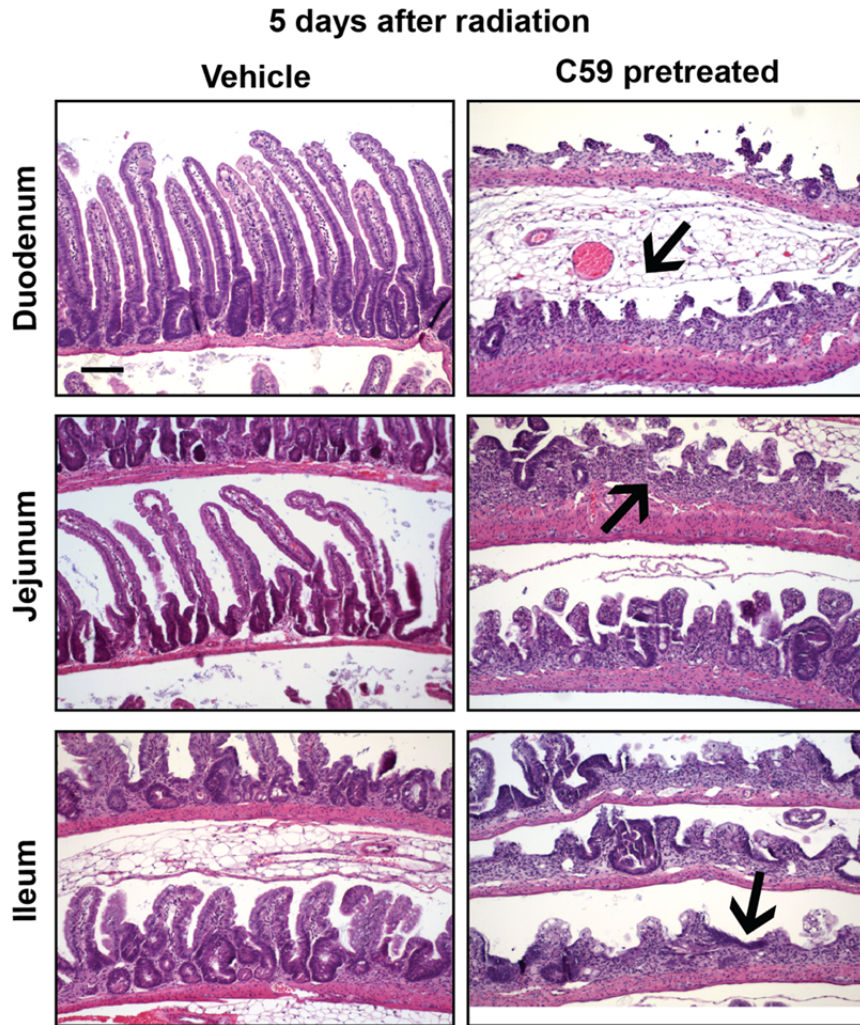


Figure 2.29 Stromal Wnts support a cell population required for epithelial regeneration in response to radiation-induced injury. *Lgr5* and *Olfm4* were suppressed by pretreatment of C57BL/6 mice with 50 mg/kg/day of C59 for 6 days followed by irradiation (12 Gy) 20 hours after the last dose. Architecture of the small intestine was analyzed 5 days after irradiation (n = 5 for each group). Note the markedly impaired crypt regeneration (indicated by arrows) in the C59-treated group (right panels). The scale bar is 200 μ m.

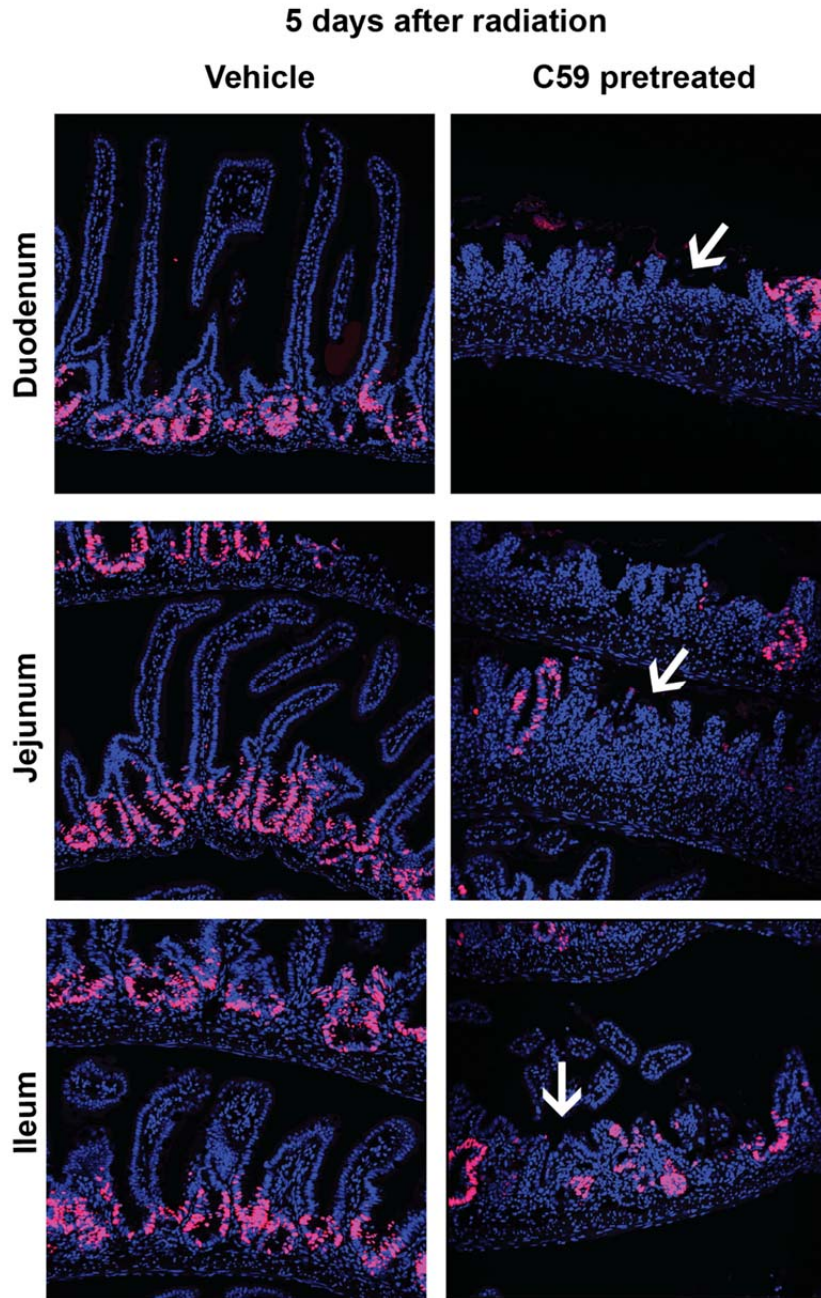


Figure 2.30 Proliferation was decreased in intestine of C59 pretreated mice. Proliferation was assessed by EdU incorporation assay 5 days after radiation damage. While proliferation was high in the epithelium of the controls (left panels), the response in C59 treated mice (right panels) was dramatically compromised. Nuclei of proliferative cells were labeled with EdU (red), and nuclei of all cells were labeled by DAPI (blue).

We tested if epithelial Wnts are required for recovery from radiation injury. *Villin-Cre/Porcⁿ^{WT}* and *Porcⁿ^{Del}* mice were treated with the same

radiation protocol as above. Three out of five wildtype, and five of five *Villin-Cre/Porcⁿ^{Del}* mice survived 8 days after radiation. All the mice were ill and had significant weight loss. Histologic examination of the intestines of surviving mice showed successful ongoing epithelial regeneration regardless of genotype, with no detectable differences between wildtype and knockout mice (Figure 2.31). Hence, epithelial Wnt production is not required for intestinal regeneration after radiation injury. The radiation sensitivity seen in C59-treated, but not *Porcn* knockout, mice is consistent with functionally important Wnts coming from the stromal niche.

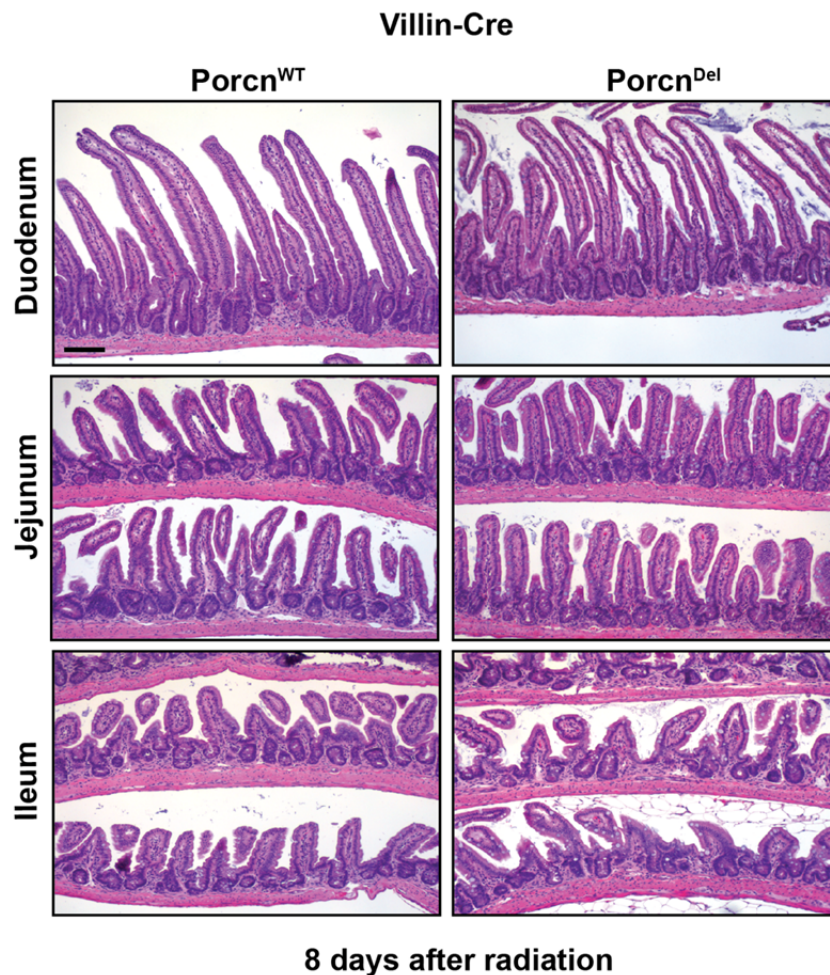


Figure 2.31 Epithelial Wnt secretion is not required for epithelial regeneration after radiation injury. Architecture of different parts of small intestine was analyzed 8 days after irradiation (n = 3 and 5 for *Villin-Cre/Porcⁿ^{WT}* and *Porcn^{Del}*, respectively). The scale bar is 200 μ m.

2.2.5 High-dose PORCN inhibition impaired intestinal homeostasis.

C59 was given once daily at 50 mg/kg significantly reduced expression of the CBC cell markers *Lgr5*, *Ascl2*, and *Olfm4*, decreased expression of Paneth cell markers and prevented an effective response to radiation injury. However, the persistence of EdU incorporation and nuclear β -catenin (Figure 2.32) in these mice suggested residual Wnt activity might be sufficient to maintain a stem cell population, as has been suggested for the related compound LGK974 (Liu et al., 2013). To test this, we increased the C59 dose to twice daily to increase trough drug levels. Mice treated with 50 mg/kg per dose, twice daily, were moribund within 6 days. At this dose intensity, intestinal crypts began to disappear in the duodenum and jejunum on the second and fourth day of treatment, respectively (Figure 2.33).

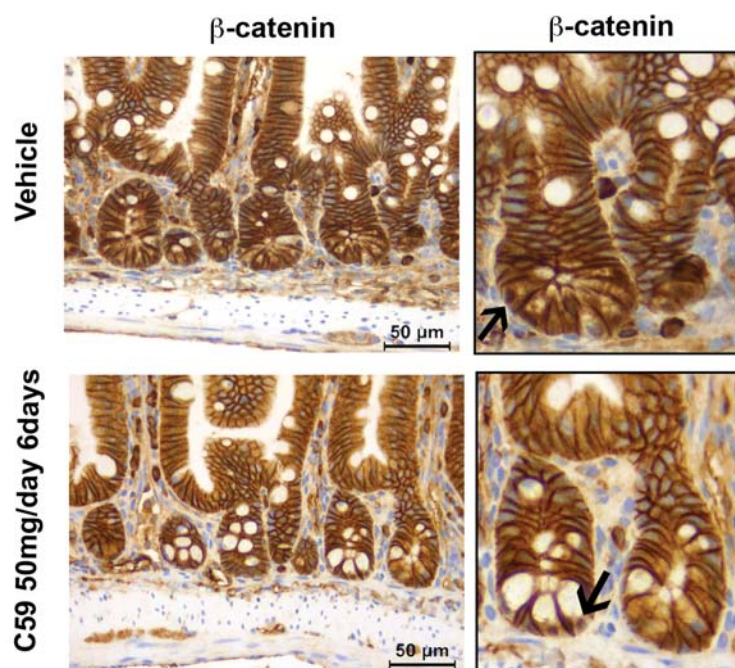


Figure 2.32 Normal β -catenin in C59 treated mice. Normal β -catenin in ileum of vehicle (top panels) and C59 treated mice (bottom panels) with 50 mg/kg/day after 6 days (right panels). Nuclear localization of β -catenin (indicated by arrows) is visible in crypt cells of both treatment groups. The scale bar equals 50 μ m.

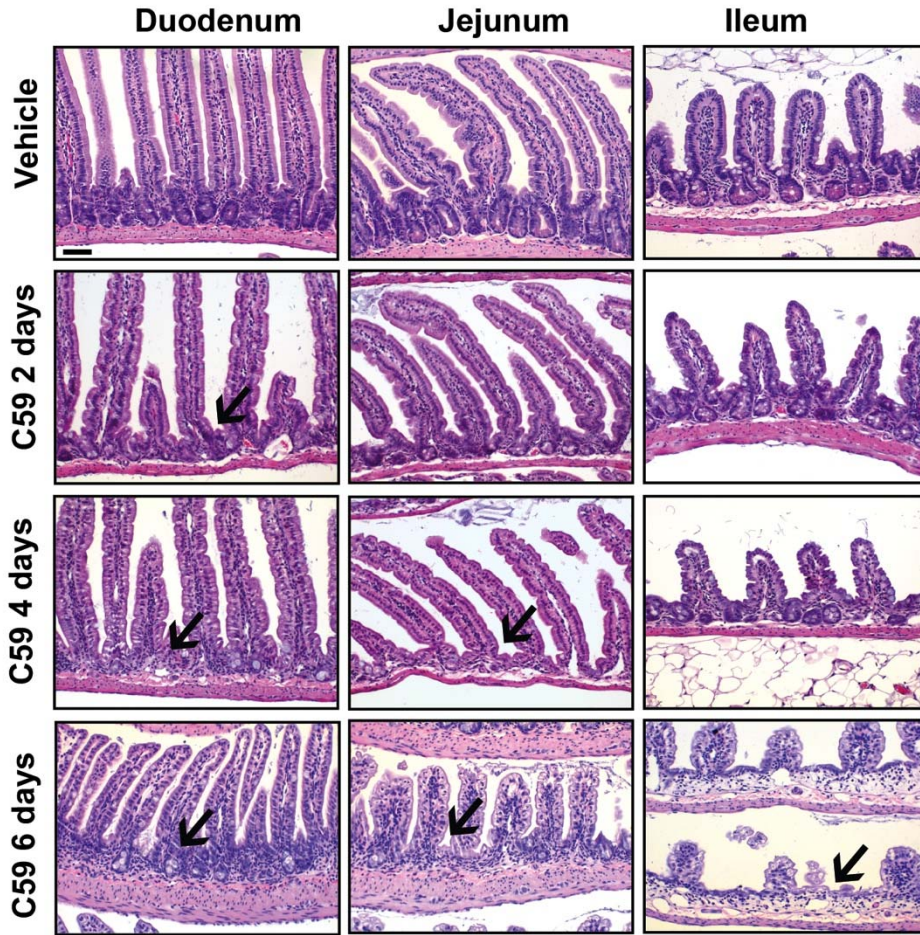


Figure 2.33 Systemic inhibition of Wnt signaling leads to impaired intestinal homeostasis. Twice daily oral administration of 50 mg/kg/dose (100 mg/kg/day) C59 leads to inhibition of gut proliferation as shown by absence of crypts and shrinkage of villi. Histology of the small intestine following treatment for 2, 4, and 6 days is shown. Data represent results derived from at least 3 mice per group.

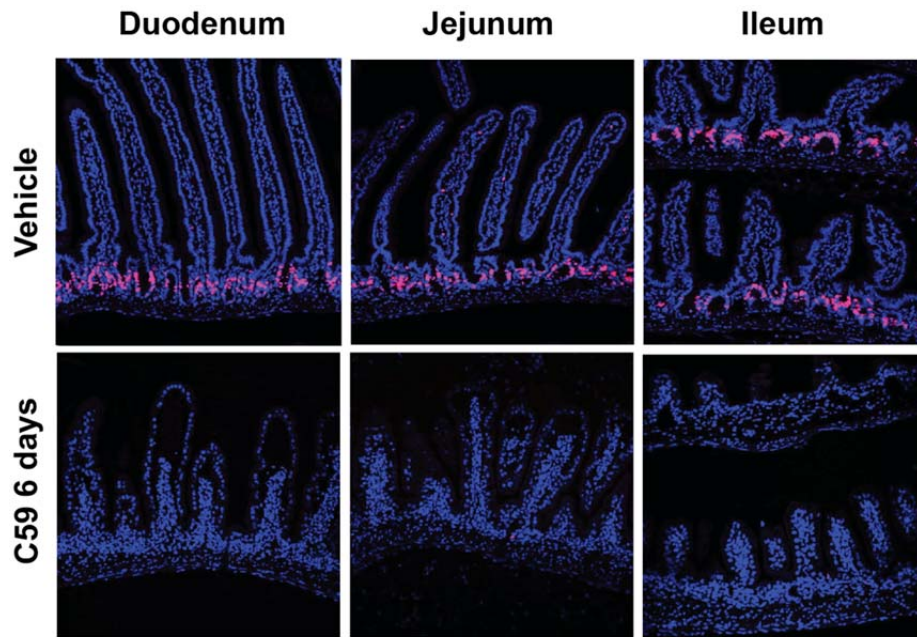


Figure 2.34 High dose C59 treatment for 6 days blocks proliferation in all regions of the small intestine. Nuclei of proliferative cells were labeled with EdU (red), nuclei of all cells were labeled by DAPI (blue). Note the lack of EdU staining in the C59-treated group, bottom panels.

After 6 days of high dose treatment, there was a global reduction in proliferation as indicated by loss of all crypts in the small intestine and absence of EdU incorporation (Figure 2.34). This toxicity is unlikely to be non-specific, since there was a decrease in proliferation rather than an increase in apoptosis (Figure 2.34 and 2.35). These dramatic findings resemble the proliferation defect observed after total loss of Wnt/ β -catenin signaling in the epithelium in mice with conditionally deleted β -catenin or *TCF4* alleles (Fevr et al., 2007; van Es et al., 2012a). We conclude that full inhibition of PORCN activity in both epithelium and stroma of the intestine blocks proliferation and intestinal homeostasis.

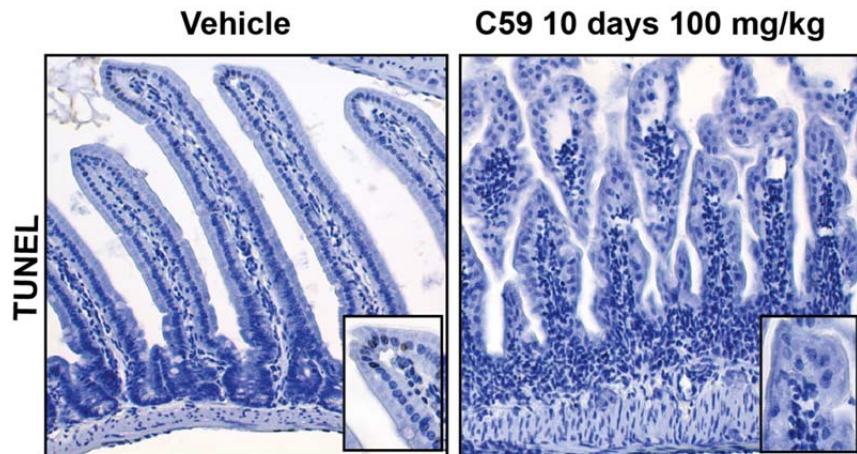


Figure 2.35 C59 treatment did not lead to increased apoptosis. Mice were treated with C59 at 100 mg/kg/day for 10 days to ensure aberrant gut homeostasis. Gut samples were processed for TUNEL staining.

2.3 Discussion

Our study indicates that stromal Wnts are sufficient to maintain mouse small intestinal homeostasis. Tissue-specific knockout of *Porcn* and *Wls* shows that epithelial Wnt production is dispensable for normal intestinal stem cell development, self-renewal, proliferation, and the response to radiation-induced injury. Conversely, using a small molecule inhibitor of Wnt production we find that varying levels of systemic PORCN inhibition produce distinct phenotypes in the gut. Moderate global inhibition of Wnt secretion markedly reduced *Lgr5* expression and impaired intestinal homeostasis after radiation injury, while more complete inhibition of Wnt secretion immediately affected stem cell function, similar to results seen after genetic knockout of key Wnt/ β -catenin pathway components. The ability to moderately inhibit PORCN function and not impair short-term intestinal homeostasis suggests that drugs inhibiting PORCN will have a therapeutic index allowing clinical use.

Purified epithelial stem cells can form organoids and expand *ex vivo* in the presence of Wnt3-producing Paneth cells and exogenous RSPO1. Here, we found epithelial Wnts supplemented with recombinant RSPO1 can be replaced by an intestinal myofibroblast-enriched stromal fraction that endogenously produces Wnts and RSPO3. Taken together, the data is consistent with the hypothesis that stromal cells can form a Wnt and RSPO3 producing niche for intestinal epithelial stem cells in the absence of epithelial Wnt production.

Is there a single essential source of Wnts in the small intestine? We found that both epithelial and hematopoietic *Porcn* function is dispensable for intestinal homeostasis. Our data on stroma as a source of both Wnts and RSPO3 *ex vivo* are consistent with myofibroblasts in close proximity to the epithelial stem cells forming the Wnt-producing niche. However, this stands in contrast to a paper published while this work was in revision (San Roman et al., 2014). They reported that inducible short-term double deletion of *Porcn* in both intestinal epithelium (in *villin-creER^{T2}/Porcn^{fllox}* mice) and sub-epithelial myofibroblasts (in *Myh11-CreER^{T2}/Porcn^{fllox}* mice) did not alter intestinal homeostasis. However, that study did not determine the efficiency of *Porcn* deletion in the myofibroblasts and whether the *Myh11-CreER^{T2}* driven excision in fact abrogated the organoid-supporting ability of the stroma.

Several publications have suggested that there are redundant sources of Wnts supporting the intestine (Farin et al., 2012; San Roman et al., 2014). Indeed, the intestinal stroma contains multiple cell types capable of making Wnts, including endothelial cells, macrophages, neurons, fibroblasts, and myofibroblasts. Wnts produced in combinations of these cells could produce a cocktail of redundant Wnt ligands maintaining intestinal homeostasis *in vivo*.

Alternatively, our data are also consistent with the niche being a specific myofibroblast population adjacent to the crypts that produces both Wnts and RSPO3.

Our study complemented the genetic knockout of PORCN with pharmacologic inhibition. One unexpected finding was the broad therapeutic range for pharmacologic PORCN inhibition. We previously reported that as little as 5 mg/kg/day of C59 blocked proliferation of a Wnt1-dependent mammary tumor, yet here, also in C57BL/6 mice, a twenty-fold higher dose was required for inhibition of intestinal stem cell proliferation. Our data suggest that even small amounts of Wnt secretion can maintain an intestinal stem cell niche in the absence of external stress. This robust network of stem cell regulators suggests that inhibition of Wnt production may be effective for diseases with pathological Wnt elevation at doses that do not perturb normal stem cell niches.

We noted that *Lgr5/Ascl2/Olfm4* expression could be reduced by C59 without immediate effect on overall intestinal architecture, similar to genetic knockout of Lgr5 cells with Diphtheria toxin (Metcalf et al., 2014). However, several of the mice treated at the intermediate dose of C59 become ill after 18 days. Examination of the small intestine revealed patchy loss of proliferation and lack of crypts in the proximal small intestine (Figure 2.36 A and B). This may be due to differential sensitivity of two distinct populations of stem cells in small intestine. Buczacki et al. recently demonstrated that label retaining cells (LRCs) in the +4 position of the crypt are secretory precursors of Lgr5 cells and serve as a reserve pool of stem cells after intestinal damage (Buczacki et al., 2013). We speculate that long-lived LRCs are relatively

insensitive to C59 mediated *Porcn* inhibition and sustain intestinal homeostasis in absence of Lgr5 stem cells. Impaired crypt homeostasis would slowly occur as the LRCs were depleted at the intermediate dose, or rapidly if they are completely deprived of Wnts at the high dose of C59.

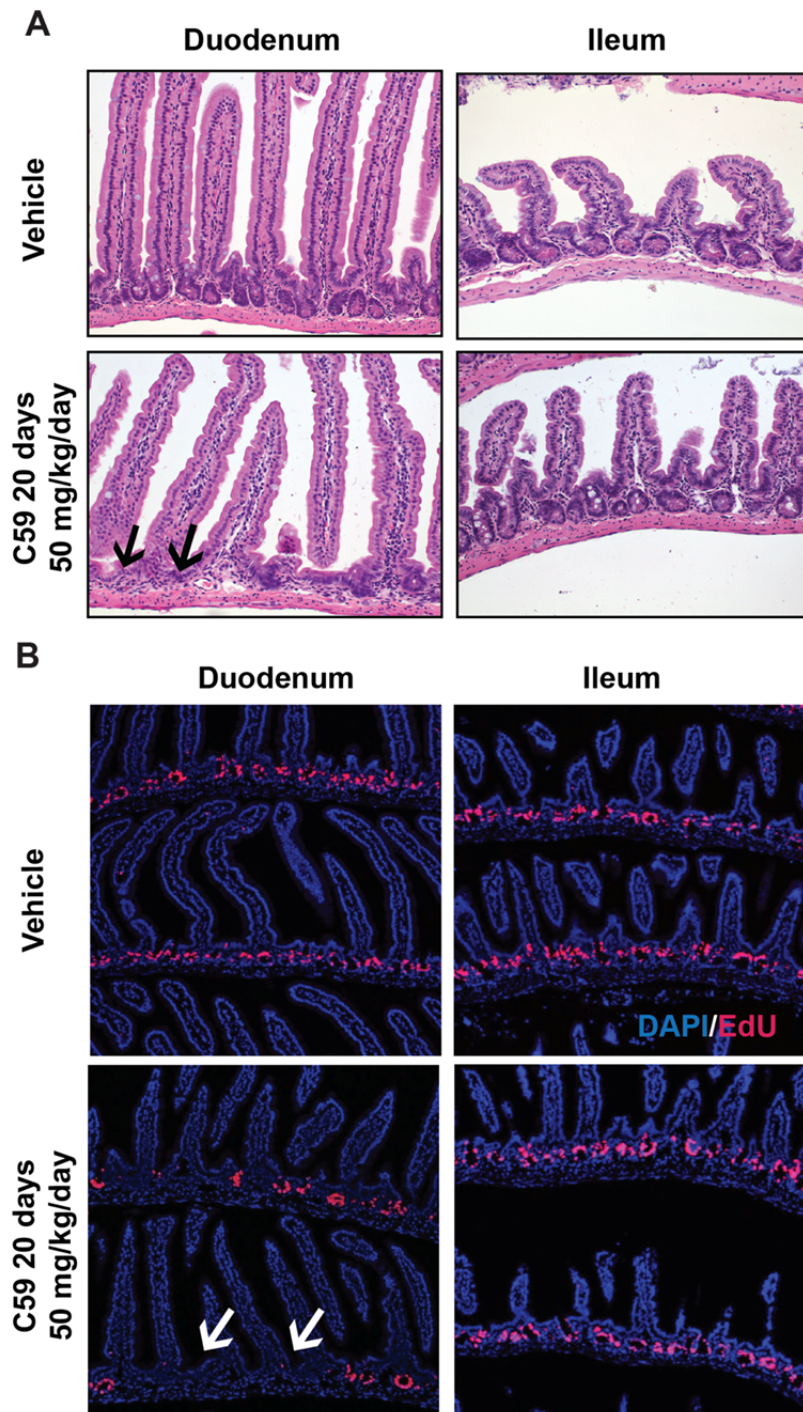


Figure 2.36 Long term treatment with intermediate dose C59 affects gut homeostasis. A) Mice were treated with 50 mg/kg/day for 20 days and

intestines were analyzed. Note the patchy absence of crypts in the duodenum (indicated by arrows), but not in ileum of C59-treated mice. This phenotype was observed in two out of four mice underwent treatment. **B)** Long term treatment with intermediate dose of C59 impacted proliferation. Mice were treated as described above and analyzed for EdU incorporation as described in Materials and Methods. Arrows indicate the patchy lack of proliferation in Duodenum, but not in ileum of C59-treated mice. This phenotype was observed in two out of four mice underwent treatment.

The role of *Lgr5*⁺ and Paneth cells in the response to radiation damage is of great recent interest (Buczacki et al., 2013; Hua et al., 2012; Metcalfe et al., 2014; Roth et al., 2012). We addressed the role of Wnt production in the radiation response and found that global pharmacologic, but not epithelial-specific, inhibition of PORCN caused markedly increased sensitivity to radiation stress in the intestine. While PORCN inhibition both reduced *Lgr5* expression and modified Paneth cell differentiation, Paneth cell depletion reportedly does not affect recovery from radiation (Metcalfe et al., 2014). Our data are therefore most consistent with the model that PORCN-dependent *Lgr5*⁺ cells are required for recovery from radiation, and suggest the possibility of synergistic toxicity in clinical settings.

In conclusion, taking advantage of the essential roles of *Porcn* and *Wls* in Wnt secretion, we have demonstrated that epithelial Wnts are not vital for intestinal homeostasis or recovery from radiation injury, while confirming that they are required for *ex vivo* cultures. In addition, we provide strong evidence that stromal Wnts play a critical role in the maintenance of small intestine homeostasis *in vivo*.

2.4 Materials and methods

2.4.1 Mouse strains and drug administration

Porcn^{fllox} mice (Biechele et al., 2013) were backcrossed to C57BL/6 mice at least for 6 generations. *Porcn*^{fllox} mice were crossed with BL/6 *Villin-Cre* mice. Age and gender-matched mice were used as controls for all experiments. *Lgr5-IRES-CreER^{T2}-EGFP* mice were obtained from Jackson Laboratories (Barker et al., 2007). *Wls*^{fllox} mice, studied at the Van Andel Research Institute, were from Richard Lang (Carpenter et al., 2010). All mouse procedures were approved by the respective Institutional Care and Use Committees (IACUC). Genotyping and PCR are described in Supplemental Methods. PORCN inhibitor C59 was suspended in a mixture of 0.5% methylcellulose and 0.1% Tween 80 by sonication for 30 minutes and then administered by gavage as described (Proffitt et al., 2013).

2.4.2 Genotyping and quantitative RT-PCR

Porcn genotyping was performed as described (Biechele et al., 2013). The *Villin-Cre* mouse has been previously described (Madison et al., 2002). RNA extraction and cDNA synthesis were done using RNEasy mini (Qiagen, cat: 74106) and i-script RT (Bio- Rad, Cat#1708891) kits following the manufacturer's instructions. Real-time PCR used the SsoFast EvaGreen PCR assay (Bio-Rad, Cat#1725205) on Bio-Rad CFX96 real-time cycling machine. Each PCR reaction was run for 40 cycles and analyzed using Bio-Rad CFX manager software version 2.1. qPCR primers are listed in Table 2.1.

Table 2.1 qRT-PCR primer sequences

q-PCR primers	5' to 3' primer sequence
Axin2 F	CTCCCCACCTTGAATGAAGA
Axin2 R	TGGCTGGTGCAAAGACATAG
Bmi1 F	AATTAGTCCCAGGGCTTTTCAA
Bmi1 R	TCTTCTCCTCATCTGCAACTTCTC
Porcn F (exon 2-3 junction)	GGAGGCTGGGGTTACCGTCTT
Porcn R (exon 4-5 junction)	GCCCCTCGCATCTTGTGCCA
PGK F	TCAAAAGCGCACGTCTGCCG
PGK R	AAGTCCACCCTCATCACGACCC
Ascl2 F1	GCCTACTCGTCGGAGGAA
ASCL2 R1	CCAACCTGGAAAAGTCAAGCA
Lgr5 F	GGGAGCGTTCACGGGCCTTC
Lgr5 R	GGTTGGCATCTAGGCGCAGGG
Olfm4 F	AGTGACCTTGTGCCTGCC
Olfm4 R	CACGCCACCATGACTACA
R-spondin 1 F	TGTGAAATGAGCGAGTGGTCC
R-spondin 1 R	TCTCCCAGATGCTCCAGTTCT
R-spondin 2 F	TTGCATAGAGGCCGCTGCTTT
R-spondin 2 R	CTGGTCAGAGGATCAGGAATG
R-spondin 3 F	GTACACTGTGAGGCCAGTGAA
R-spondin 3 R	ATGGCTAGAACACCTGTCCTG
Wnt1F	GTGGCCGATGGTGGGGCATC
Wnt1 R	AGTTCAGCGGCGGTTTCGG
Wnt2F	TCAAGAGAAACCCCCTTTCC
Wnt2 R	GGCTATGACCCTCCTCCTCT
Wnt2b F	ACGTGTTGATAGGGGATGGA
Wnt2b R	GGTTCCTTCCTGTTGCATA
Wnt3 F	TCCTCCTCGGCGCTGCTTCT
Wnt3 R	CCAGGGCCAGGGACCACCAA
Wnt3a F	TCAGGGGTGATACCAAGACC
Wnt3a R	GGGACTGCAAATCTTCCTCA
Wnt4 F	TGGACTCCCTCCCTGTCTTTGGGA
Wnt4 R	TCCTGACCACTGGAAGCCCTGTG
Wnt5a F	GTCCCTGGAAGCAGACGTTTCGG
Wnt5a R	GCGGCTCACGCCTCCTGATT
Wnt5b F	CTCTCCGCCTCACAAAAGTC
Wnt5b R	TCCAGCAAAATCCAGTCCTC
Wnt9a F	GGCCGCCTACTTCGGGCTAA
Wnt9a R	CATGCGTCAGGCCGGCAGAA
Wnt10a F	GCTCCTGAGAGAGGTGGTTG
Wnt10a R	GGGGAAGGGAAGAAGAGATG
Wnt11 F	CGGTTCCGGGAGAGAGCGGA
Wnt11R	CAGTGCCAGCCACTTGATGCCA

2.4.3 Crypt isolation and culture

Intestine was harvested, cut longitudinally, washed, and macerated in pieces not exceeding 2 millimeter in size. Fragments were incubated in ice-cold PBS containing 2 mM EDTA for 40 minutes with gentle shaking every 10 minutes. The solution was pipetted up and down for 40 times followed by 3 minutes of gravity sedimentation. Supernatant fractions containing released cells were collected after each sedimentation step. This procedure was repeated 3 times resulting in 3 collected fractions. After the first round, intestinal pellets were washed with PBS for 3 times. Fraction 3 was used for subsequent crypt isolation. Crypts were enriched by centrifugation at 200 x g for 2 minutes and counted using phase contrast microscope. As judged by microscopy, this routinely yielded >90% pure crypts. All the procedures were performed at 4°C. Crypt culture was performed in 48-well plates using 6000 crypts per well closely following conditions described by Sato et. al, (Sato et al., 2009).

2.4.4 Intestinal epithelium cell isolation

Intestines were harvested and flushed with cold PBS, cut longitudinal and washed three times with cold PBS containing 1 mM DTT. Intestines were then incubated in 30 ml buffer containing 96 mM NaCl, 27 mM sodium citrate, 1.5 mM KCl, 8 mM KH₂PO₄, 5.6 mM Na₂HPO₄ at PH 7.4 for 15 minutes on ice. Thereafter, intestines were transferred into a new tube containing 15 ml solution B (1.5 mM EDTA, 0.5 mM DTT, 1 mg/ml BSA in PBS) and shaken at 200 rpm for 10 minutes at 10 °C. This fraction contained villus cells. Next, the intestine was transferred to a second tube of 15 ml solution B and shaken

for 30 minutes. Finally, samples were transferred to a third tube and were shaken for 60 minutes. This supernatant containing crypt cells were harvested for genomic PCR and RNA isolation for microarray analysis. A 2 mm piece was cut from the remaining intestine and processed as stroma for microarray.

2.4.5 Microarray

Epithelial (crypt cells) and stromal cells from *Villin-Cre/Porcⁿ^{Del}* and *Villin-Cre/Porcⁿ^{WT}* mice were harvested as described above. RNA was isolated using RNeasy purification kit from Qiagen. Labeled cRNA was prepared and hybridized to MouseWG-6 v2.0 Expression BeadChip Kit (Illumina) according to the manufacturer's protocols. The gene expression data were extracted by GenomeStudio (v 1.7.0) software. After normalization by median centering, SAM (Significance Analysis of Microarrays) with less than 10% FDR (False Discovery Rate) was used to compare the samples. Signaling pathways are downloaded from Molecular Signatures database (MsigDB 2.5, <http://www.broadinstitute.org/gsea/msigdb/>). The genes in each pathway were centered using Cluster software and their heatmaps were generated with TreeView software.

2.4.6 Stromal Isolation for culture

Tissues remaining after crypt isolation were subjected to an additional round of pipetting for 40 times to remove most of the remaining epithelial cells, and washed once with PBS and with serum-free DMEM containing 1% Glutamax and 1% Penicillin-Streptomycin (both reagents from Life Technologies). Thereafter, tissues were digested for 3 hours in 6 ml of serum-

free DMEM containing 1% Glutamax, 1% Penicillin-Streptomycin and 2 mg/ml of Collagenase/Dispase (Roche). The digestion solution was replaced with fresh digestion solution every 60 minutes. At the end of this digestion step, tissues were further dissociated by vigorous pipetting. To inhibit proteolytic activity and cellular aggregation, at this step suspensions were supplemented with 5% fetal calf serum. Thereafter, samples were passed through a 70 μ m cell strainer, centrifuged at 400 x g for 4 minutes, washed once in PBS and counted. At this point, stromal cells were either directly mixed with epithelial cells (Fresh stroma) or cultured for 5 days in RPMI1640 containing 10% FCS, 1% Penicillin-Streptomycin and 1% Glutamax (“Cultured stroma”).

To test the ability of stroma to support epithelial crypt proliferation, fresh or cultured stroma (50000 or 25000 cells, respectively) was mixed with epithelial crypts (generally 6000 crypts) in 15 ml tubes and pelleted via centrifugation at 400g for 4 minutes. Following centrifugation, supernatant was carefully removed and then pellets were re-suspended in 50 μ l of Matrigel per well equivalent and then directly distributed into 48-well plates. The Matrigel was allowed to gel for 30 minutes at 37 °C and then each well was supplemented with complete crypt culture medium. Each experiment included wells containing stroma alone to estimate amounts of contaminating epithelial stem cells.

2.4.7 Tissue preparation for staining

Intestine was harvested immediately after sacrifice and washed extensively with PBS. The small intestine was cut in two identical lengths, small

fragments were collected for RNA isolation, and the remaining small intestine was flushed with 4% formalin and prepared for formalin fixation and paraffin embedding as a Swiss Roll.

For confocal imaging of EGFP, the small intestine was washed with PBS and then perfused with cold 4% paraformaldehyde, prepared as a Swiss Roll, and fixed for an additional two hours. Samples were then incubated in 15% sucrose solution for 24 hours, followed by 30% sucrose for another 24 hours, all at 4°C. Samples were then embedded in OCT and stored at -80°C.

2.4.8 Antibodies and staining condition

Synaptophysin (Lifespan Biosciences (LS-C49473)), β -catenin (Becton Dickinson (Cat# (421)610154)), and lysozyme (Abcam (Cat# ab108508)) antibodies were used at dilution of 1:50, 1:150, 1:5000 respectively. Antigens in formaldehyde-fixed and paraffin embedded intestinal tissues were retrieved by boiling in citrate buffer, pH 6, for 10 minutes. Thereafter, samples were blocked in 1% BSA for 60 minutes. Tissues were incubated with primary antibodies for 60 min, washed and subsequently incubated for 60 min with secondary antibody diluted 1:200. Sections were mounted in DPX medium and analyzed using a Leica DM2000 microscope. Apoptotic cells were detected by TUNEL assay, using ApopTag Plus Peroxidase In Situ (Millipore, Cat#S7101). Ki67 and β -catenin staining in Wls^{flox} samples were performed as described (Zhong et al., 2012). Stromal cells cultured for 6 days were then cultured on glass coverslips for 2 days, fixed in 2% PFA in PBS for 15 minutes and permeabilized with 0.2% Triton-X 100 for 10 minutes. Thereafter, samples were washed once in PBS followed by the staining

procedures described above using primary antibodies to Vimentin (Cell Signaling (#5741)), Desmin (Cell Signaling (#5332)), and Smooth muscle actin (α -SMA)(Abcam (#ab-7817)) diluted 1:100 in PBS containing 1% BSA. Secondary anti-rabbit and anti-mouse antibodies (Invitrogen Alexa Fluor 594 goat anti-rabbit and mouse (#A1102, #A11005) were diluted 1:500. After staining, samples were mounted in Vectashield medium containing DAPI and analyzed using a LSM710 Carl Zeiss confocal microscope.

2.4.9 Cell proliferation assay

Cell proliferation *in vivo* was assessed by EdU incorporation. EdU and Click-iT® EdU Alexa Fluor® 555 Imaging Kit, were purchased from Life Technologies (Cat#A10044 and Cat# C10338 respectively). Two hours prior to sacrifice mice were injected with 0.5 mg EdU in 150 μ l PBS (~16.66 mg/kg). Incorporated EdU was visualized following manufacturer's instructions and mounted in fluorescent mounting media with DAPI (VectaShield, Cat#H-1200). When EdU staining was performed on OCT embedded samples, incubation time for the Click iT reaction cocktail was reduced to 1 minute.

Data were analyzed using Prism 5 software and Excel. Two-tailed T-test was performed in Excel for Mac 2011 version 14.3.2.

3. Role of Wnt Signaling in Adult Murine Hematopoiesis

3.1 Introduction

The role of Wnt signaling has been implicated in hematopoiesis for decades, but remains controversial. For instance, Wnt5a has been shown to affect HSC proliferation *in vivo* and *in vitro* by inhibiting the Wnt canonical pathway, indicating a role for non-canonical Wnt pathways in hematopoiesis (Buckley et al., 2011; Liang et al., 2003; Murdoch, 2003; Nemeth and Bodine, 2007). Sugimura et al. found that non-canonical Wnt signaling through Frizzled8 and flamingo maintained the self-renewal of long-term HSCs (LT-HSCs) (Sugimura et al., 2012). Demonstrating the importance of Wnt signaling in the bone marrow, osteoblastic overexpression of DKK1 and Wif1, both inhibitors of the canonical Wnt pathway, impaired the reconstitution capacities of HSCs (Fleming et al., 2008; Schaniel et al., 2011). Moreover, embryonic deficient Wnt3a HSCs and *Vav-Cre/β-catenin* HSCs exhibited self-renewal dysfunction in secondary bone marrow transplantations (Luis et al., 2009; Zhao et al., 2007). However, *MXI-Cre/β-catenin^{-/-}*, as well as *β- and γ-catenin* double knockout mice, did not show any hematopoietic phenotype (Cobas et al., 2004; Jeannet et al., 2008). Likewise, the overexpression of HSC *β-catenin* resulted in stem cell exhaustion (Kirstetter et al., 2006). These findings present contradictory views and emphasize the need to elucidate the role of Wnt signaling in hematopoiesis.

The source of Wnt ligands for HSCs also remains unclear. Some reports have favored the niche as a source of Wnt ligands. For example, Wnt5a was proposed to have a paracrine effect in HSCs (Nemeth and Bodine, 2007). In addition, Ichii et al. found that the production of B-cells, natural killer cells and plasmocytes was blocked after HSCs were cultured on top of Wnt3a-

transduced OP9 stromal cells. These effects were reportedly due to characteristic changes of the OP9 stromal cells, but not of the HSCs. Furthermore, N-cadherin⁺ osteoblastic cells were shown to express non-canonical Wnt ligands and inhibitors of canonical Wnt ligands. In turn, this expression antagonized Wnt/ β -Catenin pathways in the HSCs, maintaining them in a quiescent stage under normal conditions (Sugimura et al., 2012). Conversely, some studies have shown that the intrinsic effect of hematopoietic Wnts is a potential source for HSCs. Liang et al. reported that Wnt5a expression in HSCs blocked B-cell proliferation (Liang et al., 2003). Moreover, stabilization of β -catenin in stromal, but not HSCs, altered the hematopoietic niche to further support self-renewal of HSCs (Kim et al., 2009). Thus, identifying the source of Wnts for hematopoiesis presents a challenge, because there are many Wnt ligands with different effects all expressed in different BM cell types.

Deregulation of Wnt pathways has been implicated in several disorders including different types of cancers, pathological fibrosis and bone diseases (Klaus and Birchmeier, 2008; Nusse, 2012). Thus, targeting Wnt secretion in Wnt-high pathologies may offer a novel therapeutic approach. Notably, it has been suggested that the maintenance of adult stem cells is dependent on Wnt signaling. Consequently, inhibition of Wnt secretion may have adverse side effects in proliferative tissues such as skin, bone marrow (BM) and intestine. It is known that hematopoietic stem cells (HSCs) maintain the proliferation of bone marrow cells, as such inhibition of Wnt signaling may affect normal hematopoiesis, resulting in bone marrow failure.

In this study, we used a genetic approach to inhibit Wnt signaling by targeting *Porcn* in adult mice in order to address the role and the source of Wnts in adult hematopoiesis. To test our hypothesis, *Porcn* conditional knockout mice were crossed into different Cre drivers including *Rosa-CreER^{T2}*, *MXI-Cre* and *Vav-Cre*. We found that the inhibition of Wnt secretion in *Rosa-CreER^{T2}/Porcn^{Del}* mice did not indicate a substantial role for Wnt signaling in hematopoiesis, except for a slight increase of granulopoiesis, which is secondary to phenotypes related to non-hematopoietic tissues. Through analyses of *MXI-Cre/Porcn^{Del}* and *Vav-Cre/Porcn^{Del}* mice, we found that hematopoietic Wnts were dispensable for the proliferation and differentiation of blood progenitors, as well as for HSC self-renewal. These results indicate that, to the extent that Wnts are involved in *in vivo* hematopoiesis, they can be fully supplied by the stroma.

3.2 Results

3.2.1 Total body knock out of *Porcn* in adult mice

Inhibition of Wnt secretion is a unique strategy to treat Wnt-high disorders but the toxicity of the therapy may be limited by the role of Wnts in adult tissue homeostasis. To assess which adult tissues are most sensitive to the loss of Wnt secretion, we crossed *Porcn^{flox}* with *Rosa-CreER^{T2}* mice to generate mice with widespread expression of a tamoxifen-sensitive Cre recombinase (Biechele et al., 2013; Hameyer et al., 2007). To induce *Porcn* inactivation, control (*Rosa-CreER^{T2}/Porcn^{WT,WT}* or *Porcn^{WT,Y}*) and inducible *Porcn* knockout mice (*Rosa-CreER^{T2}/Porcn^{flox,flox}* or *Porcn^{flox,Y}*) were fed with tamoxifen chow for 3 weeks beginning at 3 to 4 months of age. Hereafter we

denote the excised allele(s) collectively as *Porcn*^{Del}. Consistent with the well-documented role of Wnt/ β -catenin signaling in hair follicle formation (Huelsken et al., 2001), *Rosa-CreER*^{T2}/*Porcn*^{Del} mice showed progressive global alopecia beginning 5 weeks after starting the tamoxifen chow (Figure 3.1 A). Substantial excision of *Porcn* exon 3 was observed in skin samples (Figure 3.1 B). Histologically, *Porcn*^{Del} mice exhibited an impaired skin structure with lack of hair follicles in the dermis and an increased number of cells in epidermal layer (Figure 3.2), similar to the phenotype seen after inactivation of β -catenin and WLS in the skin (Augustin et al., 2013; Huelsken et al., 2001). As expected, *Porcn* inactivation was accompanied by a marked reduction of *Porcn* mRNA (Figure 3.3 A). In addition, there was a decrease in Wnt/ β -catenin signaling, shown by loss of β -catenin protein in hair follicles (Figure 3.3 B) and down-regulation of Wnt/ β -catenin target gene *Axin2* (Figure 3.3 A). These results are consistent with the established role of Wnt ligands in hair follicle development and confirm the *Porcn*^{flox} mouse as a useful tool to study the tissue specific role of Wnt secretion.

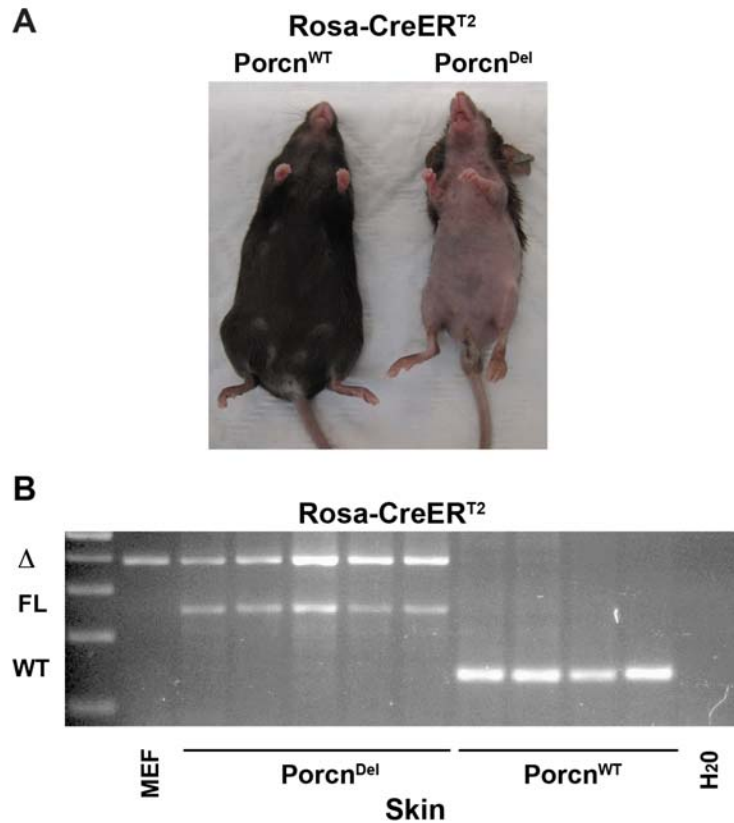


Figure 3.1 Hair loss phenotype in *Rosa-CreER^{T2}/Porcn^{Del}* mice. **A)** Tamoxifen supplementation in chow for 3 weeks caused progressive alopecia in mice. The photo was taken 7 weeks after the start of tamoxifen supplementation. **B)** Tamoxifen supplementation in chow led to Cre expression and *Porcn* deletion in skin samples of *Rosa-CreER^{T2}/Porcn^{fllox}* mice as assessed by PCR of gDNA (Del: excised *Porcn* allele, FL: floxed allele, WT: wildtype allele). Each lane represents an individual mouse.

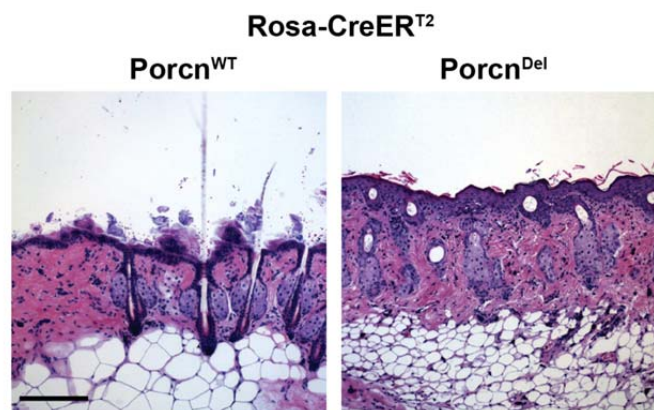


Figure 3.2 Loss of hair follicles in skin after *Porcn* inactivation. Histology of skin samples from *Rosa-CreER^{T2}/Porcn^{WT}* (n=3) and *Rosa-CreER^{T2}/Porcn^{Del}* (n = 4) mice. The scale bar equals 200 μ m.

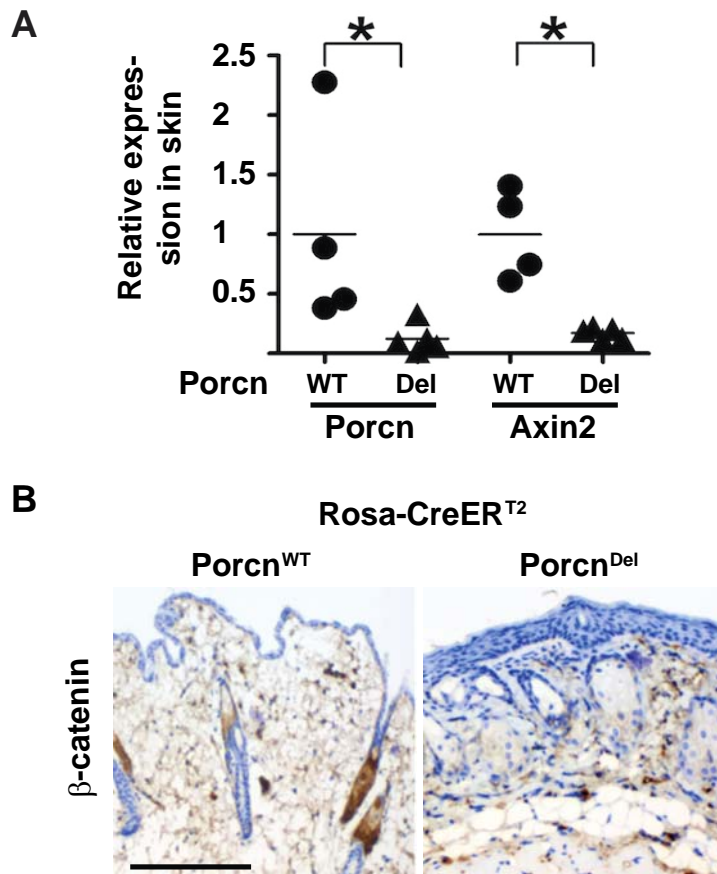


Figure 3.3 Inactivation of *Porcn* caused down-regulation of Wnt/ β -catenin target genes (*Axin2*) in the skin samples of *Rosa-CreER^{T2}/Porcn^{Del}* mice. **A) Expression level of *Porcn* and *Axin2* mRNA were normalized to *Pgk*. Mean values of respective *Rosa-CreER^{T2}/Porcn^{WT}* samples were set to 1 and compared to individual measurements within the same group (n = 4 mice per group, * p < 0.05, Mann-Whitney test) **B**) Inhibition of Wnt signaling in the skin samples of *Rosa-CreER^{T2}/Porcn^{Del}* mice. β -Catenin staining was reduced in *Porcn^{Del}* samples. This is the representative result of 5 long-term treated mice. The scale bar is 100 μ m.**

Besides alopecia, the *Porcn^{Del}* mice started to lose body weight 4 weeks after tamoxifen treatment (Figure 3.4) while the *Porcn^{WT}* mice gained weight on the same diet. Chow consumption, established by weighing the remaining pellets, was similar in the two groups. Additionally, the *Porcn^{Del}* mice developed signs of neurologic impairment including an altered gait and poor grooming, a finding consistent with a role for Wnt signaling in neuronal proliferation and differentiation (Lyu et al., 2008; Seib et al., 2013). These

mice survived 5 to 7 weeks after tamoxifen administration, when they were sacrificed due to weight loss. Necropsy did not reveal additional specific pathology beyond loss of body fat.

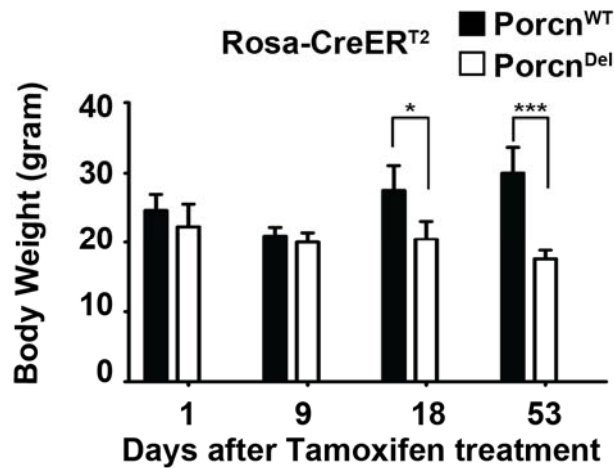


Figure 3.4 Weight loss phenotype in *Rosa-CreER^{T2}/Porcn^{Del}* mice. Progressive weight loss in *Rosa-CreER^{T2}/Porcn^{Del}* mice was observed 7 weeks after initiation of the treatment (n = 5 mice per group, * p < 0.05, *** p < 0.001, two tailed t-test). Error bars indicate standard deviation.

3.2.2 Increase of granulopoiesis after *Porcn* inactivation in the total body of adult mice.

To quantitate *Porcn* deletion in hematopoietic cells, blood samples of *Rosa-CreER^{T2}/Porcn^{Del}* mice (total body knock) were collected. Substantial excision of *Porcn* was confirmed by PCR from genomic DNA (Figure 3.5).

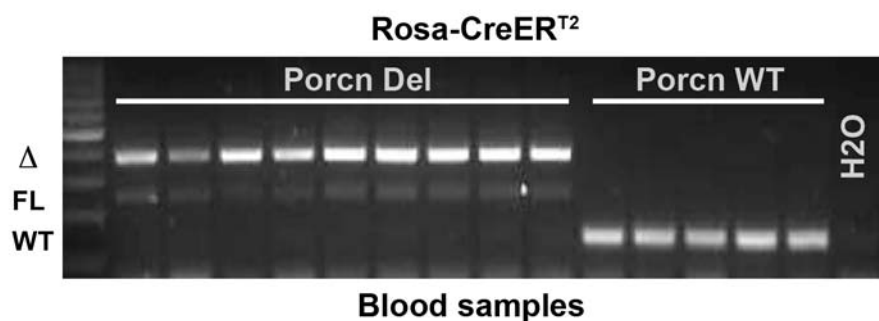


Figure 3.5 *Porcn* deletion in blood samples of *Rosa-CreER^{T2}/Porcn^{Del}* mice. Cre expression mediated great excision of *Porcn* in blood samples of *Rosa-CreER^{T2}/Porcn^{Del}* mice as assessed by PCR of genomic DNA (Del:

excised *Porcn* allele, FL: floxed allele, WT: wildtype allele). Each lane represents an individual mouse.

To test if hematopoiesis was impaired in the *Rosa-CreER^{T2}/Porcn^{Del}* mice, we first compared the blood samples with *Porcn^{WT}* mice 4 weeks after the tamoxifen chow treatment. Complete blood count (CBC) of *Porcn^{Del}* and *Porcn^{WT}* blood samples did not exhibit significant differences in hemoglobin (Hg), red blood cells (RBC), platelets (PLT), and total white blood counts (WBC) (Figure 3.6, 3.7 A, B, and C). However, *Porcn^{Del}* mice demonstrated a significantly higher number of neutrophils as compared to the control mice (Figure 3.6), a finding we attributed to inflammatory changes secondary to the total body *Porcn* knockout.

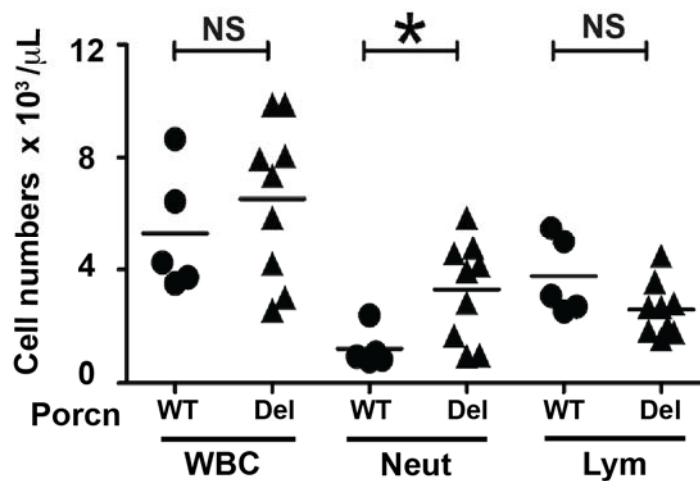


Figure 3.6 Complete blood count test showed granulocytosis after deletion of *Porcn*. Total white blood cells and lymphocytes counts did not show any significant changes in blood samples of *Rosa-CreER^{T2}/Porcn^{WT}* (n = 5) and *Porcn^{Del}* mice (n = 9, NS: not significant, p > 0.05, Mann-Whitney test). However, Neutrophil numbers were significantly increased in CBC of *Rosa-CreER^{T2}/Porcn^{Del}* (n = 9) compared to control mice (n = 5, * p = 0.019, Mann-Whitney test).

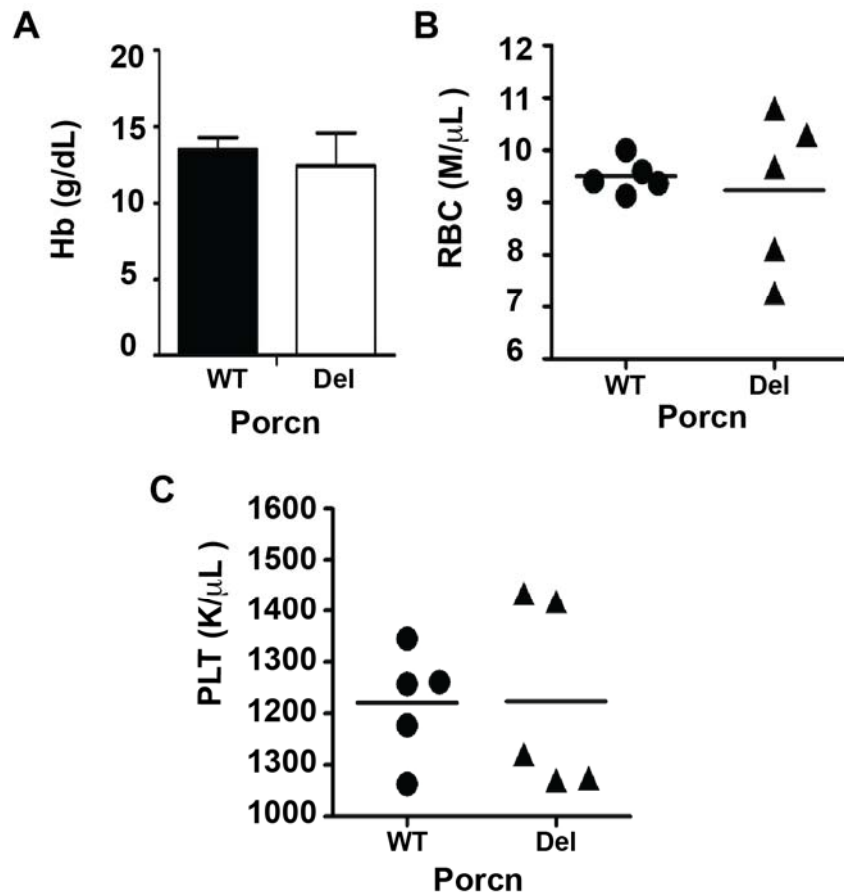


Figure 3.7 Normal Hb, RBC, and PLT in *Rosa-CreER^{T2}/Porcn^{Del}* mice. A) *Porcn^{Del}* mice had normal level of hemoglobin (Hg) in comparison to *Porcn^{WT}* (n = 5 per group). **B)** *Rosa-CreER^{T2}/Porcn^{WT}* and *Porcn^{Del}* mice (n = 5 per group). **C)** Platelet (PLT) counts was normal in both *Rosa-CreER^{T2}/Porcn^{WT}* and *Porcn^{Del}* mice (n = 5 per group).

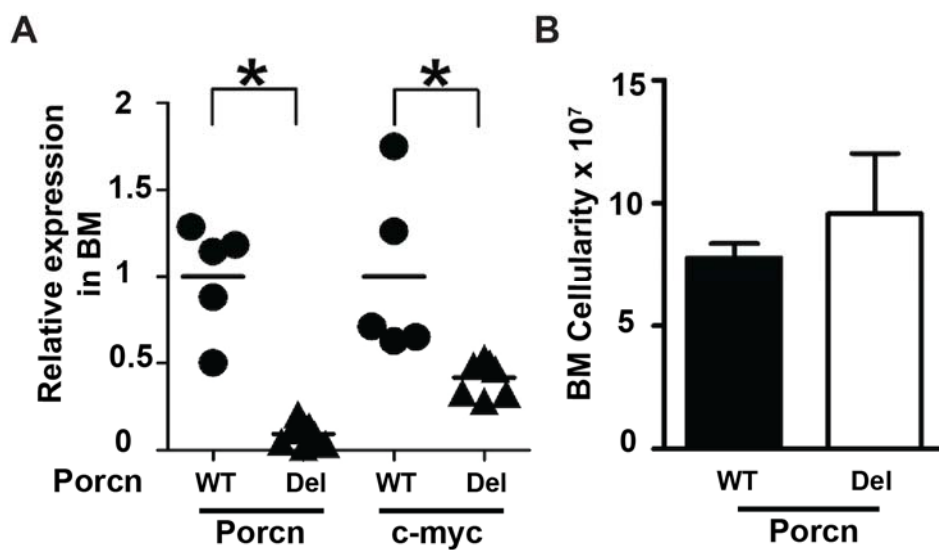


Figure 3.8 *Porcn* and *c-myc* (Wnt/ β -catenin target gene) were down-regulated in bone marrow samples of *Porcn* inactivated mice. A)

Expression levels of *Porcn*, *c-myc* mRNA were normalized to *Pgk* and β -actin. Mean values of respective *Porcn*^{WT} samples were set to 1 and compared to individual measurements within the same group (n = 5 and 6 for *Rosa-CreER*^{T2}/*Porcn*^{WT} and *Porcn*^{Del} mice, respectively, * p < 0.01, Mann-Whitney test). **B)** Total BM cell numbers from two tibia and femur were comparable in both *Rosa-CreER*^{T2}/*Porcn*^{WT} (n = 3) and *Porcn*^{Del} mice (n = 5).

To investigate the role of Wnt signaling in the maintenance of hematopoietic stem cells (HSCs) and in the proliferation of progenitor cells, bone marrow from control and knockout mice were compared. Similar to the peripheral blood, the BM of the *Porcn*^{Del} mice showed a substantial reduction of *Porcn* expression as well as Wnt target gene *c-myc* by RT-PCR (Figure 3.8 A). Unexpectedly, the total BM cells count did not significantly change between the *Porcn*^{Del} and *Porcn*^{WT} mice (Figure 3.8 B). In addition, FACS analysis did not show any changes in the frequency of LSK (Lin-, Sca-1+, c-kit+), LT-HSC (long term HSC, Lin-, Sca-1+, c-kit+, CD150+, CD48-), or ST-HSC (short term HSC, Lin-, Sca1+, c-Kit+, CD150-, CD48+) in these mice (Figure 3.9A, B, C, D and E). Moreover, the frequency of myeloid progenitors (CMP: common myeloid progenitor, GMP: granulocyte- monocyte progenitor, MEP: megakaryocyte- erythroid progenitor) in *Porcn*^{Del} mice was in the range observed in the *Porcn*^{WT} mice (Figure 3.10). Consistent with peripheral blood, there was a greater frequency of granulocytes in the BM of *Porcn*^{Del} mice (Figure 3.11 A). BM samples showed a significant reduction in frequency of common lymphoid progenitors (CLPs) and B-lymphocyte compared to *Porcn*^{WT} (Figure 3.11 B, 3.12). Some of *Rosa-CreER*^{T2}/*Porcn*^{Del} mice had thymus atrophy, but the size of spleen and liver were in the normal range in both groups of mice. Collectively, knockout of *Porcn* in the whole body of the adult *Rosa-CreER*^{T2} mice resulted in a mild increase of granulocytes and a

reduction in lymphocytes as well as CLPs, but it did not affect the total WBCs or the numbers of HSCs and myeloid progenitors.

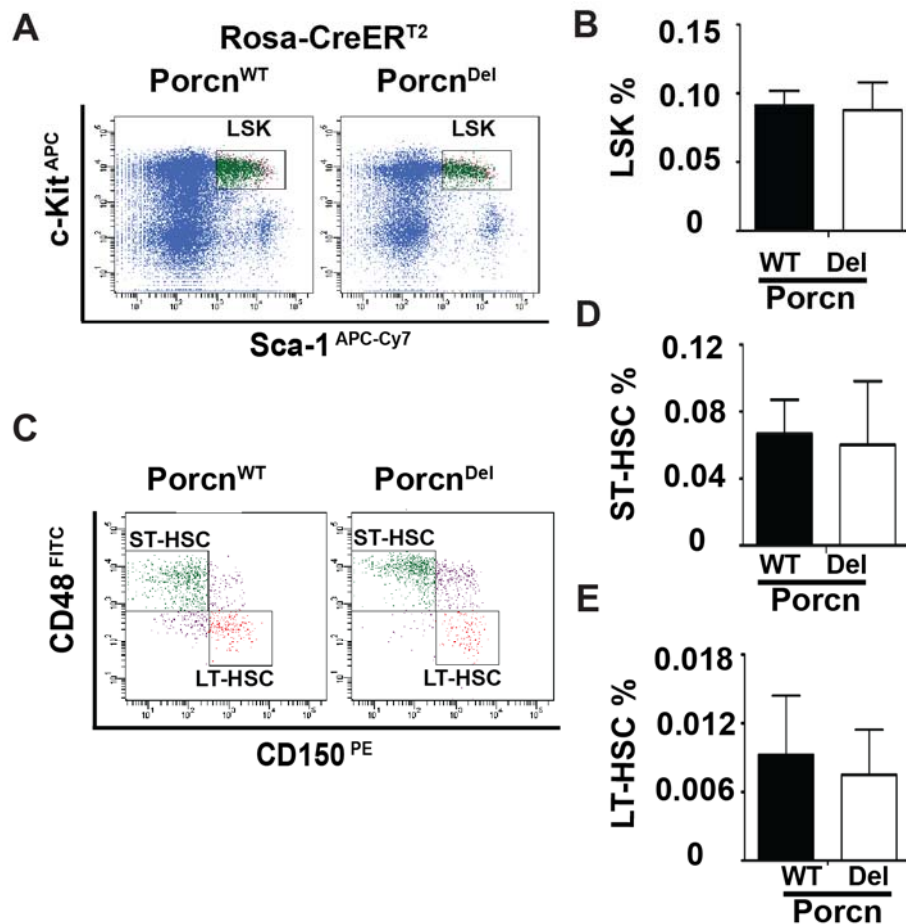


Figure 3.9 The frequency of LSK, ST-HSC, and LT-HSC in *Rosa-CreER^{T2}/Porcn^{Del}* mice were similar to *Rosa-CreER^{T2}/Porcn^{WT}* mice. **A)** Representative of LSK gating from *Porcn^{WT}* and *Porcn^{Del}* flow cytometer data were shown in scattered graphs. **B)** The frequency of LSK (Lin⁻, Sca1⁺, c-Kit⁺) did not change between *Rosa-CreER^{T2}/Porcn^{WT}* (n = 5) and *Porcn^{Del}* (n = 7) mice. **C)** Representative of LT-HSC and ST-HSC gating from *Porcn^{WT}* and *Porcn^{Del}* flow cytometer data were shown in scattered graphs. **D)** The frequency of LT-HSC (Lin⁻, Sca1⁺, c-Kit⁺, CD150⁺, CD48⁻), and **E)** the frequency of ST-HSC (Lin⁻, Sca1⁺, c-Kit⁺, CD150⁻, CD48⁺) did not change between *Rosa-CreER^{T2}/Porcn^{WT}* (n = 5) and *Porcn^{Del}* (n = 7) mice. Frequency of different HSCs (in total live BM cells) was summarized in three separated graphs (p > 0.05, Mann-Whitney test).

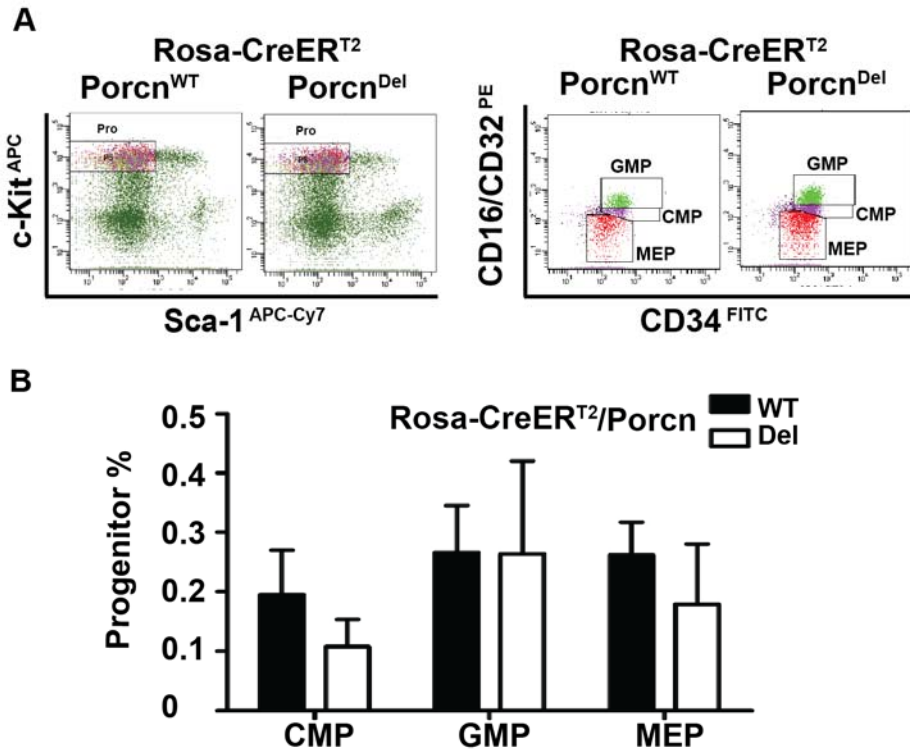


Figure 3.10 Frequency of myeloid progenitors were similar in both *Rosa-CreER^{T2}/Porcn^{WT}* and *Porcn^{Del}* mice. **A)** Representative gating for Common Myeloid progenitor (CMP), Megakaryocyte-Erythrocyte progenitor (MEP), and Granulocyte-Monocyte progenitor (GMP) from *Porcn^{WT}* (n = 5) and *Porcn^{Del}* (n = 7) flow cytometer data were shown in two scattered graphs. **B)** Frequency of different progenitors in total live BM cells was summarized in (p > 0.05, Mann-Whitney test).

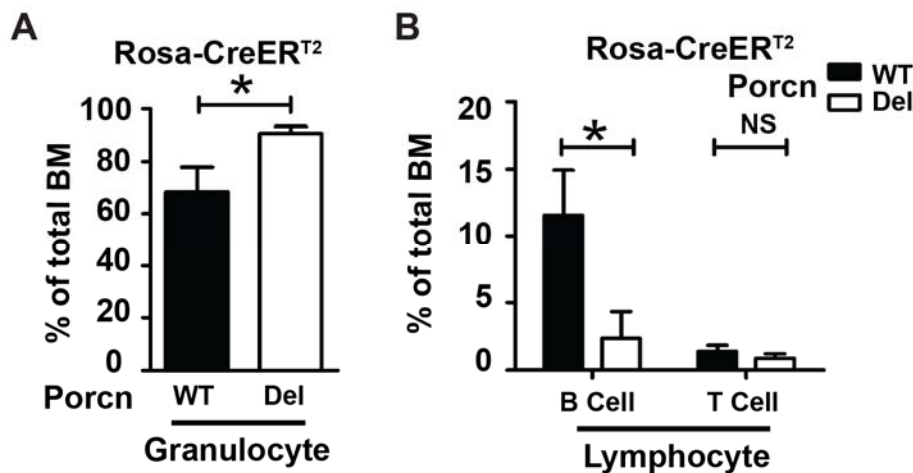


Figure 3.11 Increased granulopoiesis in *Rosa-CreER^{T2}/Porcn^{Del}* mice. **A)** Frequency of BM Granulocyte was significantly increased in *Rosa-CreER^{T2}/Porcn^{Del}* (n = 7) compared to *Rosa-CreER^{T2}/Porcn^{WT}* (n = 5) mice (Granulocyte: Mac1+, Gr1+, * p = 0.0025, Mann-Whitney test). **B)** Frequency of BM B-lymphocyte was significantly decreased in *Rosa-CreER^{T2}/Porcn^{Del}*

(n = 5) compared to *Rosa-CreER^{T2}/Porcn^{WT}* (n = 4) mice (B-Lymphocyte: CD3e⁻, CD19⁺, * p = 0.0159, T-Lymphocyte: CD3e⁺, CD19⁻, NS: not significant, p = 0.131, Mann-Whitney test).

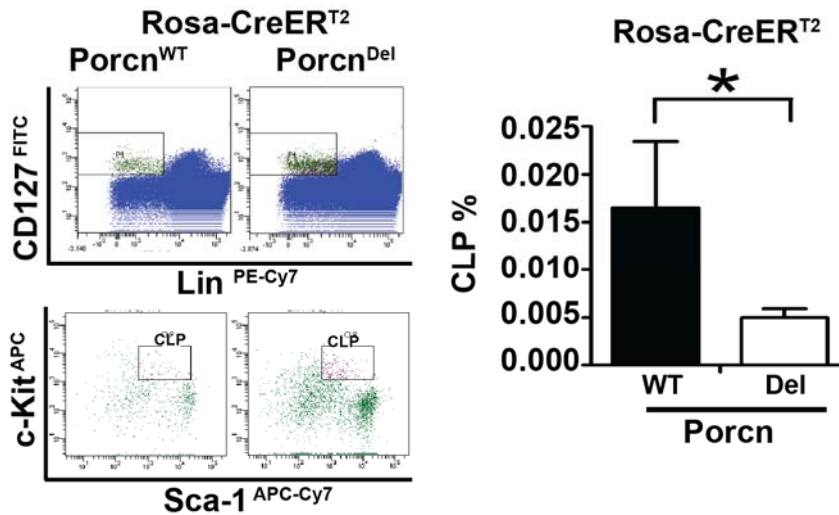


Figure 3.12 Inhibition of Wnt signaling caused reduction of Common Lymphoid progenitors (CLP) in *Rosa-CreER^{T2}/Porcn^{Del}* mice. Representative of flow cytometer gating for CLPs in *Porcn^{WT}* and *Porcn^{Del}* was shown in two scattered graphs. (Left panels). Frequency of CLPs in total live BM cells was summarized in right graphs (n = 3 in each group, * p < 0.05, two-tailed T test).

To address any cell autonomous effect of Wnt ligands in differentiation of hematopoietic progenitor cells, sorted LSK cells or BM cells were plated in colony forming assays. Unexpectedly, both *Porcn^{Del}* LSK or BM cells were able to form colonies of all lineages and they showed increased numbers of colonies compared to controls (Figure 3.13 A, and B). Again consistent with the blood counts, the increase in total colony numbers from *Porcn^{Del}* cells was due to an increase in granulocyte colonies or mixed granulocyte and monocyte colonies. Consequently, the *in vitro* culture of LSK and progenitor cells showed marked increase of granulocytes similar to *in vivo* phenotype of *Rosa-CreER^{T2}/Porcn^{Del}* mice.

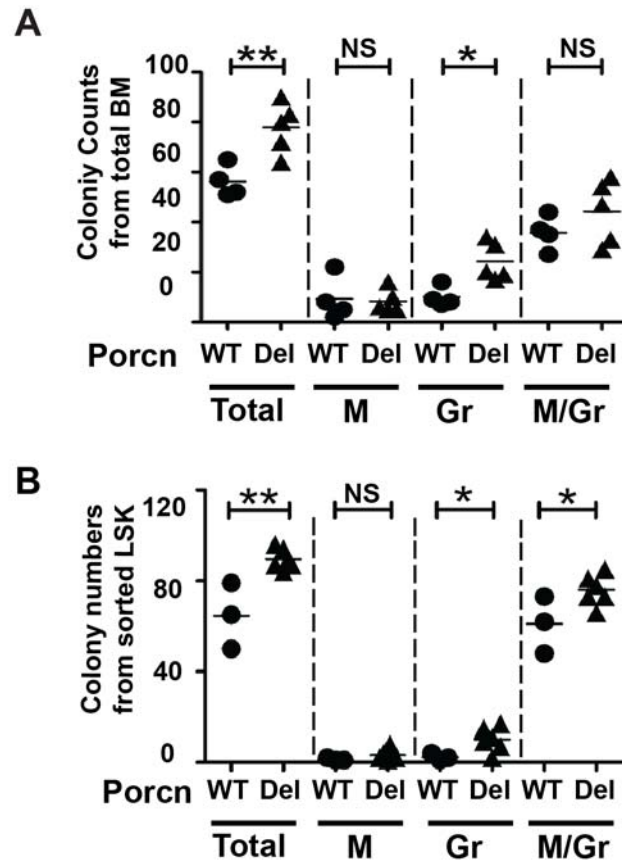


Figure 3.13 Higher granulocyte colonies from *Rosa-CreER^{T2}/Porcn^{Del}* BM samples. **A)** *Rosa-CreER^{T2}/Porcn^{Del}* bone marrow cells were able to form significantly higher number of colonies in culture compared to *Porcn^{WT}* bone marrow cells. The total and Granulocyte colonies were increased in *Porcn^{Del}* samples (n = 5 wells, 2 mice) compared to *Porcn^{WT}* (n = 4 wells, 2 mice). Total: all types of colonies including GEMM: Granulocyte, Erythrocyte, Monocyte, and Megakaryocyte colonies; Gr: Granulocyte colonies; M: Monocyte colonies; M/Gr: Monocyte and Granulocyte colonies (* p < 0.05, ** p < 0.01, NS: not significant, Mann-Whitney test). **B)** Sorted LSK cells of *Rosa-CreER^{T2}/Porcn^{Del}* mice formed higher number of colonies in culture compared to *Porcn^{WT}* LSK cells. The total, Gr, and M/Gr colonies were increased in *Porcn^{Del}* samples (n = 5 wells, 2 mice) compared to *Porcn^{WT}* (n = 4 wells, 2 mice). Total: all types of colonies; Gr: Granulocyte colonies; M: Monocyte colonies; M/Gr: Monocyte and Granulocyte colonies (* p < 0.05, ** p < 0.01, NS: not significant, Mann-Whitney test).

Luis et al. reported that *Wnt3a* deficient HSCs could not successfully reconstitute the BM of WT lethally irradiated recipient mice after a secondary BMT, indicating a role for *Wnt3a* in the maintenance of embryonic HSCs (Luis et al., 2009). To investigate adult HSC function after inhibition of *Wnt*

signaling, BM from *Rosa-CreER^{T2}/Porcn^{Del}* mice (CD45.2) was transplanted into *Porcn^{WT}* irradiated recipient mice (CD45.1). Normal BM reconstitution was confirmed by evaluating the number of donor granulocytes, and lymphocytes in blood samples from the recipient mice after 12 weeks of transplantation (data not shown). We confirmed that hematopoietic reconstitution was from *Porcn^{Del}* donor cells by genomic PCR of peripheral blood samples. This excludes the possibility that residual *Porcn^{FL}* non-excised HSCs were responsible for the successful primary BMT (Figure 3.14 A). To measure the frequency of HSCs and progenitors, primary recipient mice were sacrificed 3 months after the primary BMT. BM cells were analyzed by flow cytometry or transplanted into secondary lethally irradiated mice. Successful reconstitution of *Porcn^{WT}* and *Porcn^{Del}* donor cells was observed in primary recipient mice (Figure 3.14 B).

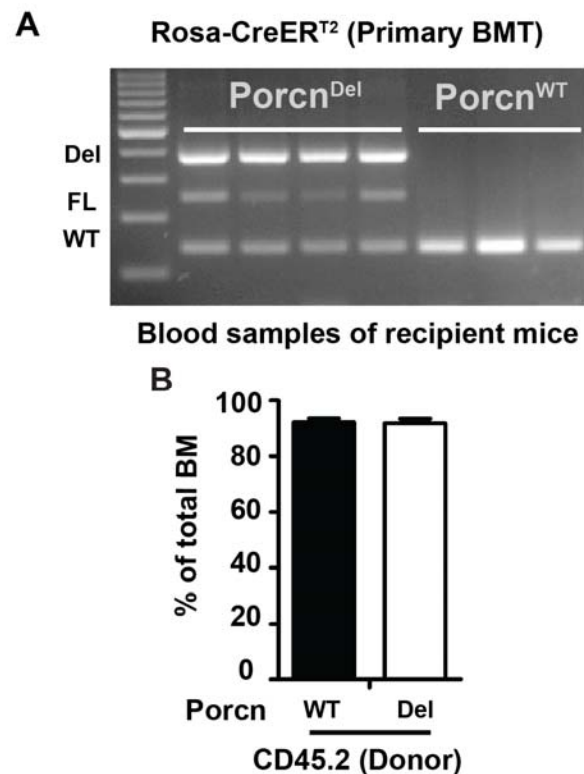


Figure 3.14 Donor *Porcn^{Del}* BM cells were able to reconstitute in primary BMT recipient mice. A) *Porcn* excised band present in genomic PCR of

blood samples from primary BMT recipient mice (Del: excised *Porcn* allele, FL: floxed allele, WT: wild type allele). Each lane represents an individual mouse. **B)** Quantification of donor reconstitution (CD45.2) in total BM cells of primary recipient mice.

The frequencies of *Porcn*^{WT} and *Porcn*^{Del} donor neutrophils (CD45.2⁺, Mac1⁺, Gr1⁺), B-(CD45.2⁺, CD19⁺, CD3e⁻) and T-lymphocytes (CD45.2⁺, CD19⁻, CD3e⁺) in the total BM cells of the primary recipient mice were similar (Figure 3.15 A, and B). Interestingly, the frequencies of donor LSKs, LT-HSCs, ST-HSCs, and myeloid progenitors (CMP, GMP, MEP) indicated a normal reconstitution of the BM from both *Rosa-CreER*^{T2}/*Porcn*^{Del} and *Porcn*^{WT} mice (Figure 3.16 A, B, Figure 3.17 A, B and Figure 3.18). Moreover, while we had observed a significant reduction of CLPs in the primary *Rosa-CreER*^{T2}/*Porcn*^{Del} mice, this was not the case in the recipients of *Porcn*^{Del} HSCs. (Figure 3.19). Thus, the changes in granulocytes and lymphocytes and thymus seen in the knockout mice were most likely due to inflammatory changes after total body *Porcn* knockout rather than an intrinsic alteration in hematopoiesis.

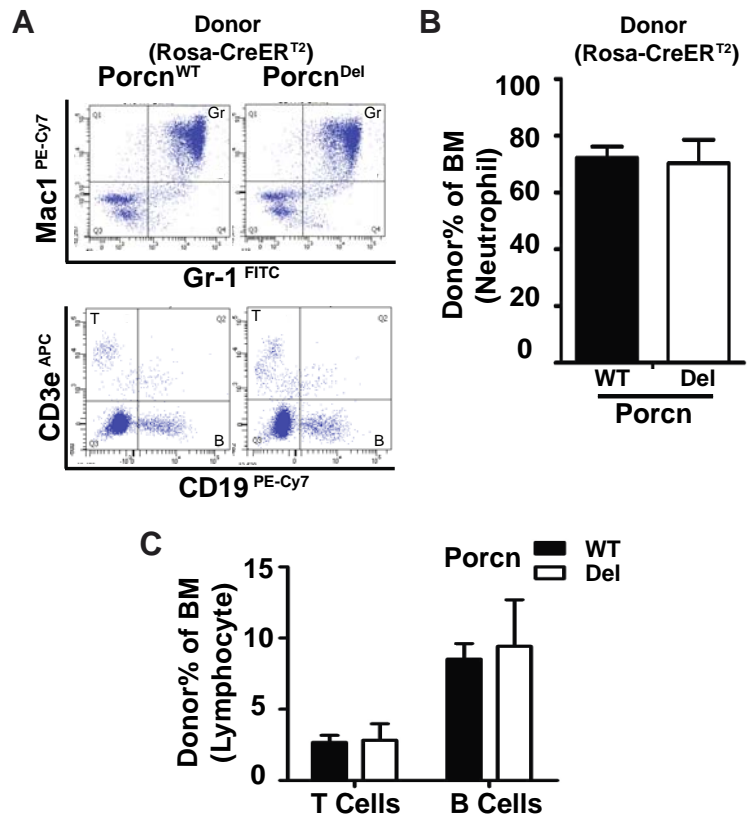


Figure 3.15 Successful reconstitution of donor *Rosa-CreER^{T2}/Porcn^{Del}* BM cells in sub-lethally irradiated recipient mice. A) Successful reconstitution of donor *Rosa-CreER^{T2}/Porcn^{Del}* and *Rosa-CreER^{T2}/Porcn^{WT}* BM cells in sub-lethally irradiated recipient mice after 5 months of BM transplantation (BMT). Representative gating for donor BM Lymphocytes and Neutrophils (CD45.2+) (n = 4 and 5 for *Porcn^{WT}* and *Porcn^{Del}* mice, respectively). B) Quantification of donor Neutrophils frequency in total BM cells of the recipient mice. C) Quantification of donor Lymphocytes frequency in total BM cells of the recipient mice.

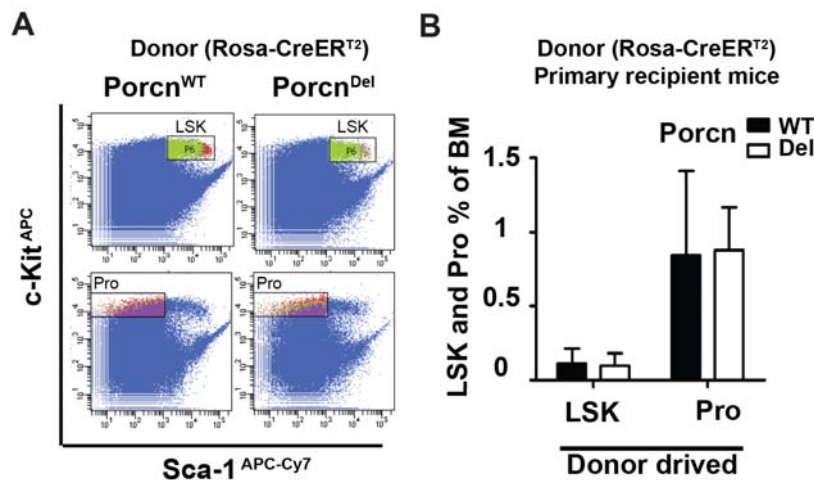


Figure 3.16 Comparable LSK and progenitors frequencies in both *Rosa-CreER^{T2}/Porcn^{Del}* and *Rosa-CreER^{T2}/Porcn^{WT}* recipient mice. A)

Representative graph of LSKs and progenitors gating based on donor gated cells (CD45.1⁺) (n = 4 and 5 for the primary recipient of *Porcn*^{WT} and *Porcn*^{Del} mice, respectively). **B)** Quantification of donor LSK and progenitors frequency in total BM cells of the recipient mice.

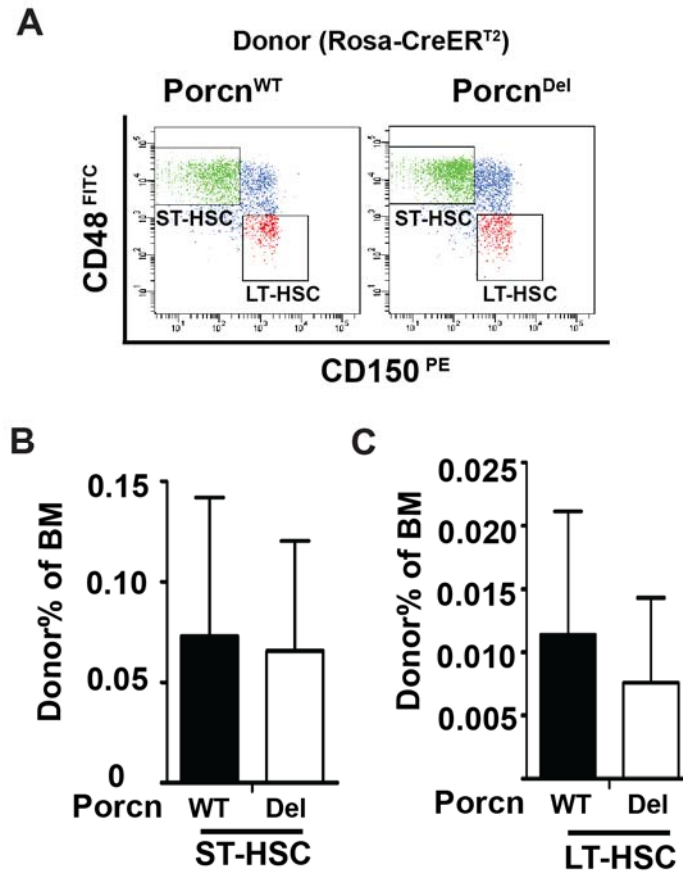


Figure 3.17 Normal LT-HSC and ST-HSC frequency in primary recipient of *Rosa-CreER*^{T2}/*Porcn*^{Del} mice. **A)** Representative graph of LT-HSC, and ST-HSC gating based on donor cells (CD45.1⁺) (n = 4 and 5 for the primary recipient of *Porcn*^{WT} and *Porcn*^{Del} mice, respectively). **B, C)** Quantification of donor LT-HSC, and ST-HSC frequency in total BM cells of the recipient mice.

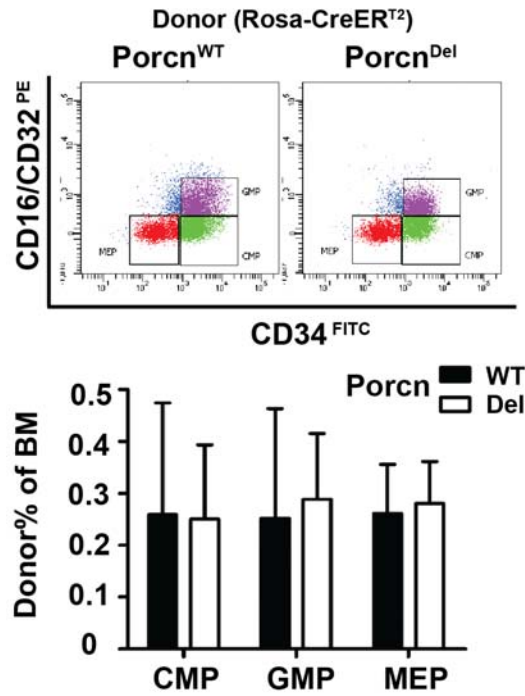


Figure 3.18 Normal myeloid progenitors frequency in primary recipient of *Rosa-CreER^{T2}/Porcn^{Del}* mice. Representative graph of Myeloid progenitors gating based on donor cells (CD45.1). (n = 4 and 5 for primary recipient of *Porcn^{WT}* and *Porcn^{Del}* mice, respectively) (Upper panel). Quantification of donor Myeloid progenitors frequency in total BM cells of recipient mice. (Lower panel)

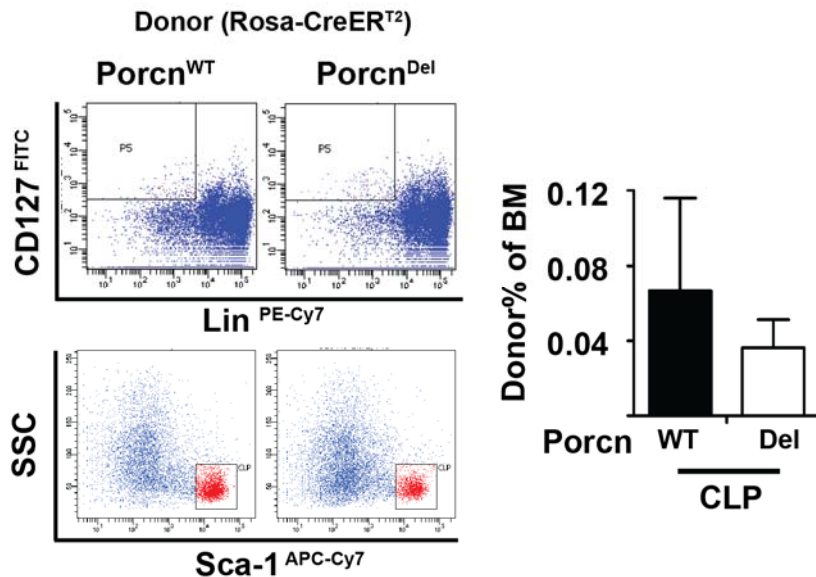


Figure 3.19 Normal CLP frequency in primary recipient of *Rosa-CreER^{T2}/Porcn^{Del}* mice. Representative graph of Common Lymphoid progenitor gating based on donor cells (CD45.1) (n = 4 and 5 for primary recipient of *Porcn^{WT}* and *Porcn^{Del}* mice, respectively, left panel). Quantification of donor CLPs frequency in total BM cells of the recipient mice (right panel, p > 0.05 Mann-Whitney test).

To test the self-renewal capacity of *Porcn*^{Del} HSCs, BM samples from the primary recipient mice were transplanted into secondary lethally irradiated mice. We observed successful reconstitution of both *Porcn*^{WT} and *Porcn*^{Del} HSC in secondary recipient mice (Figure 3.20 A and B, Figure 3.21, Figure 3.22 A and B). Thus, HSCs of the *Rosa-CreERT2/Porcn*^{Del} mice were phenotypically normal in the absence of Wnt secretion and were able to reconstitute the BM of the primary and secondary BMT recipient mice.

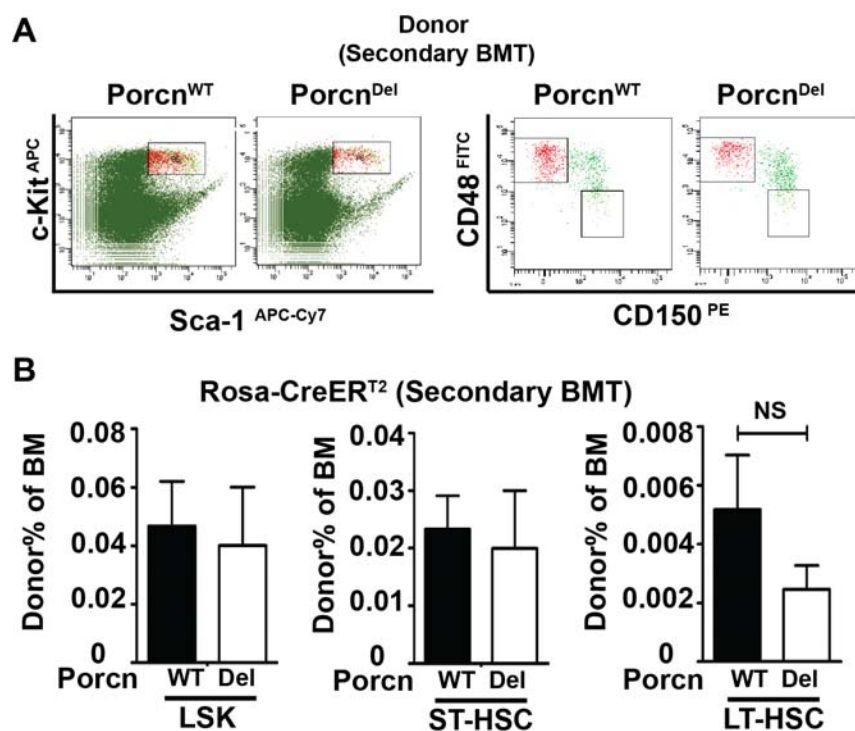


Figure 3.20 Normal HSCs frequency in Secondary BMT recipient mice. A) Representative of LSK, LT-HSC, and ST-HSC gating from *Porcn*^{WT} and *Porcn*^{Del} flow cytometer data were shown in scattered graphs. B) Frequency of different HSCs in total live Bone Marrow (BM) cells was summarized in three separate graphs ($p > 0.05$, Mann-Whitney test).

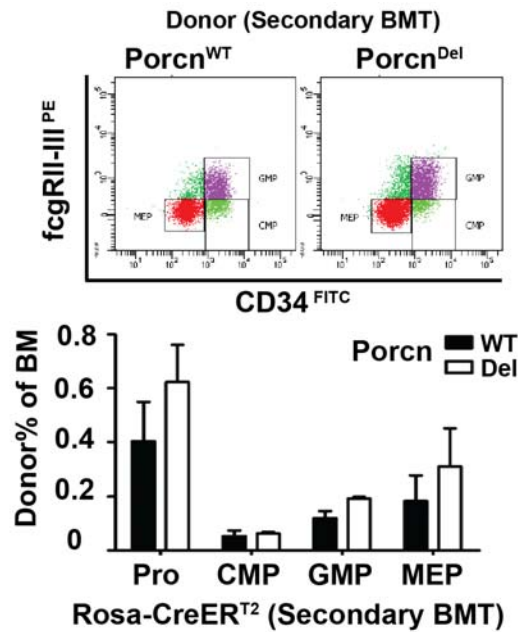


Figure 3.21 Normal frequency of Myeloid progenitors in Secondary BMT recipient mice. Representative of progenitor (Pro), CMP, GMP, and MEP gating from *Porcn*^{WT} and *Porcn*^{Del} flow cytometer data were shown in scattered graphs (Top panel). Quantification of different progenitor (Pro), CMP, GMP, and MEP in total live Bone Marrow (BM) cells (Bottom panel) ($p > 0.05$, Mann-Whitney test).

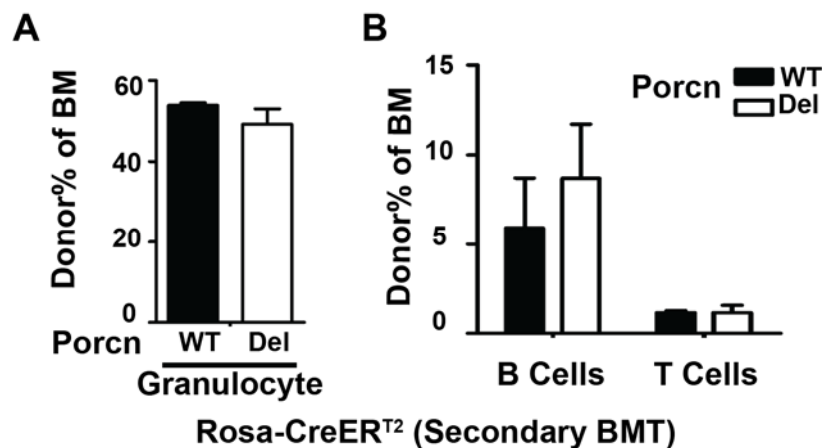


Figure 3.22 Normal WBC frequency in Secondary BMT recipient mice of *Rosa-CreER*^{T2}/*Porcn*^{Del}. **A)** Quantification of donor Neutrophils frequency in total BM cells of Secondary BMT recipient mice. **B)** Quantification of donor Lymphocytes frequency in total BM cells of Secondary BMT recipient mice.

3.2.3 Normal hematopoiesis following *Porcn* inactivation in hematopoietic cells.

The lack of significant effect on hematopoiesis after excision of *Porcn* with the *Rosa-CreER^{T2}* driver was unexpected. We considered the possibility that while we had significantly reduced PORCN function (e.g. as demonstrated by reduction of *Porcn* mRNA), subtotal excision of *Porcn* in *Rosa-CreER^{T2}/*Porcn*^{Del}* mice left sufficient Wnt secretion to maintain normal function. As a second test, we crossed *Porcn^{fllox}* mice with *Mx1-Cre* mice to get more complete and specific excision of *Porcn* in HSC after induction of *Cre* expression in adult mice.

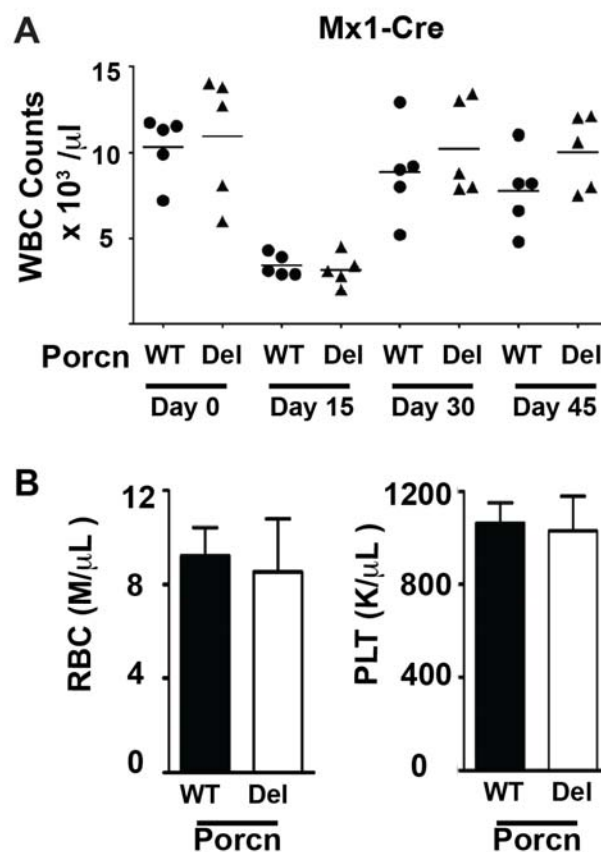


Figure 3.23 Normal WBC counts in *MX1-Cre/Porcn^{Del}* mice. **A)** Normal white blood cell (WBC) counts after *Cre* mediated inactivation of *Porcn* in *MX1-Cre/Porcn^{fllox}* mice. Injection of Poly I:C caused leukopenia within 15 days in both *Porcn^{Del}* and *Porcn^{WT}* mice; however, both control and inactivate

Porcn mice recovered to normal WBC after 30 days Poly I:C injection. ($p > 0.05$ Mann-Whitney test). **B**) Normal red blood cell (RBC) counts were observed in both *Mx1-Cre/Porcn^{WT}* and *Porcn^{Del}* mice (left panel). Platelet (PLT) counts was normal in both *Mx1-Cre/Porcn^{WT}* and *Porcn^{Del}* mice (right panel) ($n = 5$ per group).

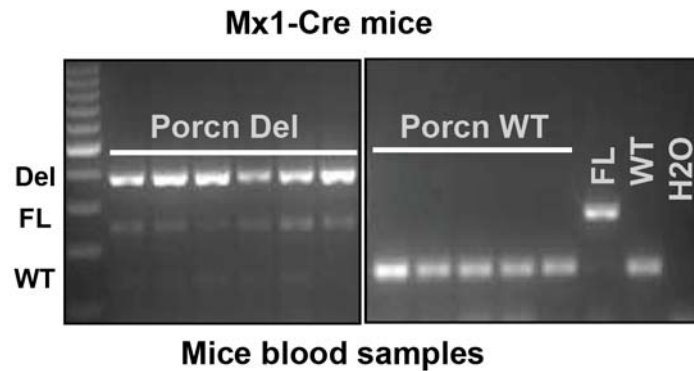


Figure 3.24 *Porcn* deletion in blood samples of *Mx1-Cre/Porcn^{Del}* mice. Cre expression leads to *Porcn* deletion in blood samples of *Mx1-Cre/Porcn^{Del}* mice as assessed by PCR of gDNA (Del: excised *Porcn* allele, FL: floxed allele, WT: wild type allele). Each lane represents an individual mouse.

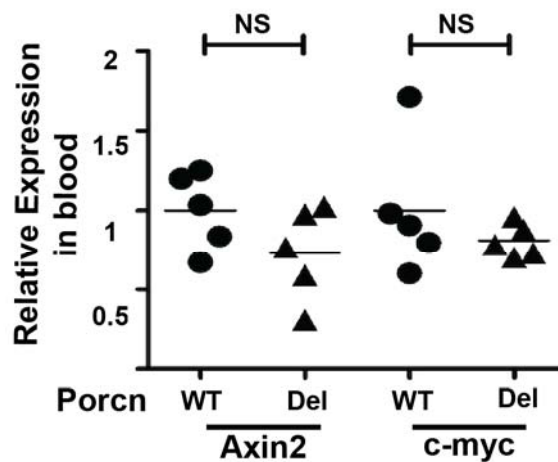


Figure 3.25 Wnt/ β -catenin target genes were not down-regulated in blood samples of *Mx1-Cre/Porcn^{Del}* mice. Expression of *Axin2*, and *c-myc* were normalized to *Pgk* and *HPRT* ($n = 5$ mice in each group, $p > 0.05$, Mann-Whitney test).

To excise *Porcn* in hematopoietic cells, *Mx1-Cre/Porcn^{fllox}* and *Porcn^{WT}* mice received poly I:C every other day for 7 doses. The blood counts of mice were then monitored over three months. A normal recovery of WBCs was

observed in both the *Porcn*^{WT} and *Porcn*^{Del} mice 15 days after the poly I:C injections (Figure 3.23 A). In addition, RBCs and platelets were in the normal range (Figure 3.23 B). Extensive excision of *Porcn* was confirmed in blood samples from the *Mx1-Cre/Porcn*^{Del} mice (Figure 3.24). However, unlike what was seen with the *Rosa-CreER*^{T2} driven more extensive knockout, expression of Wnt target genes did not change after the more restricted *Mx1-Cre*-driven *Porcn* knockout (Figure 3.25).

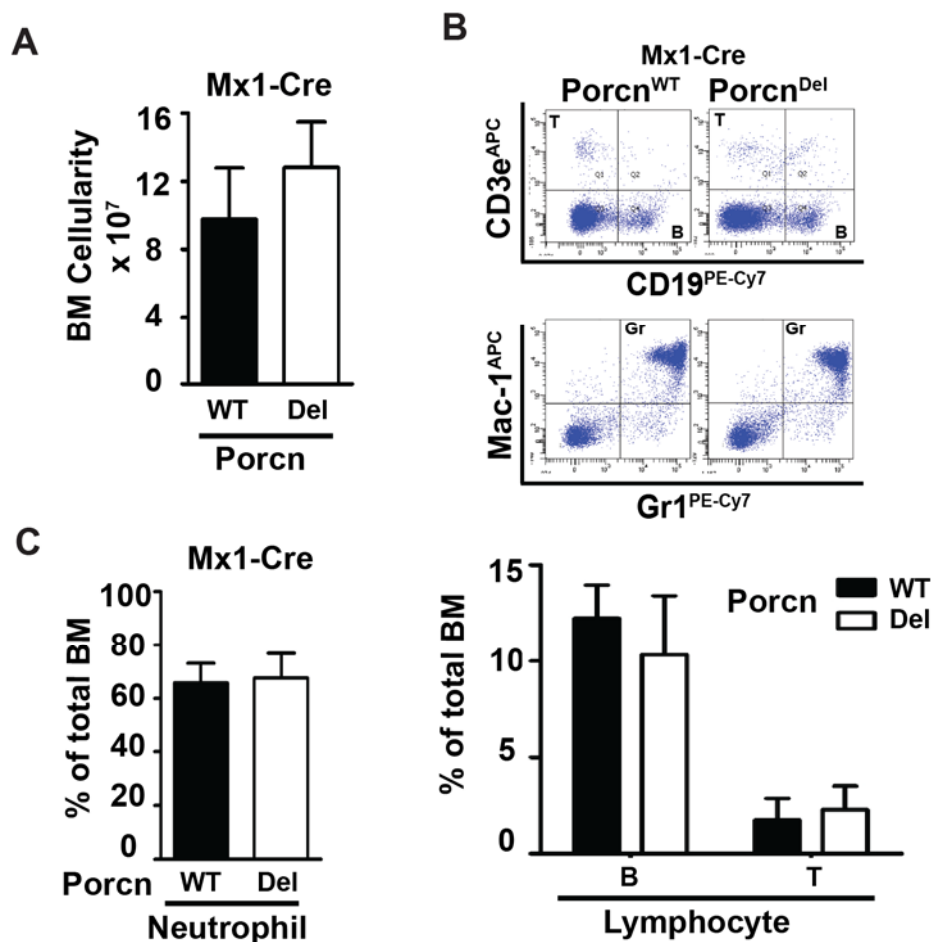


Figure 3.26 Neutrophils and Lymphocytes present at the normal ratio in *Mx1-Cre/Porcn*^{Del} mice. **A)** Total BM cell numbers were comparable in both *Mx1-Cre/Porcn*^{WT} (n = 3) and *Porcn*^{Del} mice (n = 3, 2 tibia and femur, p = 0.4, Mann-Whitney test). **B)** Representative gating of flow cytometer data for B- and T-lymphocyte (top panel), monocyte and neutrophil (bottom panel). **C)** BM differentiated cells (Neutrophils and Lymphocytes) present at the normal ratio in *Mx1-Cre/Porcn*^{Del} mice compared to *Mx1-Cre/Porcn*^{WT} mice after 6 months of *Porcn* excision. Quantification of Neutrophils frequency in live BM

cells was shown in left graph and quantification of Lymphocytes frequencies were shown in right graph (n = 4 per group of mice).

To test hematopoiesis, mice were sacrificed 4 months after poly I:C treatment, with subsequent analysis of their BM cells. The BM cell counts were within normal range in both *Mx1-Cre/Porcn^{Del}* mice and *Porcn^{WT}* mice (Figure 3.26 A). The frequency of BM neutrophils and lymphocytes were not different in *Porcn^{WT}* and *Porcn^{Del}* mice as measured by flow cytometry (Figures 3.26 B and C).

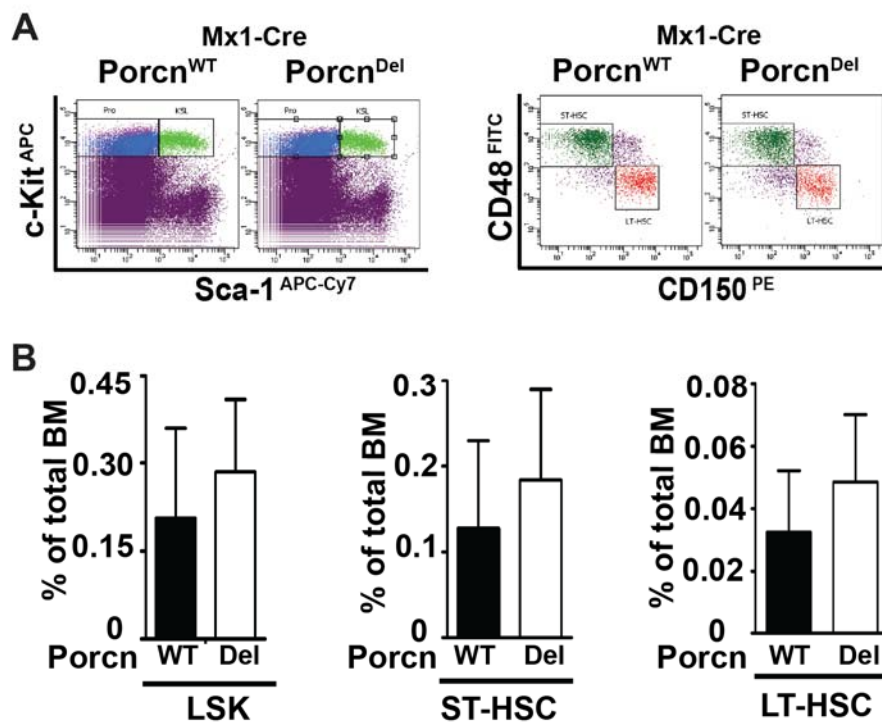


Figure 3.27 The frequency of LSK, LT-HSC, and ST-HSC did not change between *Mx1-Cre/Porcn^{WT}* and *Porcn^{Del}* mice. **A)** Representative gating of flow cytometer data for HSCs. **B)** LSK cells (Lin⁻, Sca1⁺, c-Kit⁺), ST-HSC, and LT-HSC frequency of BM cells in *Mx1-Cre/Porcn^{WT}* and *Mx1-Cre/Porcn^{Del}* (n = 4 per group).

In addition, the frequencies of HSCs and progenitors did not significantly change in the BM of *Mx1-Cre/Porcn^{Del}* and *Porcn^{WT}* mice (Figure 3.27 and 3.28). Moreover, *Porcn^{Del}* BM cells were able to form all types of myeloid and

erythroid colonies (Figure 3.29 A). Quantitative real time PCR on genomic DNA from BM, blood as well as hematopoietic colonies confirmed a near total excision of *Porcn* (Figure 3.29 B) in *Mx1-Cre/Porcn^{Del}* mouse.

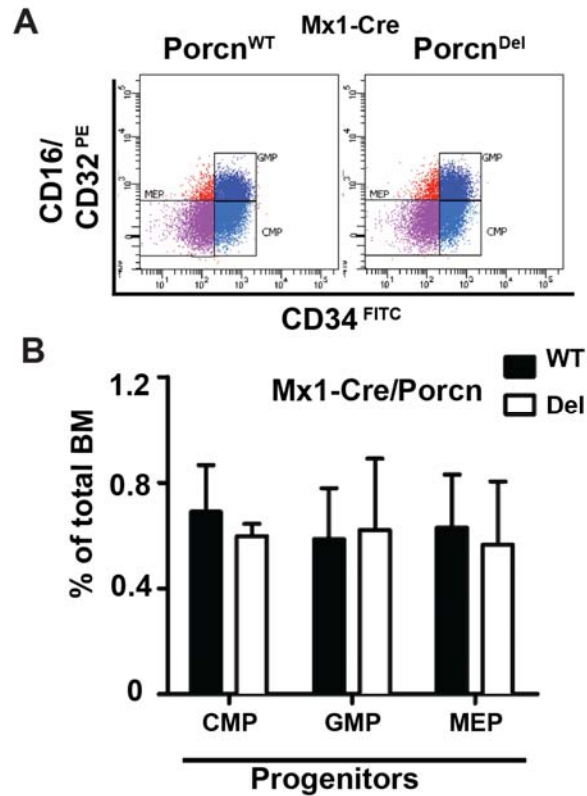


Figure 3.28 The frequency of myeloid progenitors did not change between *MX1-Cre/Porcn^{WT}* and *Porcn^{Del}* mice. **A)** Representative gating of flow cytometer data for myeloid progenitor. **B)** Myeloid progenitors frequency of BM cells in *Mx1-Cre/Porcn^{WT}* and *Mx1-Cre/Porcn^{Del}* (n = 4 per group).

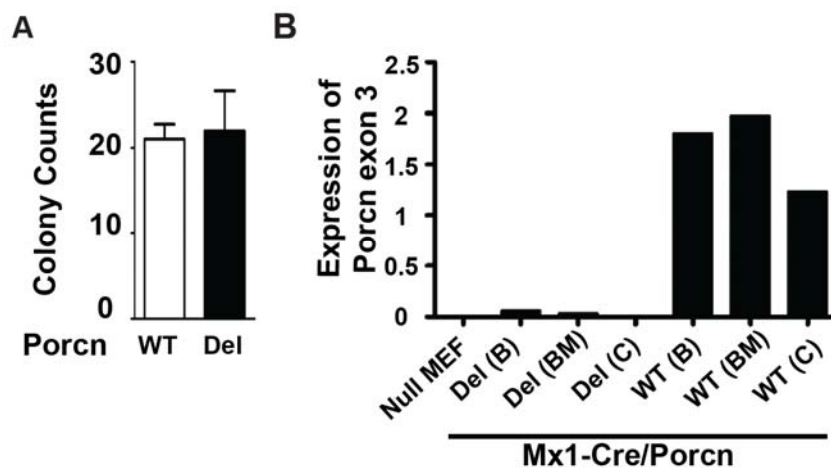


Figure 3.29 Normal differentiation ability of *Porcn* deleted HSC in colony forming assay. **A)** Quantification of total number of colonies (CFU-GM,

BFU-E, and CFU-GEMM) from 3 wells in each group. **B)** Relative expression of genomic *Porcn* exon3 by Real Time-PCR. Expression of *Porcn* exon3 assessed in Null MEF (*Porcn*^{Del} Mouse Embryonic Fibroblast), blood (B), bone marrow (BM), and colonies (C) of *Mx1-Cre/Porcn*^{Del} and *Porcn*^{WT} mice.

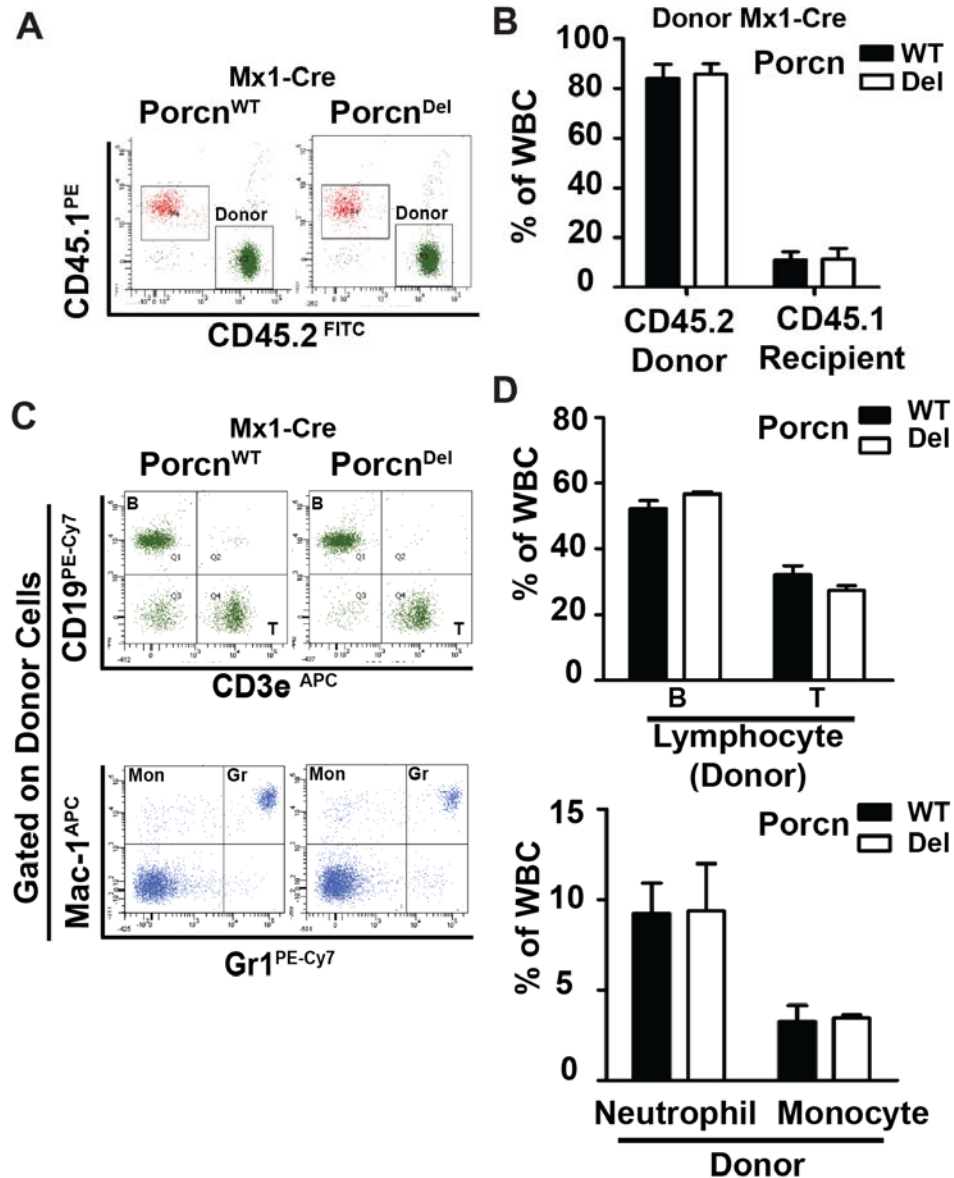


Figure 3.30 Successful BM reconstitution of *Porcn* inactivated donor HSCs in recipient mice. **A)** Blood cells were stained for CD45.1⁺ (recipient) and CD45.2⁺ (donor). **B)** Successful primary bone marrow transplantation after 8 weeks in recipient mice from both *Mx1-Cre/Porcn*^{Del} and *Porcn*^{WT} bone marrow. **C)** Donor cells (CD45.2⁺, CD45.1⁻) were gated for B-Lymphocyte (CD19⁺, CD3e⁻) and T-lymphocyte (CD19⁻, CD3e⁺) (top panel), and Monocytes (Mac1⁺, Gr1⁻) and Neutrophil (Mac1⁺, Gr1⁺) (bottom panel) (n = 4 mice per group). **D)** *Porcn*^{Del} donor cells were able to reconstitute BM of irradiated recipient mice with the same ratio as *Porcn*^{WT} donors. Quantification of blood donor Lymphocytes and Neutrophils were summarized in left and right panels, respectively.

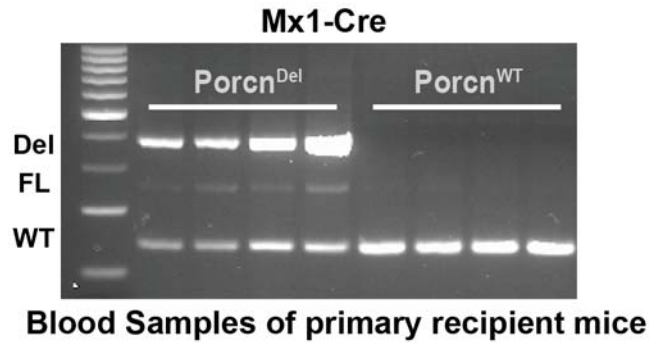


Figure 3.31 Donor *Mx1-Cre/Porcn^{Del}* BM cells were able to reconstitute in primary BMT recipient mice. *Porcn* excised band was present in genomic PCR of blood samples from primary BMT recipient mice (Del: excised *Porcn* allele, FL: floxed allele, WT: wildtype allele). Each lane represents an individual recipient mouse.

To test the self-renewal ability of *Mx1-Cre/Porcn^{Del}* HSCs, BM samples from the *Porcn^{Del}* and *Porcn^{WT}* mice (CD45.2) were transplanted into lethally irradiated recipient mice (CD45.1). The successful reconstitution of the donor BM cells was shown by FACS analysis of the primary recipient's blood samples (Figure 3.30 A, and B). *Porcn* excised blood cells were identified within blood samples of primary BMT mice by genomic PCR, again ruling out the possibility that non-excised *Porcn* HSCs were responsible for hematopoietic (Figure 3.31). To test the normal function of *Porcn^{Del}* HSCs, the primary recipient mice were sacrificed 6 months following BMT and their BM was subsequently transplanted to into secondary recipient mice. The secondary recipient mice survived more than one year and their BM analysis showed successful reconstitution from donor BM cells. A representative FACS analysis of BM from primary and secondary transplanted mice is shown in tables 1 and 2.

Table 3.1 Frequency of HSCs and progenitors in total live BM cells from primary BMT recipients of *Mxl-Cre/Porc^{WT}* and *Porc^{Del}* mice (n = 2 for each group).

Donor Genotypes	KSL%	Short term HSC%	Long Term HSC%	CLP%	CMP%	GMPP%	MEP%
<i>MXI-Cre/Porc^{WT}</i>	0.0636	0.0446	0.0052	0.0012	0.31	0.27	0.33
<i>MXI-Cre/Porc^{WT}</i>	0.0348	0.193	0.0069	0.0315	0.23	0.44	0.52
<i>MXI-Cre/Porc^{Del}</i>	0.0410	0.279	0.33	0.0025	0.31	0.22	0.34
<i>MXI-Cre/Porc^{Del}</i>	0.377	0.192	0.0081	0.0648	0.33	0.27	0.36

Table 3.2 Frequency of HSCs and progenitors in total live BM cells from secondary BMT recipients of *Mx1-Cre/Porcⁿ^{WT}* and *Porcⁿ^{Del}* mice (n = 2 for each group).

Donor Genotypes	KSL%	Short term HSC%	Long Term HSC%	CLP%	CMIP%	GMP%	MEIP%
<i>MXI-Cre/Porcⁿ^{WT}</i>	0.01021	0.00256	0.00306	0.0260	0.05	0.03	0.24
<i>MXI-Cre/Porcⁿ^{WT}</i>	0.00654	0.01084	0.00275	0.0215	0.09	0.10	0.15
<i>MXI-Cre/Porcⁿ^{Del}</i>	0.00512	0.00208	0.00056	0.0139	0.04	0.07	0.09
<i>MXI-Cre/Porcⁿ^{Del}</i>	0.01668	0.00429	0.00103	0.0154	0.16	0.14	0.35

Overall, deletion of *Porcn* and inhibition of Wnt secretion from hematopoietic cells did not affect proliferation, differentiation, and self-renewal of HSC in *MX1-Cre/Porcn^{Del}* mice. These results suggest that hematopoietic Wnts are dispensable for maintenance of HSCs. In addition, there was no increase of granulopoiesis in colony forming assay and in *MX1-Cre/Porcn^{Del}* mice. Therefore, the increased granulopoiesis in *Rosa-CreER^{T2}/Porcn^{Del}* mice could be secondary to other phenotypes such as hair loss and neurological phenotypes, but not inhibition of Wnt secretion in HSCs or progenitor cells.

One confounding issue was the subtotal excision of *Porcn* in the hematopoietic system by using Mx1-Cre mice, evidenced by observation of a faint floxed, non-excised band in the genomic PCR of blood and BM samples. This raised the possibility that hematopoiesis was rescued by a small population of *Porcn^{flox}* cells. To address this issue, *Porcn^{flox}* mice were crossed to *Vav-Cre* (constitutive Cre expression in adult hematopoietic and endothelial cells) mice to obtain complete *Porcn* excision in hematopoietic cells.

3.2.4 Murine hematopoietic Wnts are dispensable for adult hematopoiesis.

To achieve a complete inhibition of Wnt secretion from hematopoietic cells, *Porcn^{flox}* mice were bred with *Vav-Cre* mice (de Boer et al., 2003), where there is constitutive expression of Cre in all hematopoietic lineages from early in development. If hematopoietic Wnts are essential at any point after *Vav* expression begins, *Vav-Cre/Porcn^{Del}* mice should exhibit impaired hematopoiesis. Again unexpectedly, *Vav-Cre/Porcn^{Del}* mice were developmentally normal, fertile and they did not show any gross phenotype.

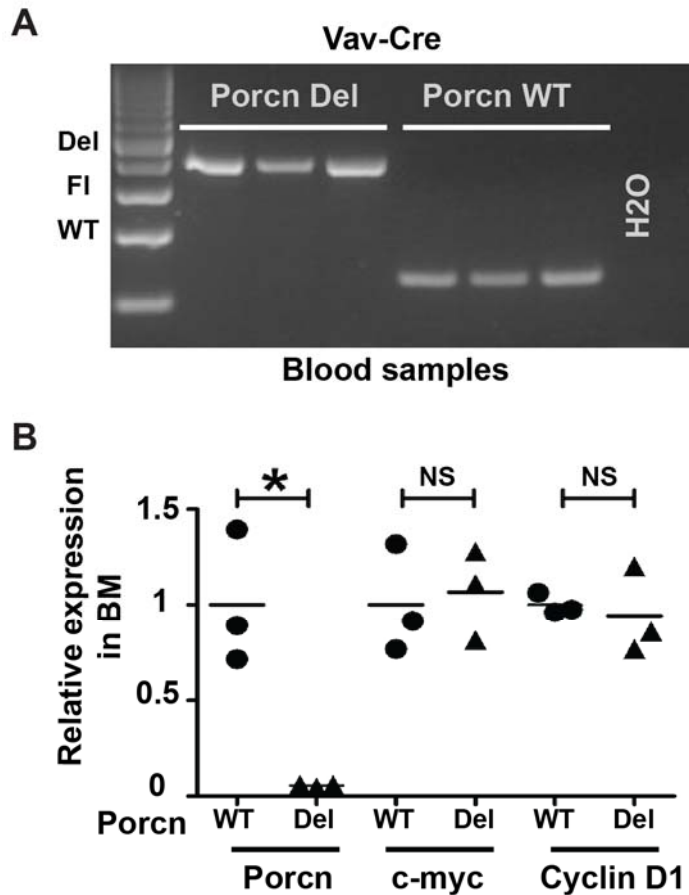


Figure 3.32. Complete deletion of *Porcn* in blood samples of *Vav-Cre/Porcn^{Del}* mice. **A) A complete excision of *Porcn* in blood samples of *Vav-Cre/Porcn^{lox}* mice was assessed by PCR of gDNA (Del: excised *Porcn* allele, FL: floxed allele, WT: wild type allele). Each lane represents an individual mouse. **B)** Expression of Wnt target genes (*c-myc* and *Cyclin D1*) was not down-regulated in *Porcn* inactivated BM samples. No expression of *Porcn* was detected in BM samples of *Vav-Cre/Porcn^{Del}* mice (n = 3 per group, two tailed T test).**

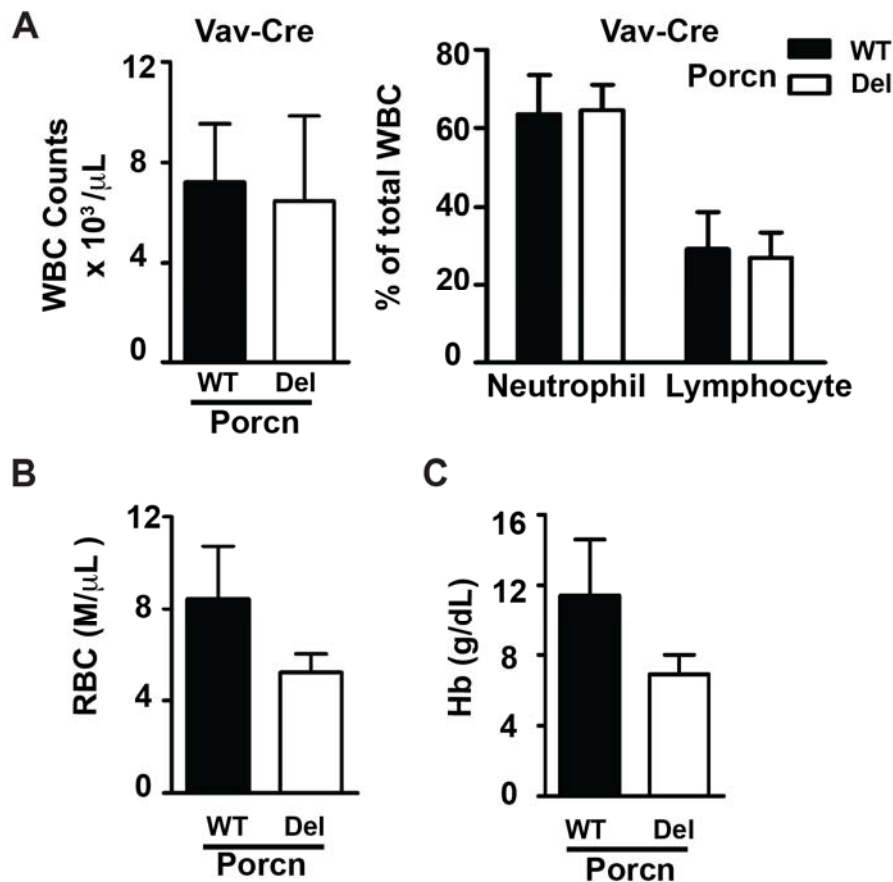


Figure 3.33 Normal CBC in *Vav-Cre/Porcn*^{Del} mice. **A)** Normal white blood cell counts was observed in blood samples of *Vav-Cre/Porcn*^{WT} (n = 4) and *Porcn*^{Del} mice (n = 4) (left panel). Frequency of lymphocyte and neutrophils were in normal range in both group of mice (right panel) (p > 0.05, Mann-Whitney test). **B)** Normal red blood cell counts was observed in both *Vav-Cre/Porcn*^{WT} and *Porcn*^{Del} mice (n = 4 per group, p > 0.05, Mann-Whitney test). **C)** *Porcn*^{Del} mice had normal level of hemoglobin (Hb) in comparison to *Porcn*^{WT}. (n = 4 per group, p > 0.05, Mann-Whitney test).

Complete deletion of the *Porcn* gene in the hematopoietic lineage was confirmed in the blood and BM samples of the *Vav-Cre/Porcn*^{Del} mice by genomic PCR and RT-PCR (Figure 3.32 A, and B). However, the expression of Wnt target genes including *c-myc* and *Cyclin D1* were not affected in the BM of the *Vav-Cre/Porcn*^{Del} mice (Figure 3.32 B). Additionally, the CBC revealed normal WBC, RBC and Hb level in both *Vav-Cre/Porcn*^{WT} and *Vav-Cre/Porcn*^{Del} mice (Figure 3.33 A, B and C). Furthermore, there was no

difference in the frequencies of BM granulocytes, and lymphocytes, BM myeloid progenitors or common lymphoid progenitors in both the control and *Porcn^{Del}* mice (Figure 4C, D, E, and F S4 A, B, and C). Analysis of thymic cells also showed a normal population of double negative (DN), double Positive (DP), CD4 T-cells and CD8 T-cells in the *Vav-Cre/Porcn^{Del}* mice (Figure 4G, and 4H). In summary, *Vav-Cre/Porcn^{Del}* mice exhibited normal hematopoiesis in the absence of Wnt secretion from hematopoietic cells.

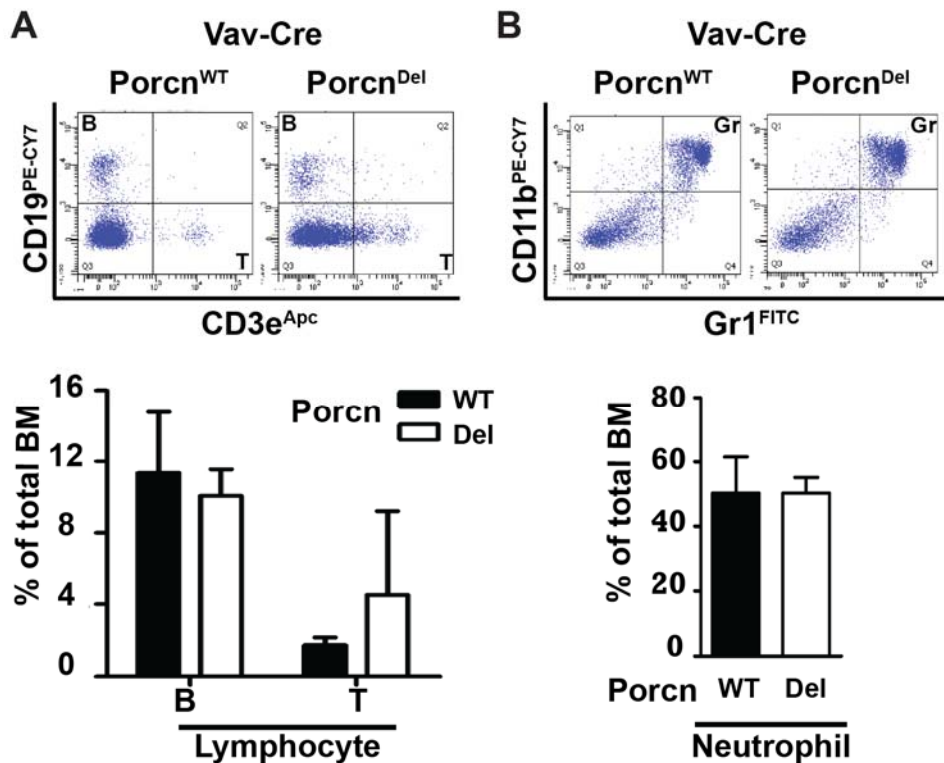


Figure 3.34 Normal lymphocyte and neutrophil frequency in BM samples of *Vav-Cre/Porcn^{Del}* mice. A) *Vav-Cre/Porcn^{Del}* mice had normal frequency of lymphocytes in their BM cells compared to *Vav-Cre/Porcn^{WT}* mice (n = 3 per group, Mann-Whitney test). Representative gating of flow cytometer data for B- and T-lymphocyte (upper panel) B) *Vav-Cre/Porcn^{Del}* mice had normal frequency of neutrophils in their BM cells compared to *Vav-Cre/Porcn^{WT}* mice (n = 3 per group, Mann-Whitney test). Representative gating of flow cytometer data for monocyte and neutrophil (upper panel).

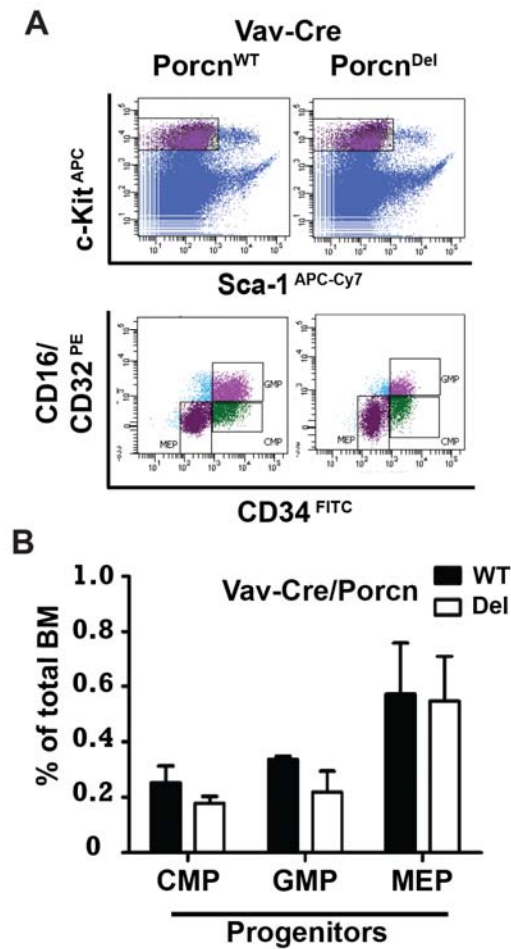


Figure 3.35 Normal myeloid progenitors numbers in *Vav-Cre/Porcn^{Del}* mice. A) Representative gating of flow cytometer data for myeloid progenitors. B) Similar myeloid progenitors frequency was observed in total BM cells of *Vav-Cre/Porcn^{WT}* and *Porcn^{Del}* mice. (n = 3 per group, Mann-Whitney test).

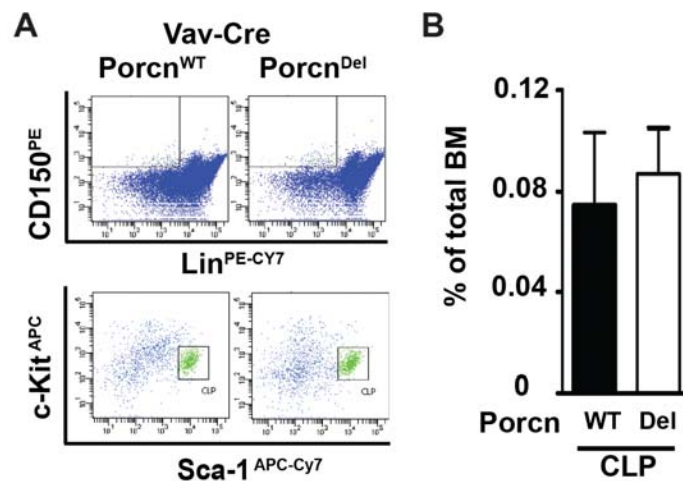


Figure 3.36 Normal lymphoid progenitor numbers in *Vav-Cre/Porcn^{Del}* mice. A) Representative gating of flow cytometer data for common lymphoid

progenitor **B**) Similar Common Lymphoid progenitors (CLP) frequency was observed in total BM cells of *Vav-Cre/Porcⁿ^{WT}* and *Porcⁿ^{Del}* mice (n = 3 per group, Mann-Whitney test).

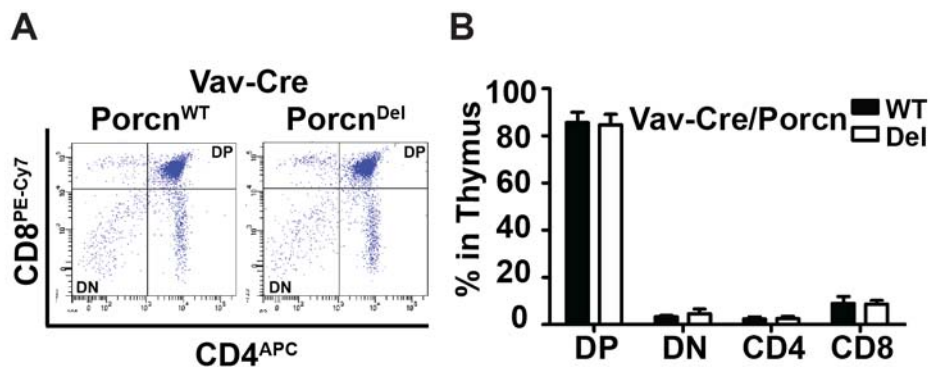


Figure 3.37 Normal differentiation of T-lymphocytes in thymus of *Vav-Cre/Porcⁿ^{Del}* mice. **A)** Representative graph of flow cytometer data from isolated cells of thymus in two groups of mice. **B)** Normal frequency of differentiated and undifferentiated T cell types was observed in *Vav-Cre/Porcⁿ^{Del}* compared to *Vav-Cre/Porcⁿ^{WT}* mice (DP: double positive (CD8⁺,CD4⁺), DN: double negative (CD8⁻,CD4⁻), CD4 T cells (CD4⁺,CD8⁻), CD8 T cells (CD4⁻, CD8⁺), n = 3 per group, Mann-Whitney test).

3.3 Discussion

In this study, we genetically inhibit Wnt secretion by targeting *Porcn* in hematopoietic system and confirmed that hematopoietic production of Wnts is entirely dispensable for the maintenance, proliferation and differentiation of adult HSCs. *Porcn* excision using three different Cre drivers consistently produced no overt hematopoietic phenotype. This result suggests that if Wnts are important in the maintenance of hematopoiesis, they must be coming from the stroma or stem cell niche. However, no significant hematopoietic phenotype was observed even with the *Rosa-CreER^{T2}* driver where some stromal excision is expected. One limitation of the study is that we did not completely excise *Porcn* in the bone marrow niche. Further studies will be needed to address the role of niche as a source of Wnts for maintenance of HSCs.

The role of stroma as stem cell niche was recently established in the mouse intestine, where we showed that epithelial cell Wnt secretion was not essential, and that stromal myofibroblasts could supply the Wnts required for epithelial proliferation.

Because, we did not target *Porcn* in the BM niche of *MX1-Cre* and *Vav-Cre* mice and deletion of *Porcn* in BM niche of *Rosa-CreER^{T2}/Porcn^{Del}* mice was not also complete.

The role of Wnts in self-renewal of HSC has been proposed long time ago, but it still remains controversial. Studies that support role of Wnts in maintenance of HSC mostly targeted the key proteins downstream of canonical Wnt signaling pathways such as β -catenin, APC, and GSK β (Inoki et al., 2006; Qian et al., 2008; Trowbridge et al., 2006; Zhao et al., 2007). However, these proteins especially β -catenin can be regulated by other signaling pathways not only Wnts (Katoh and Katoh, 2006; Qiang et al., 2009). There are few studies that focus on Wnt ligands to address role of Wnts in self-renewal of HSC (Louis et al., 2008; Luis et al., 2009). Luis et al. showed Wnt3a deficient fetal HSC are not able to reconstitute the secondary BMT, indicating self-renewal defect of Wnt3a^{-/-} HSCs in Wnt3a^{+/+} recipient mice. These results could show autonomous or non-autonomous effect of Wnt3a, since fetal Wnt3a^{-/-} HSCs were collected from total body Wnt3a^{-/-} mice, where the niche of HSCs is also Wnt3a deficient. Moreover, Wnts might have differential role during embryonic or adult hematopoiesis, both Luis et al. and Louis et al. evaluated the role of Wnt3a^{-/-} and Wnt4^{-/-} in fetal HSC, not adult HSCs. We focus on adult hematopoiesis and could not find any role of Wnts in adult hematopoiesis by targeting Wnt secretion in hematopoietic cells.

This discrepancy could be due to difference in embryonic hematopoiesis and adult hematopoiesis, or due to targeting HSCs, but not BM niche.

The source of Wnts for hematopoiesis is also unclear. Both stromal niche and hematopoietic cells express different Wnt ligands and were proposed to be involved in different steps of hematopoiesis (Austin et al., 1997; Van Den Berg et al., 1998). For example, non-canonical Wnts such as Wnt5a is widely expressed in HSCs, progenitors, differentiated blood cells, and stromal cells. Wnt5a was previously shown to be involved in maintenance of HSCs by inhibiting canonical Wnt signaling (Buckley et al., 2011; Nemeth and Bodine, 2007; Nemeth et al.). In addition, Wnt5a could negatively regulate B lymphopoiesis in mice. This phenotype was explained as a cell autonomous effect of Wnt5a from HSCs, because the wildtype recipient mice that received donor fetal Wnt5^{-/-} HSCs showed more B cell numbers in spleen and their BM (Liang et al., 2003). However, these Wnt5a^{-/-} progenitors were obtained from a Wnt5a^{-/-} niche (Wnt5a^{-/-} mice), where the lack of Wnt5a might reprogram the fate of HSCs and progenitors towards B cell proliferation, a possible non-autonomous effect of Wnt5a. Recently, Sugimura et al. also found that non-canonical Wnts could maintain self-renewal of HSCs by keeping LT-HSCs in quiescent stage through the interaction of Flamingo and Frizzled-8 in BM osteoblasts niche (Sugimura et al., 2012). In contrast, Floria et al. demonstrate a crucial role for stem-cell-intrinsic, but not extrinsic, effect of Wnt5a signaling in HSC ageing and exclude the niche involvement in aging process. Our results from *Porcn^{Del}/Mx1-cre* and *Porcn^{Del}/Vav-cre*, can exclude any autonomous effect of canonical and non-canonical Wnts in murine adult hematopoiesis. Thus, if Wnts are important for adult hematopoiesis, they

might come from different cell types of the niche and support hematopoiesis, but not from the hematopoietic cells.

Canonical and non-canonical Wnt signaling might inversely regulate hematopoiesis. For instance, the pattern of canonical and non-canonical Wnt expression is distinctive in hematopoietic tissue. Wnt3a and Wnt10b are only expressed in HSCs, while the non-canonical Wnt5a is expressed in many hematopoietic cells and stromal cells. Non-canonical Wnt signaling could antagonize Wnt/ β -catenin signaling in HSCs and enhances their repopulation capacity (Nemeth and Bodine, 2007). However, inhibition of Wnt/ β -catenin signaling in HSCs showed impaired hematopoiesis in mice (Fleming et al., 2008; Luis et al., 2011; Schaniel et al., 2011; Zhao et al., 2007). In our study, we suppress both canonical and non-canonical Wnts in all hematopoietic cells and partially in BM niche (using the *Rosa-CreER^{T2}* driver), but we observed intact hematopoiesis. It is possible that there is a balance between canonical and non-canonical pathways to control precise hematopoiesis. Consequently, disruption of each Wnt/ β -catenin or non-canonical Wnt pathways could affect hematopoiesis. In contrast, targeting all Wnt pathways together by inhibiting Wnt secretion might have limited effects on hematopoiesis. This is a reassuring finding as novel agents that pharmacologically inhibit Porcn function enter clinical trials.

3.4 Materials and methods

3.4.1 Mouse strains

Generation of *Porcn* conditional null allele was described previously (Biechele et al., 2013). *Porcn^{fllox}* mice were backcrossed to C57BL/6 mice. To

generate conditional deletion of *Porcn* in hematopoietic cells, *Porcn^{fllox}* mice were crossed with *Rosa-CreER^{T2}* (Hameyer et al., 2007), *Mx1-Cre* (Kühn et al., 1995), and *Vav-Cre* (de Boer et al., 2003). We used age and gender-matched mice as controls for all experiments. For BM transplantation C57BL6/Ly5.1 mice were used. All mouse procedures were applied based on approval of Institutional Care and Use Committees (IACUC).

3.4.2 Genotyping and quantitative RT-PCR

Porcn genotyping was done based on Biechele et al. RNA extraction was performed using RNEasy mini (Qiagen, cat: 74106) and cDNA synthesis were done based on i-script RT (Bio- Rad, Cat#1708891) kits following the manufacturer's instructions. SsoFast EvaGreen PCR kit (Bio-Rad, Cat#1725205) was used for Real-time PCR assay on Bio-Rad CFX96 real-time cycling machine. Each PCR reaction was run for at least 40 cycles and data were analyzed by Bio-Rad CFX manager version 2.1 software. Q-PCR primers are listed in Table 2.1.

3.4.3 Inducible *Porcn* deletion

To induce systemic *Porcn* deletion in *Porcn^{fllox/Y}* or *Rosa-CreER^{T2}/Porcn^{fllox,fllox}*, mice were fed with Tamoxifen chow (80 mg/kg/BW assuming 20 gram mice eat 3 gram chow per day) for 5 days followed by normal chow for 2 days. This treatment was repeated for 3 consecutive weeks and then mice were fed normal chow for 2 to 4 weeks prior to sacrifice.

To induce *Porcn* deletion in hematopoietic cells and lymphocytes in *Porcn^{fllox/Y}* or *Mx1-Cre /Porcn^{fllox,fllox}*, mice were injected with 800 µg Poly I:C

every other day for 7 doses. Mice were monitored for 4 months after Poly I:C injection.

3.4.4 Complete Blood Counts (CBC)

Murine peripheral blood was collected from facial vein into EDTA-coated glass capillary tubes. The complete blood count (CBC) was done with a HemaVet.

3.4.5 Flow cytometry.

Single-cell suspensions from BM, blood, spleen, and thymus were analyzed by flow cytometry. Monoclonal antibodies conjugated with various dyes including allophycocyanin (APC), APC-Cy7, phycoerythrin (PE), PE-CY7, eFluor 450 or fluorescein isothiocyanate obtained from BD Pharmingen (BD), eBioscience or BioLegend. Here is the list of antibody used in our study: Gr-1 (8C5), CD3 (KT31.1), Mac-1/CD11b (M1/70), B220 (RA3-6B2), CD19 (1D3), TER119 (TER-119), CD4 (GK1.5), CD8 (53-6.7), c-Kit (2B8), Sca1 (E13-161-7), CD16/32 (2.4G3), CD48 (HM48-1), CD150 (TC15-12F12.2), CD45.1 (A20), and CD45.2 (104). Stained cells were examined with an LSRII flow cytometer (BD Biosciences) and sorted using a FACS Aria. Propidium iodide staining was performed to exclude the dead cells in our analysis. The same numbers of total bone marrow cells from *Porcn^{Del}* or control bone marrow were subjected to flow cytometry analysis. Diva software (BD) and FlowJo (Tree Star) were respectively used for data acquisition and analysis.

3.4.6 Bone Marrow Transplantation (BMT)

The total 1×10^6 bone marrow cells from either the control and *Rosa-CreER^{T2}/Porcn^{Del}* mice or *MXI-Cre/Porcn^{Del}* mice (CD45.2) were transplanted through tail vein injection into lethally irradiated CD45.1⁺ congenic recipient mice. To assess the successful BMT, blood samples of recipient mice were collected 8 weeks after transplantation and analyzed by FACS. Primary recipient mice were culled after 16 weeks of BMT and the BM cells were harvest for FACS analysis or secondary BMT assay. The total 1×10^6 BM cells from both control and *Porcn^{Del}* primary recipient mice (CD45.2) were transplanted through tail vein injection into lethally irradiated CD45.1⁺ congenic mice. To assess the successful secondary BMT, blood samples or BM cell of recipient mice were collected after 16 weeks of transplantation and analyzed by FACS.

3.4.7 Colony forming Assay

1×10^4 BM cells were incubated in the presence of Methocult M3434. After two weeks of incubation, the colony numbers were counted. All the assays were conducted in triplicate.

3.4.8 Tissue preparation for staining

Skin was harvested after sacrifice; washed with PBS and placed in 4% formalin over night, then transfer to 70% ethanol for 24 hours. Tissue processing, embedding, and Hematoxilin & Eosin staining were performed based on standard protocols. β -catenin antibody was purchased from Becton Dickinson (BD, Cat# 610154) and used at dilution of 1:150. Antigens retrieval

was done with boiling in citrate buffer, pH 6, for 10 minutes. Thereafter, samples were blocked in 1% BSA for 60 minutes. Tissues were incubated with primary antibody for 60 min, washed and subsequently incubated for 60 min with secondary antibody (BD, Cat #1706516) diluted 1:200. Sections were mounted in DPX medium and analyzed using a Leica DM2000 microscope.

3.4.9 Statistical analysis

Data were analyzed using Prism 5 software and Excel. Two-tailed T-test was performed in Excel for mac 2011 version 14.3.2.

4. Discussion and Conclusions

Pharmacological and genetic approaches were used in this thesis to identify the role of Wnt secretion in adult tissue homeostasis. Targeting PORCN, a key regulatory enzyme of the Wnt secretion pathway, we confirmed the role of Wnts in intestinal homeostasis and hair regeneration. In addition, we found that hematopoietic Wnts are dispensable for hematopoiesis. However, we were unable to identify the importance of Wnt signaling in murine adult hematopoiesis, likely due to the challenge in targeting *Porcn* within the BM niche. Additionally, *Porcn* deletion within the whole body of adult mice (*Rosa-CreER^{T2}/Porcn^{Del}*) demonstrated toxicity, such that the mice exhibited severe weight loss and neurological signs and symptoms. Collectively, these results indicate a potential role of Wnts in the maintenance of neural cells and their function. In this thesis, we focus on the role of Wnts in adult hematopoiesis and intestinal homeostasis.

4.1 Wnts in intestinal homeostasis

4.1.1 Conclusion

To identify the general toxicity of *Porcn* inhibition in adult mice, we crossed *Porcn^{fllox}* and *Rosa-CreER^{T2}* mice to generate *Rosa-CreER^{T2}/Porcn^{Del}* mice following tamoxifen administration. *Porcn* deletion in the adult mice was toxic, and the mice started to lose body weight after 3 weeks of tamoxifen administration. The experimental design and results are described in Chapter 3. To determine if the weight loss was due to abnormal intestinal homeostasis, mice were sacrificed 6-7 weeks after tamoxifen administration. Unlike the skin, there were no detectable gross or microscopic differences between the intestines of the *Rosa-CreER^{T2}/Porcn^{Del}* and *Rosa-CreER^{T2}/Porcn^{WT}* mice

(Figure 4.1 A, left and right top panels). Furthermore, immunohistochemical staining for β -catenin confirmed its nuclear localization in the small intestinal crypts of both the *Porcn*^{WT} and *Porcn*^{Del} mice (Figure 4.1 A left and right lower panels), indicating intact Wnt/ β -catenin signaling in the *Rosa-CreER*^{T2}/*Porcn*^{Del} crypt base cells. Accordingly, expression of the Wnt/ β -catenin target gene *Lgr5*, as well as intestinal stem cell markers such as *Olfm4* and *Bmi1*, did not differ between the *Rosa-CreER*^{T2}/*Porcn*^{Del} and *Rosa-CreER*^{T2}/*Porcn*^{WT} intestines (Figure 4.1 B). These data indicate that the Wnt/ β -catenin pathway is intact and functional in intestinal crypts when *Rosa-CreER*^{T2} is used for widespread inactivation of *Porcn*.

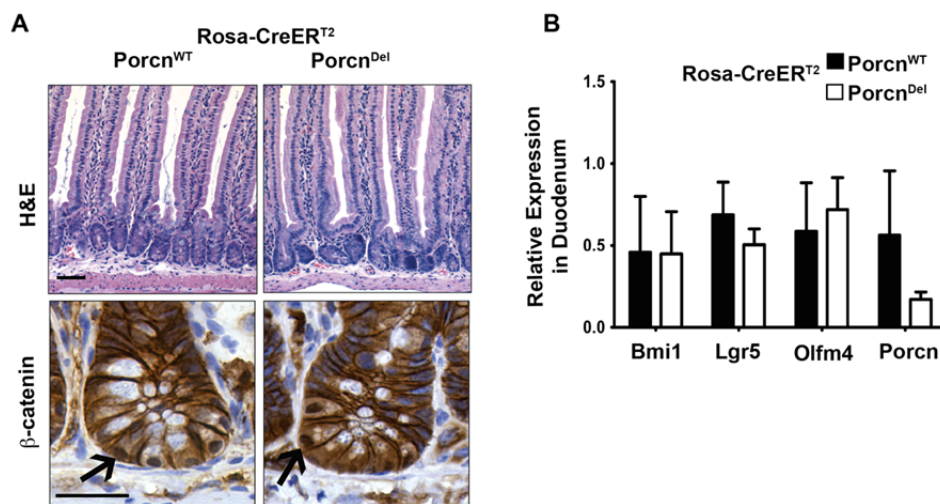


Figure 4.1 Normal small intestine histology and β -catenin distribution in *Porcn*-inactivated mice. A) β -catenin IHC shown in lower panels. Images show representative histopathology of at least 5 mice in each group. Note nuclear β -catenin localization in bottom of crypt (arrows). Scale bar = 100 μ m and 50 μ m in upper and lower panels, respectively. **B)** *Porcn* inactivation by *Rosa-CreER*^{T2} affects *Porcn* mRNA, but not expression of intestinal stem cell markers. qRT-PCR of samples from duodenum of *Porcn*^{WT} (n = 5, black bars) and *Porcn*^{Del} (n = 4, white bars) mice.

We confirmed by genomic PCR that there was substantial inactivation of *Porcn* in all regions of the gastrointestinal (GI) tract (Figure 4.2 A). There was no difference in the degree of *Porcn* inactivation in the mice examined up to 7 weeks after tamoxifen administration, suggesting there was no positive selection for crypts with the residual non-recombined alleles. Similar to the suggestion by Hameyer et al. that *Rosa-CreER^{T2}* gives satisfactory epithelial and poor stromal recombination in the small intestine, we confirmed that recombination appeared markedly less effective in the stroma (Figure 4.2 B) (Hameyer et al., 2007).

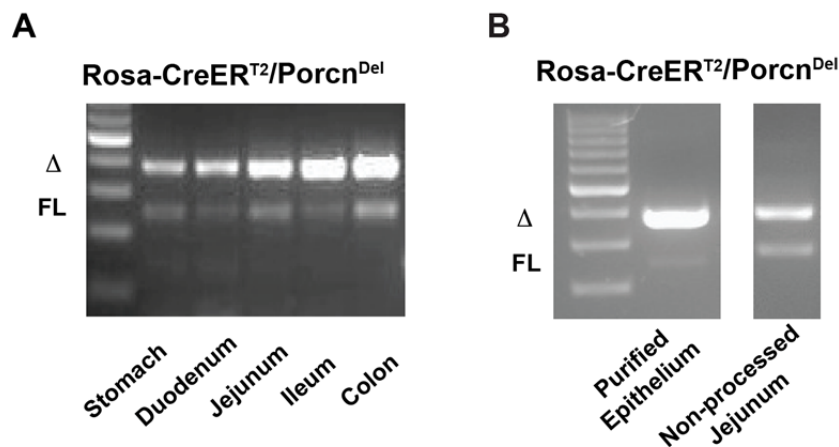


Figure 4.2 Preferential inactivation of *Porcn* in epithelium rather than stroma of *CreER^{T2}/Porcn^{Del}* intestine. **A)** Genomic PCR demonstrates substantial inactivation of *Porcn* in *Rosa-CreER^{T2}/Porcn^{Del}* intestine. Results from one mouse typical of > at least 5 mice per genotype tested. (Δ : excised *Porcn* allele, FL: floxed allele). **B)** Preferential inactivation of *Porcn* in epithelium rather than stroma after tamoxifen administration in *Rosa-CreER^{T2}/Porcn^{Del}* intestine. Note a substantial deletion of *Porcn* in epithelial compared to non-processed intestinal samples from the same mouse.

To functionally test if *Rosa-CreER^{T2}*-driven recombination resulted in a decrease in Wnt secretion, we assessed the ability of *Porcn^{Del}* intestinal epithelial crypt cells to form intestinal organoids, an *in vitro* assay that requires a source of active Wnts (Sato et al., 2011). Organoid formation was

reduced 6-fold when crypts from *Rosa-CreER^{T2}/Porcn^{Del}* mice were tested, consistent with the inactivation of Porcn in most, if not all, Paneth cells of the intestine (Figure 4.3 A and B). Substantial inactivation of Porcn (Figure 4.2 B), and hence functional Wnt secretion, in the intestinal epithelium (but not in the stroma of *Rosa-CreER^{T2}* mice) resulted in markedly impaired *ex vivo* organoid formation but normal intestinal homeostasis. Thus, we were ruled out the possible abnormal function of the small intestine as a potential cause of weight loss in the *Rosa-CreER^{T2}/Porcn^{Del}* mice.

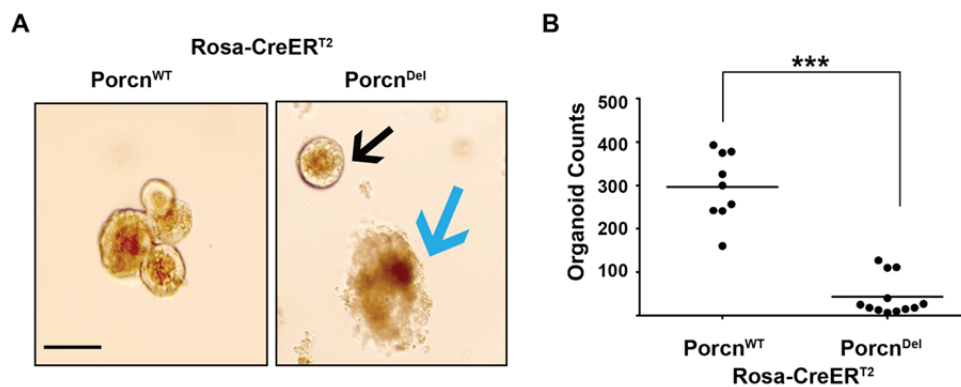


Figure 4.3 *Rosa-CreER^{T2}/Porcn^{Del}* crypts form less organoid than *Rosa-CreER^{T2}/Porcn^{WT}* crypts. A) *Rosa-CreER^{T2}/Porcn^{Del}* organoid cultures contain a small numbers of normal organoids (black arrows) and a large number of growth defective crypt cells (blue arrow). Scale bar equals 200 μ m. B) Quantification of organoids. Each data point is the number of organoids present per well. The figure combines data from three independent experiments (***) $p < 0.001$, two-tailed t-test).

Multiple Wnts (especially Wnt3, 6 and 9b) are expressed in murine intestinal epithelial cells, and Paneth cells in particular have been shown to be an important source of Wnts *in vivo* and in *ex vivo* culture (Gregorieff et al., 2005; Sato et al., 2009). Because the *Rosa-CreER^{T2}* driver did not inactivate Porcn in all Wnt-producing epithelial cells, we next crossed *Porcn^{fllox}* mice

with *Villin-Cre* mice (Madison et al., 2002). *Villin* expression begins in late embryogenesis in all epithelial cells of the intestine. Therefore, we predicted that embryonic epithelial inactivation of *Porcn* would be lethal in the neonatal period. To our surprise, *Villin-Cre/Porcn^{Del}* mice were viable and exhibited normal development. Further validation of *Porcn* deletion in *Villin-Cre/Porcn^{Del}* mice and phenotypes of these mice are reviewed in Chapter 2.

Below are our findings regarding the deletion of *Porcn* and the inhibition of Wnt secretion in intestinal epithelial cells:

1. Epithelial Wnts were dispensable for intestinal homeostasis in mice.
2. *Ex vivo* culture of intestinal epithelial cells (organoid culture) were dependent on epithelial Wnts and exogenous RSPO1.
3. Stromal cells, especially myofibroblast-like cells, expressed several Wnt ligands and RSPO3.
4. Stromal cells could support *ex vivo* culture of intestinal epithelial cells in the absence of epithelial Wnts and exogenous RSPO1.
5. Microarray data showed no compensation in any other signaling pathways in the stroma or epithelial cells of *Villin-Cre/Porcn^{Del}* mice compared to the *Villin-Cre/Porcn^{WT}* mice.
6. Intestinal epithelial Wnts were not required for regeneration of the intestinal epithelial cells following radiation stress.

Porcn deletion in the intestinal epithelial cells did not indicate the role of Wnt signaling in mouse intestinal stem cell self-renewal *in vivo*; however, this approach clearly confirmed the role of Wnts for maintenance of intestinal stem cells and their proliferation in organoid culture (*in vitro*).

Genetic deletion of *Porcn* in the stroma is difficult. Due to incomplete deletion of *Porcn* in the stromal cells of the *Rosa-CreER^{T2}/Porcn^{Del}* mice, we did not find any intestinal phenotype *in vivo*. Therefore, we decided to use a pharmacological approach to inhibit PORCN in the intestinal stroma cells *in vivo*. Details of the C59 treatment are explained in Chapter 2.

Here is a summary of our observations as a result of pharmacological inhibition of PORCN and Wnt secretion in both the stromal and epithelial cells:

1. C59 completely inhibited organoid formation of epithelial cells in the B6 mice similar to the IWP treatment (a PORCN inhibitor, which can only be used in *in vitro* studies) and in the *Villi-Cre/Porcn^{Del}* mice.
2. An intermediate dose of C59 (50 mg/kg/day) suppressed Wnt target gene expressions and stem cell markers such as *Axin2*, *Lgr5*, *ASCL2* and *Olfm4*.
3. Reduction of *Lgr5* stem cells by an intermediate dose of C59 did not affect intestinal homeostasis over a time period of a few weeks.
4. A high dose of C59 (50 mg/kg/BID) caused impaired intestinal homeostasis in the mice within 5 to 6 days.
5. An intermediate dose of C59 inhibited differentiation of Paneth cells in the mice.
6. Stromal Wnts and *Lgr5* stem cells were required for regeneration of intestinal epithelial cells after radiation damage.
7. The therapeutic dose of C59 in a mouse model of breast tumor is 5 mg/kg/day; however, a 20-fold higher dose of C59 was required to show

the toxicity in normal intestinal homeostasis. Thus, PORCN inhibitors exhibit a therapeutic index allowing for clinical use.

8. The combination of C59 treatment (50 mg/kg/day) with radiation caused impaired intestinal homeostasis in the mice within 5 days, indicating the possibility of synergistic toxicity in clinical settings.

In conclusion, a combination of genetic and pharmacological approaches helped us to better understand the role of Wnt signaling in adult intestinal homeostasis and to identify the possible source of Wnt-producing cells for intestinal stem cells. Additionally, our data suggest that patients with high Wnt diseases may benefit from a low dose treatment of PORCN inhibitors without intestinal toxicity.

4.1.2 Discussion

Identifying the intestinal stem cells markers, their niche and essential factors required for their self-renewal are the focus of many studies throughout the past decade. Understanding how intestinal stem cells maintain tissue homeostasis can help researchers to elucidate the pathophysiology and treatment approaches of intestinal diseases. A breakthrough discovery in the field of intestinal stem cells was performed in the research laboratory of Hans Clever by identifying a method to grow epithelial intestine in culture for several months (Sato et al., 2009). Sato et al. reported that Paneth cells formed the niche for Lgr5 stem cells *in vivo* and *in vitro* by expressing TGF, EGF, Wnt3 and DII4, all essential signals required for the maintenance of stem cells (Sato et al., 2011). However, several additional components including RSPO1, EGF and Noggin were also added to these epithelial crypt cultures to support

growth of intestinal epithelial cells in the absence of stromal cells. Such exogenous factors are essential for small intestine culture. Moreover, depletion of Paneth cells, albeit not complete, did not affect intestinal homeostasis *in vivo*, indicating other niche cells may maintain self-renewal of intestinal stem cells *in vivo* (Durand et al., 2012; Kim et al., 2012). In our study, we found that epithelial Wnts (mostly secreted by Paneth cells) were dispensable for intestinal homeostasis *in vivo*; however they were required for *in vitro* culture in the absence of stromal cells. We also showed that myofibroblast-like cells from the stroma expressed several Wnt ligands and Rspo3. Furthermore, these cells could support the culture of *Porcn* depleted epithelial crypts in the absence of RSPO1, suggesting the potential role of stroma, but not Paneth cells, for the maintenance of intestinal stem cells.

Wnt signaling and RSPO1 have been proposed to promote regeneration of intestinal epithelium following radiation (Bhanja et al., 2009; Davies et al., 2008; Zhou et al., 2013). Expression of several Wnt ligands (Wnt3, 6 and 9b) reportedly increased more than 50-fold within 24 hours post radiation and returned back to normal levels after 72 hours (Davies et al., 2008). Additionally, Wnt target gene expression and β -Gal reporter mice showed increased levels of Wnt signaling in the bottom of crypts 24 hours post radiation (Davies et al., 2008). Therefore, we proposed that epithelial Wnts may be required for the regeneration of epithelial cells following radiation. However, both *Villin-Cre/Porcn^{Del}* and *Villin-Cre/Porcn^{WT}* mice completely regenerated the intestinal epithelial cells after a lethal dose of gamma radiation. These data suggest that stroma Wnts are most likely sufficient to

support regenerative responses to radiation stress, similar to their roles in normal intestinal homeostasis.

Bmi1 quiescent stem cells are sensitive to 1 Gray (Gy) radiation; however, Lgr5 stem cells are more radioresistant, and they can tolerate 8-12 Gy doses of radiation (Hua et al., 2012). Although the majority of Lgr5 cells have been shown to die after 12 Gy of radiation, a small population of these stem cells can repair their DNA and start to regenerate the intestinal epithelial layer after 18 hours of radiation. Such stem cell populations undergo massive proliferation from 18 to 24 hours post radiation and then return back to normal stages after 48 hours of radiation (Hua et al., 2012). These data suggest that, although Lgr5 stem cells may not be required for normal homeostasis (Tian et al., 2011), they may be critical for the regeneration of intestine following radiation (Hua et al., 2012). Thus, we hypothesized that the intestine may become sensitive to radiation after depletion of Lgr5 stem cells by C59 treatment. Next, we confirmed that intermediate doses of C59, which significantly reduced Lgr5 stem cells and did not affect intestinal homeostasis in the short period, affected the regeneration of the intestinal epithelial layer after 12 Gy radiation. Collectively, our data demonstrates a potential role of Lgr5 stem cells for intestinal regeneration following radiation. In accordance with our results, Metcalfe et al. used a genetic approach to eliminate Lgr5 stem cells prior to radiation and reported impaired intestinal homeostasis in mice following 5 days of radiation (Metcalfe et al., 2014). In conclusion, we observed that the CBC stem cells, but not the +4 stem cells, were radioresistant and responded to radiation injuries in the experimental mice.

Wnt/ β -catenin signaling has also been proposed to influence Paneth cell

maturation and localization in crypts. It is known that β -catenin and TCF4 can regulate expression of several genes involved in maturation and positioning of Paneth cells, including Cryptdins (1-6), defensin5, MMP7 and EphB3 (van Es et al., 2005). Moreover, matrix metalloproteinase 7 (MMP7) can activate and process Cryptdin precursors for maturation of Paneth cells. Indeed, mice lacking MMP7 were unable to process procryptdin precursors, resulting in impairment to clear intestinal infections (Ayabe et al., 2002; Wilson et al., 1999).

In our study, we found that expression of MMP7 and Cryptdin1 were reduced in mice intestinal samples after 6 days of C59 treatment (intermediate dose). Additionally, the lysozyme staining (Paneth cell marker) showed a reduction of mature Paneth cells in the entire small intestine of the C59-treated mice. These data confirm the importance of Wnt ligands for the maturation of Paneth cells in mice. However, this process is independent of epithelial Wnt secretion, as the Paneth cell numbers and maturation were not affected in the *Villi-Cre/PorcⁿDel* mice. Hence, stromal Wnts, but not epithelial Wnts, are responsible for Paneth cell differentiation in the small intestine of mice.

4.1.3 Future plans

In our study, we found that the stroma formed the intestinal stem cell niche by secreting essential Wnts and RSPO3. In future studies, we would like to identify the exact role of RSPO3 for the maintenance of intestinal stem cells *in vitro* and *in vivo*. Thus, generating mice lacking RSPO3 in stromal cells and characterization of the phenotype in these mice will be informative.

To better determine the nature of the stromal cell niche, we cultured

stromal cells and stained them with different markers for various cell types. The immunofluorescent staining confirmed the nature of the cultured stroma as myofibroblast cells. We excluded the hematopoietic cells as a potential niche source by generating *Villin-Cre/Vav-Cre/Porcⁿ^{Del}* mice, where *Porcn* was deleted in the epithelial and all of the hematopoietic lineages, including the intestinal stromal myeloid cells and lymphoid cells. To confirm the *in vivo* role of myofibroblasts as a Wnt producing niche, we needed to generate mice lacking *Porcn* within these cells by using a specific *Cre* driver for this cell population. However, this approach is challenging, because constitutive *Cre* mice, which allow for targeting of fibroblasts and myofibroblasts, may cause FDH or other lethal phenotypes due to the inactivation of *Porcn* in the early embryonic stage.

4.2 Role of Wnt signaling in hematopoiesis

4.2.1 Conclusions

To investigate the role of Wnt signaling in hematopoiesis, *Porcn^{fllox}* mice were crossed with inducible *Rosa-CreER^{T2}* (*Cre* expression in all tissues), *Mx1-Cre* (hematopoietic and liver cells) and constitutive *Vav-Cre* (hematopoietic and endothelial cells) mice. First, we evaluated hematopoiesis in the *Rosa-CreER^{T2}/Porcn^{Del}* mice, and details of the results are described in Chapter 3. Below is a summary of the hematopoietic phenotype in the *Rosa-CreER^{T2}/Porcn^{Del}* mice:

1. *Porcn* was excised in most of the BM cells, and *Porcn* mRNA expression was significantly decreased. Additionally, expression of c-myc (Wnt target gene) was also reduced in the BM samples of the *Rosa-*

CreER^{T2}/Porcn^{Del} mice.

2. Blood counts of the mice showed a slight increase in total WBC, but were not statistically significant. Moreover, there was a significant reduction of lymphocytes and an increased number of neutrophils in the blood samples of *Rosa-CreER^{T2}/Porcn^{Del}* mice.

3. *Rosa-CreER^{T2}/Porcn^{Del}* mice exhibited thymus atrophy.

4. The BM analysis showed a significant increase in neutrophils in the *Rosa-CreER^{T2}/Porcn^{Del}* mice.

5. The analysis of BM cells showed a substantial reduction of B-lymphocyte and CLPs, but not CMPs or GMPs.

6. There were no differences between HSC frequencies (including LT-HSCs and ST-HSCs) in both the control and *Rosa-CreER^{T2}/Porcn^{Del}* mice.

7. *Rosa-CreER^{T2}/Porcn^{Del}* BM cells were able to differentiate normally and to form all colonies in the absence of hematopoietic Wnt secretion. The *Porcn^{Del}* samples exhibited a higher number of colonies compared to the *Porcn^{WT}* samples, which was due to a higher number of granulocyte colonies.

8. *Rosa-CreER^{T2}/Porcn^{Del}* HSCs were able to successfully reconstitute the BM of irradiated primary and secondary recipient mice.

9. The primary and secondary recipient mice did not demonstrate any increase in granulocyte number or any decrease in B-lymphocytes and CLP frequencies.

These results suggest that an increase in granulocytes was most likely due to the inhibition of Wnt secretion in other organs, such as the skin, which indirectly impacted the production of granulocytes. We concluded that the

Rosa-CreER^{T2}/Porcn^{Del} mouse model was not ideal, because *Porcn* was not completely excised in the BM or in the blood samples of these mice. Afterwards, *Porcn^{fllox}* mice were crossed to *Mx1-Cre* mice to generate *Mx1-Cre/Porcn^{Del}* mice, which was believed to completely inactivate *Porcn* in the hematopoietic and liver cells after poly I:C treatment. The effects of *Porcn* deletion in the *Mx1* mice are described in Chapter 3. Below is a summary of our observations of the *Mx1-Cre/Porcn^{Del}* mice:

1. Although *Porcn* was substantially excised from the blood and BM samples, we did not achieve 100% excision.
2. Expression of c-myc remained unchanged in both the control and *Mx1-Cre/Porcn^{Del}* mice.
3. Normal hematopoiesis was observed in the *Mx1-Cre/Porcn^{Del}* mice.
4. *Mx1-Cre/Porcn^{Del}* progenitor cells were able to normally differentiate and to form all type of colonies in the absence of Wnt secretion from the hematopoietic cells.
5. *Mx1-Cre/Porcn^{Del}* HSCs could normally reconstitute the BM of primary and secondary recipient mice.

The results from the *Mx1-Cre/Porcn^{Del}* mice suggest that hematopoietic Wnts are dispensable for proliferation and differentiation of HSCs. Although the *Mx1-Cre/Porcn^{Del}* mice showed near complete excision of *Porcn* in their blood and BM samples, there remained a fraction of blood cells that were not excised by applying genomic PCR in the blood samples of the *Mx1-Cre/Porcn^{Del}* mice. Therefore, we next examined the constitutive *Vav-Cre* mice to achieve a complete deletion of *Porcn* in the hematopoietic tissues. To our surprise, the *Vav-Cre/Porcn^{Del}* pups were viable and exhibited normal

development. We then evaluated hematopoiesis in these mice, of which the details are presented in Chapter 3. Below is a summary of our findings regarding hematopoiesis in the *Vav-Cre/Porcⁿ^{Del}* mice:

1. Porcn excision was complete in the blood and BM samples.
2. The expression of c-myc as a Wnt target gene was not altered in the BM samples.
3. The analysis of hematopoietic tissues, including the thymus, spleen, BM and blood, revealed normal hematopoiesis in these mice.
4. The mice aged up to two years now.

4.2.2 Discussion

Three different Porcn knockout mouse models in hematopoietic tissues have been used to identify the role of Wnt signaling in hematopoiesis. However, we were unable to completely target Wnt secretion in both the BM niche and the hematopoietic cells, challenging our ability to elucidate the exact role of Wnt signaling in hematopoiesis. Although, we are the first to clearly demonstrate that hematopoietic Wnts are dispensable for murine hematopoiesis.

In addition, we found that hematopoietic Wnts were dispensable for the differentiation of HSCs towards all progenitors, as well as towards mature blood cells. In previous studies, Wnt3a condition-medium or overexpression of Wnt3a in OP9 stromal cells inhibited B cell and myeloid production of HSCs *in vitro* (Ichii et al., 2012; Yamane et al., 2001). Conversely, knockouts of Wnt3a^{-/-} in HSCs showed a severe reduction of CMP and GMP cells, B cell progenitors and CLP cells, in secondary recipient mice (Luis et al., 2009).

Furthermore, Wnt5a was shown to negatively regulate B cell proliferation through cell autonomous effects (Liang et al., 2003). In contrast to previous studies, we found that HSCs lacking Wnt secretion in the *Mx1-Cre/Porcⁿ^{Del}* and *Vav-cre/Porcⁿ^{Del}* mice could normally differentiate towards all blood cell types *in vivo* and *in vitro*. Additionally, *Rosa-CreER^{T2}/Porcn^{Del}* mice exhibited a marked increase in granulocytes and a severe reduction in lymphocytes and CLP cells in the BM and blood samples, but these phenotypes were not observed in the *Porcn^{Del}* primary and secondary BMT recipient mice. Thus, a lack of hematological phenotypes in the *Rosa-CreER^{T2}/Porcn^{Del}* recipient mice further supports our conclusion that hematopoietic Wnts are dispensable for differentiation of blood progenitors. Notably, the increased granulopoiesis and decreased lymphopoiesis in the *Rosa-CreER^{T2}/Porcn^{Del}* mice may be related to mouse illness due to the whole body knockout of *Porcn* or due to the partial targeting of Wnt secretion in the BM niche of the *Rosa-CreER^{T2}/Porcn^{Del}* mice.

4.2.3 Future plans

Inhibiting Wnt secretion in the BM niche is challenging, because there are several identified niche cell types that are capable of providing different Wnt ligands for HSCs. To completely inhibit Wnt secretion in the BM niche, it is necessary to cross several *Cre* drivers (targeting all types of niche cells) together with *Porcn^{fllox}* mice or use C59 for systemic inhibition of Wnt signaling.

A high dose-C59 approach is not practical, because complete inhibition of *Porcn* results in mouse death in less than one week due to impaired intestinal

homeostasis, and the time interval to see any effects of C59 in hematopoiesis is quite long. Alternatively, we can use a lower dose of C59 for at least one or two months and observe hematopoiesis in the C59-treated mice. Hematopoietic Wnts are not required for normal hematopoiesis; however, they may be required during responses to several environmental stresses. Thus, it would be interesting to challenge *Porcn^{Del}* HSC function by injection of G-CSF, IL-3 and 5-FU, or to test the response of *Porcn^{Del}* HSCs to infectious reagents, such as Candida.

Bibliography

Alonso, L., and Fuchs, E. (2003). Stem cells in the skin: waste not, Wnt not. *Genes Dev* 17, 1189-1200.

Atit, R., Sgaier, S.K., Mohamed, O.A., Taketo, M.M., Dufort, D., Joyner, A.L., Niswander, L., and Conlon, R.A. (2006). Beta-catenin activation is necessary and sufficient to specify the dorsal dermal fate in the mouse. *Dev Biol* 296, 164-176.

Augustin, I., Goidts, V., Bongers, A., Kerr, G., Vollert, G., Radlwimmer, B., Hartmann, C., Herold-Mende, C., Reifenberger, G., von Deimling, A., *et al.* (2012). The Wnt secretion protein Evi/Gpr177 promotes glioma tumorigenesis. *EMBO Mol Med* 4, 38-51.

Augustin, I., Gross, J., Baumann, D., Korn, C., Kerr, G., Grigoryan, T., Mauch, C., Birchmeier, W., and Boutros, M. (2013). Loss of epidermal Evi/Wls results in a phenotype resembling psoriasiform dermatitis. *J Exp Med* 210, 1761-1777.

Austin, T.W., Solar, G.P., Ziegler, F.C., Liem, L., and Matthews, W. (1997). A role for the Wnt gene family in hematopoiesis: expansion of multilineage progenitor cells. *Blood* 89, 3624-3635.

Ayabe, T., Satchell, D.P., Pesendorfer, P., Tanabe, H., Wilson, C.L., Hagen, S.J., and Ouellette, A.J. (2002). Activation of Paneth cell alpha-defensins in mouse small intestine. *J Biol Chem* 277, 5219-5228.

Baarsma, H.A., Königshoff, M., and Gosens, R. (2013). The WNT signaling pathway from ligand secretion to gene transcription: molecular mechanisms and pharmacological targets. *Pharmacol Ther* 138, 66-83.

- Bafico, A., Liu, G., Goldin, L., Harris, V., and Aaronson, S.A. (2004). An autocrine mechanism for constitutive Wnt pathway activation in human cancer cells. *Cancer Cell* *6*, 497-506.
- Barker, N., van Es, J.H., Kuipers, J., Kujala, P., van den Born, M., Cozijnsen, M., Haegebarth, A., Korving, J., Begthel, H., Peters, P.J., *et al.* (2007). Identification of stem cells in small intestine and colon by marker gene *Lgr5*. *Nature* *449*, 1003-1007.
- Baron, R., and Kneissel, M. (2013). WNT signaling in bone homeostasis and disease: from human mutations to treatments. *Nat Med* *19*, 179-192.
- Barrott, J.J., Cash, G.M., Smith, A.P., Barrow, J.R., and Murtaugh, L.C. (2011). Deletion of mouse *Porc1* blocks Wnt ligand secretion and reveals an ectodermal etiology of human focal dermal hypoplasia/Goltz syndrome. *Proc Natl Acad Sci USA* *108*, 12752-12757.
- Bhanja, P., Saha, S., Kabarriti, R., Liu, L., Roy-Chowdhury, N., Roy-Chowdhury, J., Sellers, R.S., Alfieri, A.A., and Guha, C. (2009). Protective role of R-spondin1, an intestinal stem cell growth factor, against radiation-induced gastrointestinal syndrome in mice. *PLoS ONE* *4*, e8014.
- Bhanot, P., Brink, M., Samos, C.H., Hsieh, J.C., Wang, Y., Macke, J.P., Andrew, D., Nathans, J., and Nusse, R. (1996). A new member of the frizzled family from *Drosophila* functions as a Wingless receptor. *Nature* *382*, 225-230.
- Biechele, S., Cockburn, K., Lanner, F., Cox, B.J., and Rossant, J. (2013). *Porc1*-dependent Wnt signaling is not required prior to mouse gastrulation. *Development* *140*, 2961-2971.

Biechele, S., Cox, B.J., and Rossant, J. (2011). Porcupine homolog is required for canonical Wnt signaling and gastrulation in mouse embryos. *Dev Biol* 355, 275-285.

Bovolenta, P., Esteve, P., Ruiz, J.M., Cisneros, E., and Lopez-Rios, J. (2008). Beyond Wnt inhibition: new functions of secreted Frizzled-related proteins in development and disease. *J Cell Sci* 121, 737-746.

Buckley, S.M., Ulloa-Montoya, F., Abts, D., Oostendorp, R.A.J., Dzierzak, E., Ekker, S.C., and Verfaillie, C.M. (2011). Maintenance of HSC by Wnt5a secreting AGM-derived stromal cell line. *Exp Hematol* 39, 114-123.e111-115.

Buczacki, S., Davies, R.J., and Winton, D.J. (2011). Stem cells, quiescence and rectal carcinoma: an unexplored relationship and potential therapeutic target. *Br J Cancer* 105, 1253-1259.

Buczacki, S.J.A., Zecchini, H.I., Nicholson, A.M., Russell, R., Vermeulen, L., Kemp, R., and Winton, D.J. (2013). Intestinal label-retaining cells are secretory precursors expressing Lgr5. *Nature* 495, 65-69.

Buechling, T., Chaudhary, V., Spirohn, K., Weiss, M., and Boutros, M. (2011). p24 proteins are required for secretion of Wnt ligands. *EMBO Rep* 12, 1265-1272.

Carpenter, A.C., Rao, S., Wells, J.M., Campbell, K., and Lang, R.A. (2010). Generation of mice with a conditional null allele for Wntless. *Genesis* 48, 554-558.

Cervantes, S., Yamaguchi, T.P., and Hebrok, M. (2009). Wnt5a is essential for intestinal elongation in mice. *Dev Biol* 326, 285-294.

Chen, B., Dodge, M.E., Tang, W., Lu, J., Ma, Z., Fan, C.-W., Wei, S., Hao, W., Kilgore, J., Williams, N.S., *et al.* (2009). Small molecule-mediated

disruption of Wnt-dependent signaling in tissue regeneration and cancer. *Nat Chem Biol* 5, 100-107.

Chen, H.-Z., Ouseph, M.M., Li, J., Pécot, T., Chokshi, V., Kent, L., Bae, S., Byrne, M., Duran, C., Comstock, G., *et al.* (2012). Canonical and atypical E2Fs regulate the mammalian endocycle. *Nat Cell Biol* 14, 1192-1202.

Clevers, H., and Nusse, R. (2012). Wnt/ β -catenin signaling and disease. *Cell* 149, 1192-1205.

Cobas, M., Wilson, A., Ernst, B., Mancini, S.J.C., MacDonald, H.R., Kemler, R., and Radtke, F. (2004). Beta-catenin is dispensable for hematopoiesis and lymphopoiesis. *J Exp Med* 199, 221-229.

Coombs, G.S., Schmitt, A.A., Canning, C.A., Alok, A., Low, I.C.C., Banerjee, N., Kaur, S., Utomo, V., Jones, C.M., Pervaiz, S., *et al.* (2012). Modulation of Wnt/ β -catenin signaling and proliferation by a ferrous iron chelator with therapeutic efficacy in genetically engineered mouse models of cancer. *Oncogene* 31, 213-225.

Coombs, G.S., Yu, J., Canning, C.A., Veltri, C.A., Covey, T.M., Cheong, J.K., Utomo, V., Banerjee, N., Zhang, Z.H., Jadulco, R.C., *et al.* (2010). WLS-dependent secretion of WNT3A requires Ser209 acylation and vacuolar acidification. *J Cell Sci* 123, 3357-3367.

Covey, T.M., Kaur, S., Tan Ong, T., Proffitt, K.D., Wu, Y., Tan, P., and Virshup, D.M. (2012). PORCN moonlights in a Wnt-independent pathway that regulates cancer cell proliferation. *PLoS ONE* 7, e34532.

Cox, B.J., Vollmer, M., Tamplin, O., Lu, M., Biechele, S., Gertsenstein, M., van Campenhout, C., Floss, T., Kühn, R., Wurst, W., *et al.* (2010). Phenotypic annotation of the mouse X chromosome. *Genome Res* 20, 1154-1164.

Dann, C.E., Hsieh, J.C., Rattner, A., Sharma, D., Nathans, J., and Leahy, D.J. (2001). Insights into Wnt binding and signalling from the structures of two Frizzled cysteine-rich domains. *Nature* *412*, 86-90.

Davies, P.S., Dismuke, A.D., Powell, A.E., Carroll, K.H., and Wong, M.H. (2008). Wnt-reporter expression pattern in the mouse intestine during homeostasis. *BMC Gastroenterol* *8*, 57.

De, A. (2011). Wnt/Ca²⁺ signaling pathway: a brief overview. *Acta Biochim Biophys Sin (Shanghai)* *43*, 745-756.

de Boer, J., Williams, A., Skavdis, G., Harker, N., Coles, M., Tolaini, M., Norton, T., Williams, K., Roderick, K., Potocnik, A.J., *et al.* (2003). Transgenic mice with hematopoietic and lymphoid specific expression of Cre. *Eur J Immunol* *33*, 314-325.

Durand, A., Donahue, B., Peignon, G., Letourneur, F., Cagnard, N., Slomianny, C., Perret, C., Shroyer, N.F., and Romagnolo, B. (2012). Functional intestinal stem cells after Paneth cell ablation induced by the loss of transcription factor Math1 (Atoh1). *Proc Natl Acad Sci USA* *109*, 8965-8970.

Farin, H.F., van Es, J.H., and Clevers, H. (2012). Redundant sources of Wnt regulate intestinal stem cells and promote formation of Paneth cells. *Gastroenterology* *143*, 1518-1529.e1517.

Fevr, T., Robine, S., Louvard, D., and Huelsken, J. (2007). Wnt/beta-catenin is essential for intestinal homeostasis and maintenance of intestinal stem cells. *Mol Cell Biol* *27*, 7551-7559.

Fleming, H.E., Janzen, V., Lo Celso, C., Guo, J., Leahy, K.M., Kronenberg, H.M., and Scadden, D.T. (2008). Wnt signaling in the niche enforces

hematopoietic stem cell quiescence and is necessary to preserve self-renewal in vivo. *Cell Stem Cell* 2, 274-283.

Fossat, N., Jones, V., Khoo, P.-L., Bogani, D., Hardy, A., Steiner, K., Mukhopadhyay, M., Westphal, H., Nolan, P.M., Arkell, R., *et al.* (2011). Stringent requirement of a proper level of canonical WNT signalling activity for head formation in mouse embryo. *Development* 138, 667-676.

Fu, J., Jiang, M., Mirando, A.J., Yu, H.-M.I., and Hsu, W. (2009). Reciprocal regulation of Wnt and Gpr177/mouse Wntless is required for embryonic axis formation. *Proceedings of the National Academy of Sciences* 106, 18598–18603.

Fuchs, E. (2007). Scratching the surface of skin development. *Nature* 445, 834-842.

Galli, L.M., Barnes, T.L., Secret, S.S., Kadowaki, T., and Burrus, L.W. (2007). Porcupine-mediated lipid-modification regulates the activity and distribution of Wnt proteins in the chick neural tube. *Development* 134, 3339-3348.

Gong, Y., Bourhis, E., Chiu, C., Stawicki, S., DeAlmeida, V.I., Liu, B.Y., Phamluong, K., Cao, T.C., Carano, R.A.D., Ernst, J.A., *et al.* (2010). Wnt Isoform-Specific Interactions with Coreceptor Specify Inhibition or Potentiation of Signaling by LRP6 Antibodies. *PLoS ONE* 5, e12682.

Gregorieff, A., Pinto, D., Begthel, H., Destrée, O., Kielman, M., and Clevers, H. (2005). Expression pattern of Wnt signaling components in the adult intestine. *Gastroenterology* 129, 626-638.

Gross, J.C., and Boutros, M. (2013). Secretion and extracellular space travel of Wnt proteins. *Curr Opin Genet Dev* 23, 385-390.

Grzeschik, K.-H., Bornholdt, D., Oeffner, F., König, A., del Carmen Boente, M., Enders, H., Fritz, B., Hertl, M., Grasshoff, U., Höfling, K., *et al.* (2007). Deficiency of PORCN, a regulator of Wnt signaling, is associated with focal dermal hypoplasia. *Nat Genet* 39, 833-835.

Hameyer, D., Loonstra, A., Eshkind, L., Schmitt, S., Antunes, C., Groen, A., Bindels, E., Jonkers, J., Krimpenfort, P., Meuwissen, R., *et al.* (2007). Toxicity of ligand-dependent Cre recombinases and generation of a conditional Cre deleter mouse allowing mosaic recombination in peripheral tissues. *Physiol Genomics* 31, 32-41.

Harterink, M., and Korswagen, H.C. (2012). Dissecting the Wnt secretion pathway: key questions on the modification and intracellular trafficking of Wnt proteins. *Acta Physiol (Oxf)* 204, 8-16.

He, B., Reguart, N., You, L., Mazieres, J., Xu, Z., Lee, A.Y., Mikami, I., McCormick, F., and Jablons, D.M. (2005). Blockade of Wnt-1 signaling induces apoptosis in human colorectal cancer cells containing downstream mutations. *Oncogene* 24, 3054-3058.

He, B., You, L., Uematsu, K., Xu, Z., Lee, A.Y., Matsangou, M., McCormick, F., and Jablons, D.M. (2004). A monoclonal antibody against Wnt-1 induces apoptosis in human cancer cells. *Neoplasia* 6, 7-14.

Herr, P., and Basler, K. (2012). Porcupine-mediated lipidation is required for Wnt recognition by Wls. *Dev Biol* 361, 392-402.

Herr, P., Hausmann, G., and Basler, K. (2012). WNT secretion and signalling in human disease. *Trends Mol Med* 18, 483-493.

Hikasa, H., and Sokol, S.Y. (2013). Wnt signaling in vertebrate axis specification. *Cold Spring Harb Perspect Biol* 5, a007955.

Hsieh, J.-C., Lee, L., Zhang, L., Wefer, S., Brown, K., DeRossi, C., Wines, M.E., Rosenquist, T., and Holdener, B.C. (2003). Mesd encodes an LRP5/6 chaperone essential for specification of mouse embryonic polarity. *Cell* *112*, 355-367.

Hua, G., Thin, T.H., Feldman, R., Haimovitz-Friedman, A., Clevers, H., Fuks, Z., and Kolesnick, R. (2012). Crypt base columnar stem cells in small intestines of mice are radioresistant. *Gastroenterology* *143*, 1266-1276.

Huelsken, J., Vogel, R., Brinkmann, V., Erdmann, B., Birchmeier, C., and Birchmeier, W. (2000). Requirement for beta-catenin in anterior-posterior axis formation in mice. *J Cell Biol* *148*, 567-578.

Huelsken, J., Vogel, R., Erdmann, B., Cotsarelis, G., and Birchmeier, W. (2001). beta-Catenin controls hair follicle morphogenesis and stem cell differentiation in the skin. *Cell* *105*, 533-545.

Hughes, K.R., Sablitzky, F., and Mahida, Y.R. (2011). Expression profiling of Wnt family of genes in normal and inflammatory bowel disease primary human intestinal myofibroblasts and normal human colonic crypt epithelial cells. *Inflamm Bowel Dis* *17*, 213-220.

Ichii, M., Frank, M.B., Iozzo, R.V., and Kincade, P.W. (2012). The canonical Wnt pathway shapes niches supportive of hematopoietic stem/progenitor cells. *Blood*.

Inoki, K., Ouyang, H., Zhu, T., Lindvall, C., Wang, Y., Zhang, X., Yang, Q., Bennett, C., Harada, Y., Stankunas, K., *et al.* (2006). TSC2 integrates Wnt and energy signals via a coordinated phosphorylation by AMPK and GSK3 to regulate cell growth. *Cell* *126*, 955-968.

Janda, C.Y., Waghray, D., Levin, A.M., Thomas, C., and Garcia, K.C. (2012). Structural basis of Wnt recognition by Frizzled. *Science* 337, 59-64.

Jeannot, G., Scheller, M., Scarpellino, L., Duboux, S., Gardiol, N., Back, J., Kuttler, F., Malanchi, I., Birchmeier, W., Leutz, A., *et al.* (2008). Long-term, multilineage hematopoiesis occurs in the combined absence of beta-catenin and gamma-catenin. *Blood* 111, 142-149.

Jubb, A.M., Chalasani, S., Frantz, G.D., Smits, R., Grabsch, H.I., Kavi, V., Maughan, N.J., Hillan, K.J., Quirke, P., and Koeppen, H. (2006). Achaete-scute like 2 (*ascl2*) is a target of Wnt signalling and is upregulated in intestinal neoplasia. *Oncogene* 25, 3445-3457.

Kadowaki, T., Wilder, E., Klingensmith, J., Zachary, K., and Perrimon, N. (1996). The segment polarity gene porcupine encodes a putative multitransmembrane protein involved in Wingless processing. *Genes Dev* 10, 3116-3128.

Kanazawa, A., Tsukada, S., Sekine, A., Tsunoda, T., Takahashi, A., Kashiwagi, A., Tanaka, Y., Babazono, T., Matsuda, M., Kaku, K., *et al.* (2004). Association of the gene encoding wingless-type mammary tumor virus integration-site family member 5B (WNT5B) with type 2 diabetes. *Am J Hum Genet* 75, 832-843.

Katoh, M., and Katoh, M. (2006). Cross-talk of WNT and FGF signaling pathways at GSK3beta to regulate beta-catenin and SNAIL signaling cascades. *Cancer Biol Ther* 5, 1059-1064.

Keller, R.E., Danilchik, M., Gimlich, R., and Shih, J. (1985). The function and mechanism of convergent extension during gastrulation of *Xenopus laevis*. *J Embryol Exp Morphol* 89, 185-209.

- Kelly, O.G., Pinson, K.I., and Skarnes, W.C. (2004). The Wnt co-receptors Lrp5 and Lrp6 are essential for gastrulation in mice. *Development* *131*, 2803-2815.
- Kim, J.A., Kang, Y.J., Park, G., Kim, M., Park, Y.O., Kim, H., Leem, S.H., Chu, I.S., Lee, J.S., Jho, E.H., *et al.* (2009). Identification of a stroma-mediated Wnt/beta-catenin signal promoting self-renewal of hematopoietic stem cells in the stem cell niche. *Stem Cells* *27*, 1318-1329.
- Kim, T.-H., Escudero, S., and Shivdasani, R.A. (2012). Intact function of Lgr5 receptor-expressing intestinal stem cells in the absence of Paneth cells. *Proc Natl Acad Sci USA* *109*, 3932-3937.
- Kirstetter, P., Anderson, K., Porse, B.T., and Jacobsen, S.E.W. (2006). Activation of the canonical Wnt pathway leads to loss of hematopoietic stem cell repopulation and multilineage differentiation block - *Nature Immunology*. *Nature* *7*, 1048-1056.
- Klaus, A., and Birchmeier, W. (2008). Wnt signalling and its impact on development and cancer. *Nat Rev Cancer* *8*, 387-398.
- Kleinschmit, A., Koyama, T., Dejima, K., Hayashi, Y., Kamimura, K., and Nakato, H. (2010). *Drosophila* heparan sulfate 6-O endosulfatase regulates Wingless morphogen gradient formation. *Dev Biol* *345*, 204-214.
- Korinek, V., Barker, N., Moerer, P., van Donselaar, E., Huls, G., Peters, P.J., and Clevers, H. (1998). Depletion of epithelial stem-cell compartments in the small intestine of mice lacking Tcf-4. *Nat Genet* *19*, 379-383.
- Kühn, R., Schwenk, F., Aguet, M., and Rajewsky, K. (1995). Inducible gene targeting in mice. *Science* *269*, 1427-1429.

Kuhnert, F., Davis, C.R., Wang, H.-T., Chu, P., Lee, M., Yuan, J., Nusse, R., and Kuo, C.J. (2004). Essential requirement for Wnt signaling in proliferation of adult small intestine and colon revealed by adenoviral expression of Dickkopf-1. *Proc Natl Acad Sci USA* *101*, 266-271.

Kusserow, A., Pang, K., Sturm, C., Hrouda, M., Lentfer, J., Schmidt, H.A., Technau, U., von Haeseler, A., Hobmayer, B., Martindale, M.Q., *et al.* (2005). Unexpected complexity of the Wnt gene family in a sea anemone. *Nature* *433*, 156-160.

Lahar, N., Lei, N.Y., Wang, J., Jabaji, Z., Tung, S.C., Joshi, V., Lewis, M., Stelzner, M., Martín, M.G., and Dunn, J.C.Y. (2011). Intestinal subepithelial myofibroblasts support in vitro and in vivo growth of human small intestinal epithelium. *PLoS ONE* *6*, e26898.

Lavergne, E., Hendaoui, I., Coulouarn, C., Ribault, C., Leseur, J., Eliat, P.A., Mebarki, S., Corlu, A., Clément, B., and Musso, O. (2011). Blocking Wnt signaling by SFRP-like molecules inhibits in vivo cell proliferation and tumor growth in cells carrying active β -catenin. *Oncogene* *30*, 423-433.

Li, V.S.W., Ng, S.S., Boersema, P.J., Low, T.Y., Karthaus, W.R., Gerlach, J.P., Mohammed, S., Heck, A.J.R., Maurice, M.M., Mahmoudi, T., *et al.* (2012). Wnt signaling through inhibition of β -catenin degradation in an intact Axin1 complex. *Cell* *149*, 1245-1256.

Liang, H., Chen, Q., Coles, A.H., Anderson, S.J., Pihan, G., Bradley, A., Gerstein, R., Jurecic, R., and Jones, S.N. (2003). Wnt5a inhibits B cell proliferation and functions as a tumor suppressor in hematopoietic tissue. *Cancer Cell* *4*, 349-360.

Lintern, K.B., Guidato, S., Rowe, A., Saldanha, J.W., and Itasaki, N. (2009). Characterization of wise protein and its molecular mechanism to interact with both Wnt and BMP signals. *J Biol Chem* 284, 23159-23168.

Liu, J., Pan, S., Hsieh, M.H., Ng, N., Sun, F., Wang, T., Kasibhatla, S., Schuller, A.G., Li, A.G., Cheng, D., *et al.* (2013). Targeting Wnt-driven cancer through the inhibition of Porcupine by LGK974. *Proc Natl Acad Sci USA* 110, 20224-20229.

Liu, P., Wakamiya, M., Shea, M.J., Albrecht, U., Behringer, R.R., and Bradley, A. (1999). Requirement for Wnt3 in vertebrate axis formation. *Nat Genet* 22, 361-365.

Liu, W., Shaver, T.M., Balasa, A., Ljungberg, M.C., Wang, X., Wen, S., Nguyen, H., and Van den Veyver, I.B. (2012). Deletion of Porcn in mice leads to multiple developmental defects and models human focal dermal hypoplasia (Goltz syndrome). *PLoS ONE* 7, e32331.

Louis, I., Heinonen, K.M., Chagraoui, J., Vainio, S., Sauvageau, G., and Perreault, C. (2008). The signaling protein Wnt4 enhances thymopoiesis and expands multipotent hematopoietic progenitors through beta-catenin-independent signaling. *Immunity* 29, 57-67.

Luis, T.C., Naber, B.A.E., Roozen, P.P.C., Brugman, M.H., de Haas, E.F.E., Ghazvini, M., Fibbe, W.E., van Dongen, J.J.M., Fodde, R., and Staal, F.J.T. (2011). Canonical wnt signaling regulates hematopoiesis in a dosage-dependent fashion. *Cell Stem Cell* 9, 345-356.

Luis, T.C., Weerkamp, F., Naber, B.A.E., Baert, M.R.M., de Haas, E.F.E., Nikolic, T., Heuvelmans, S., De Krijger, R.R., van Dongen, J.J.M., and Staal, F.J.T. (2009). Wnt3a deficiency irreversibly impairs hematopoietic stem cell

self-renewal and leads to defects in progenitor cell differentiation. *Blood* 113, 546-554.

Lyu, J., Yamamoto, V., and Lu, W. (2008). Cleavage of the Wnt receptor Ryk regulates neuronal differentiation during cortical neurogenesis. *Dev Cell* 15, 773-780.

Madison, B.B., Dunbar, L., Qiao, X.T., Braunstein, K., Braunstein, E., and Gumucio, D.L. (2002). Cis elements of the villin gene control expression in restricted domains of the vertical (crypt) and horizontal (duodenum, cecum) axes of the intestine. *J Biol Chem* 277, 33275-33283.

Mazieres, J., He, B., You, L., Xu, Z., and Jablons, D.M. (2005). Wnt signaling in lung cancer. *Cancer Lett* 222, 1-10.

Merrill, B.J., Pasolli, H.A., Polak, L., Rendl, M., García-García, M.J., Anderson, K.V., and Fuchs, E. (2004). Tcf3: a transcriptional regulator of axis induction in the early embryo. *Development* 131, 263-274.

Metcalfe, C., Kljavin, N.M., Ybarra, R., and de Sauvage, F.J. (2014). Lgr5(+) stem cells are indispensable for radiation-induced intestinal regeneration. *Cell Stem Cell* 14, 149-159.

Mii, Y., and Taira, M. (2011). Secreted Wnt “inhibitors” are not just inhibitors: Regulation of extracellular Wnt by secreted Frizzled-related proteins. *Develop Growth Differ* 53, 911-923.

Miller, R.K., and McCrea, P.D. (2010). Wnt to build a tube: contributions of Wnt signaling to epithelial tubulogenesis. *Dev Dyn* 239, 77-93.

Montgomery, R.K., Carlone, D.L., Richmond, C.A., Farilla, L., Kranendonk, M.E.G., Henderson, D.E., Baffour-Awuah, N.Y., Ambruzs, D.M., Fogli, L.K., Algra, S., *et al.* (2011). Mouse telomerase reverse transcriptase (mTert)

expression marks slowly cycling intestinal stem cells. *Proc Natl Acad Sci USA* *108*, 179-184.

Mulligan, K.A., Fuerer, C., Ching, W., Fish, M., Willert, K., and Nusse, R. (2012). Secreted Wingless-interacting molecule (Swim) promotes long-range signaling by maintaining Wingless solubility. *Proc Natl Acad Sci USA* *109*, 370-377.

Murakami, C., de Oliveira Lira Ortega, A., Guimarães, A.S., Gonçalves-Bittar, D., Bönecker, M., and Ciamponi, A.L. (2011). Focal dermal hypoplasia: a case report and literature review. *Oral Surg Oral Med Oral Pathol Oral Radiol Endod* *112*, e11-18.

Murdoch, B. (2003). Wnt-5A augments repopulating capacity and primitive hematopoietic development of human blood stem cells *in vivo*. *Proc Natl Acad Sci USA* *100*, 3422-3427.

Myung, P.S., Takeo, M., Ito, M., and Atit, R.P. (2013). Epithelial Wnt ligand secretion is required for adult hair follicle growth and regeneration. *J Invest Dermatol* *133*, 31-41.

Najdi, R., Proffitt, K., Sprowl, S., Kaur, S., Yu, J., Covey, T.M., Virshup, D.M., and Waterman, M.L. (2012). A uniform human Wnt expression library reveals a shared secretory pathway and unique signaling activities. *Differentiation* *84*, 203-213.

Nemeth, M.J., and Bodine, D.M. (2007). Regulation of hematopoiesis and the hematopoietic stem cell niche by Wnt signaling pathways. *Cell Res* *17*, 746-758.

Nemeth, M.J., Topol, L., Anderson, S.M., Yang, Y., and Bodine, D.M. (2007). Wnt5a inhibits canonical Wnt signaling in hematopoietic stem cells and

enhances repopulation. *Proceedings of the National Academy of Sciences* *104*, 15436–15441.

Neumann, S., Coudreuse, D.Y.M., van der Westhuyzen, D.R., Eckhardt, E.R.M., Korswagen, H.C., Schmitz, G., and Sprong, H. (2009). Mammalian Wnt3a is released on lipoprotein particles. *Traffic* *10*, 334-343.

Niehrs, C. (2006). Function and biological roles of the Dickkopf family of Wnt modulators. *Oncogene* *25*, 7469-7481.

Niehrs, C. (2012). The complex world of WNT receptor signalling. In *Nat Rev Mol Cell Biol* (Nature Publishing Group), pp. 767-779.

Nusse, R. (2012). Wnt signaling. *Cold Spring Harb Perspect Biol* *4*.

Nusse, R., and Varmus, H.E. (1982). Many tumors induced by the mouse mammary tumor virus contain a provirus integrated in the same region of the host genome. *Cell* *31*, 99-109.

Ong, C.K., Subimerb, C., Pairojkul, C., Wongkham, S., Cutcutache, I., Yu, W., McPherson, J.R., Allen, G.E., Ng, C.C.Y., Wong, B.H., *et al.* (2012). Exome sequencing of liver fluke-associated cholangiocarcinoma. *Nat Genet* *44*, 690-693.

Ootani, A., Li, X., Sangiorgi, E., Ho, Q.T., Ueno, H., Toda, S., Sugihara, H., Fujimoto, K., Weissman, I.L., Capecchi, M.R., *et al.* (2009). Sustained in vitro intestinal epithelial culture within a Wnt-dependent stem cell niche. *Nat Med* *15*, 701-706.

Panáková, D., Sprong, H., Marois, E., Thiele, C., and Eaton, S. (2005). Lipoprotein particles are required for Hedgehog and Wingless signalling. *Nature* *435*, 58-65.

- Pinto, D., Gregorieff, A., Begthel, H., and Clevers, H. (2003). Canonical Wnt signals are essential for homeostasis of the intestinal epithelium. *Genes Dev* 17, 1709-1713.
- Proffitt, K.D., Madan, B., Ke, Z., Pendharkar, V., Ding, L., Lee, M.A., Hannoush, R.N., and Virshup, D.M. (2013). Pharmacological inhibition of the Wnt acyltransferase PORCN prevents growth of WNT-driven mammary cancer. *Cancer Res* 73, 502-507.
- Proffitt, K.D., and Virshup, D.M. (2012). Precise regulation of porcupine activity is required for physiological Wnt signaling. *J Biol Chem* 287, 34167-34178.
- Pulkkinen, K., Murugan, S., and Vainio, S. (2008). Wnt signaling in kidney development and disease. *Organogenesis* 4, 55-59.
- Qian, Z., Chen, L., Fernald, A.A., Williams, B.O., and Le Beau, M.M. (2008). A critical role for Apc in hematopoietic stem and progenitor cell survival. *J Exp Med* 205, 2163-2175.
- Qiang, Y.-W., Hu, B., Chen, Y., Zhong, Y., Shi, B., Barlogie, B., and Shaughnessy, J.D. (2009). Bortezomib induces osteoblast differentiation via Wnt-independent activation of beta-catenin/TCF signaling. *Blood* 113, 4319-4330.
- Rijsewijk, F., Schuermann, M., Wagenaar, E., Parren, P., Weigel, D., and Nusse, R. (1987). The Drosophila homolog of the mouse mammary oncogene int-1 is identical to the segment polarity gene wingless. *Cell* 50, 649-657.
- Rios-Esteves, J., Haugen, B., and Resh, M.D. (2014). Identification of Key Residues and Regions Important for Porcupine-mediated Wnt Acylation. *J Biol Chem* 289, 17009-17019.

Rossi, L., Lin, K.K., Boles, N.C., Yang, L., King, K.Y., Jeong, M., Mayle, A., and Goodell, M.A. (2012). Less is more: unveiling the functional core of hematopoietic stem cells through knockout mice. *Cell Stem Cell* 11, 302-317.

Roth, S., Franken, P., Sacchetti, A., Kremer, A., Anderson, K., Sansom, O., and Fodde, R. (2012). Paneth cells in intestinal homeostasis and tissue injury. *PLoS ONE* 7, e38965.

Ruiz-Herguido, C., Guiu, J., D'Altri, T., Inglés-Esteve, J., Dzierzak, E., Espinosa, L., and Bigas, A. (2012). Hematopoietic stem cell development requires transient Wnt/ β -catenin activity. *J Exp Med* 209, 1457-1468.

San Roman, A.K., Jayewickreme, C.D., Murtaugh, L.C., and Shivdasani, R.A. (2014). Wnt secretion from epithelial cells and subepithelial myofibroblasts is not required in the mouse intestinal stem cell niche in vivo. *Stem Cell Reports* 2, 127-134.

Sangiorgi, E., and Capecchi, M.R. (2008). *Bmi1* is expressed in vivo in intestinal stem cells. *Nat Genet* 40, 915-920.

Sato, T., van Es, J.H., Snippert, H.J., Stange, D.E., Vries, R.G., van den Born, M., Barker, N., Shroyer, N.F., van de Wetering, M., and Clevers, H. (2011). Paneth cells constitute the niche for *Lgr5* stem cells in intestinal crypts. *Nature* 469, 415-418.

Sato, T., Vries, R.G., Snippert, H.J., van de Wetering, M., Barker, N., Stange, D.E., van Es, J.H., Abo, A., Kujala, P., Peters, P.J., *et al.* (2009). Single *Lgr5* stem cells build crypt-villus structures in vitro without a mesenchymal niche. *Nature* 459, 262-265.

Savina, A., Vidal, M., and Colombo, M.I. (2002). The exosome pathway in K562 cells is regulated by Rab11. *J Cell Sci* 115, 2505-2515.

Schaniel, C., Sirabella, D., Qiu, J., Niu, X., Lemischka, I.R., and Moore, K.A. (2011). Wnt-inhibitory factor 1 dysregulation of the bone marrow niche exhausts hematopoietic stem cells. *Blood* *118*, 2420-2429.

Schreck, C., Bock, F., Grziwok, S., Oostendorp, R.A.J., and Istvanffy, R. (2014). Regulation of hematopoiesis by activators and inhibitors of Wnt signaling from the niche. *Ann N Y Acad Sci* *1310*, 32-43.

Scoville, D.H., Sato, T., He, X.C., and Li, L. (2008). Current view: intestinal stem cells and signaling. *Gastroenterology* *134*, 849-864.

Seib, D.R.M., Corsini, N.S., Ellwanger, K., Plaas, C., Mateos, A., Pitzer, C., Niehrs, C., Celikel, T., and Martin-Villalba, A. (2013). Loss of dickkopf-1 restores neurogenesis in old age and counteracts cognitive decline. *Cell Stem Cell* *12*, 204-214.

Semënov, M., Tamai, K., and He, X. (2005). SOST Is a Ligand for LRP5/LRP6 and a Wnt Signaling Inhibitor. *Journal of Biological Chemistry* *280*, 26770–26775.

Slusarski, D.C., Yang-Snyder, J., Busa, W.B., and Moon, R.T. (1997). Modulation of embryonic intracellular Ca²⁺ signaling by Wnt-5A. *Dev Biol* *182*, 114-120.

Sugimura, R., He, X.C., Venkatraman, A., Arai, F., Box, A., Semerad, C., Haug, J.S., Peng, L., Zhong, X.-B., Suda, T., *et al.* (2012). Noncanonical Wnt signaling maintains hematopoietic stem cells in the niche. *Cell* *150*, 351-365.

Taelman, V.F., Dobrowolski, R., Plouhinec, J.-L., Fuentealba, L.C., Vorwald, P.P., Gumper, I., Sabatini, D.D., and De Robertis, E.M. (2010). Wnt signaling requires sequestration of glycogen synthase kinase 3 inside multivesicular endosomes. *Cell* *143*, 1136-1148.

Takada, R., Satomi, Y., Kurata, T., Ueno, N., Norioka, S., Kondoh, H., Takao, T., and Takada, S. (2006). Monounsaturated fatty acid modification of Wnt protein: its role in Wnt secretion. *Dev Cell* 11, 791-801.

Takeda, N., Jain, R., LeBoeuf, M.R., Wang, Q., Lu, M.M., and Epstein, J.A. (2011). Interconversion between intestinal stem cell populations in distinct niches. *Science* 334, 1420-1424.

Tanaka, K., Kitagawa, Y., and Kadowaki, T. (2002). Drosophila segment polarity gene product porcupine stimulates the posttranslational N-glycosylation of wingless in the endoplasmic reticulum. *J Biol Chem* 277, 12816-12823.

Tanaka, K., Kitagawa, Y., and Kadowaki, T. (2003). Misexpression of mouse porcupine isoforms modulates the differentiation of P19 embryonic carcinoma cells. *Cell Biol Int* 27, 549-557.

Tanaka, K., Okabayashi, K., Asashima, M., Perrimon, N., and Kadowaki, T. (2000). The evolutionarily conserved porcupine gene family is involved in the processing of the Wnt family. *Eur J Biochem* 267, 4300-4311.

Tang, X., Wu, Y., Belenkaya, T.Y., Huang, Q., Ray, L., Qu, J., and Lin, X. (2012). Roles of N-glycosylation and lipidation in Wg secretion and signaling. *Dev Biol* 364, 32-41.

Tian, H., Biehs, B., Warming, S., Leong, K.G., Rangell, L., Klein, O.D., and de Sauvage, F.J. (2011). A reserve stem cell population in small intestine renders Lgr5-positive cells dispensable. *Nature* 478, 255-259.

Trowbridge, J.J., Xenocostas, A., Moon, R.T., and Bhatia, M. (2006). Glycogen synthase kinase-3 is an in vivo regulator of hematopoietic stem cell repopulation. *Nat Med* 12, 89-98.

van Amerongen, R. (2012). Alternative Wnt pathways and receptors. *Cold Spring Harb Perspect Biol* 4.

van Amerongen, R., and Berns, A. (2006). Knockout mouse models to study Wnt signal transduction. *Trends Genet* 22, 678-689.

van Amerongen, R., and Nusse, R. (2009). Towards an integrated view of Wnt signaling in development. *Development* 136, 3205-3214.

Van Den Berg, D.J., Sharma, A.K., Bruno, E., and Hoffman, R. (1998). Role of members of the Wnt gene family in human hematopoiesis. *Blood* 92, 3189-3202.

van der Flier, L.G., Haegebarth, A., Stange, D.E., van de Wetering, M., and Clevers, H. (2009a). OLFM4 is a robust marker for stem cells in human intestine and marks a subset of colorectal cancer cells. *Gastroenterology* 137, 15-17.

van der Flier, L.G., van Gijn, M.E., Hatzis, P., Kujala, P., Haegebarth, A., Stange, D.E., Begthel, H., van den Born, M., Guryev, V., Oving, I., *et al.* (2009b). Transcription factor achaete scute-like 2 controls intestinal stem cell fate. *Cell* 136, 903-912.

van Es, J.H., Haegebarth, A., Kujala, P., Itzkovitz, S., Koo, B.-K., Boj, S.F., Korving, J., van den Born, M., van Oudenaarden, A., Robine, S., *et al.* (2012a). A critical role for the Wnt effector Tcf4 in adult intestinal homeostatic self-renewal. *Mol Cell Biol* 32, 1918-1927.

van Es, J.H., Jay, P., Gregorieff, A., van Gijn, M.E., Jonkheer, S., Hatzis, P., Thiele, A., van den Born, M., Begthel, H., Brabletz, T., *et al.* (2005). Wnt signalling induces maturation of Paneth cells in intestinal crypts. *Nat Cell Biol* 7, 381-386.

van Es, J.H., Sato, T., van de Wetering, M., Lyubimova, A., Nee, A.N.Y., Gregorieff, A., Sasaki, N., Zeinstra, L., van den Born, M., Korving, J., *et al.* (2012b). Dll1⁺ secretory progenitor cells revert to stem cells upon crypt damage. *Nat Cell Biol* *14*, 1099-1104.

Wang, X., Reid Sutton, V., Omar Peraza-Llanes, J., Yu, Z., Rosetta, R., Kou, Y.-C., Eble, T.N., Patel, A., Thaller, C., Fang, P., *et al.* (2007). Mutations in X-linked PORCN, a putative regulator of Wnt signaling, cause focal dermal hypoplasia. *Nat Genet* *39*, 836-838.

Wilson, C.L., Ouellette, A.J., Satchell, D.P., Ayabe, T., López-Boado, Y.S., Stratman, J.L., Hultgren, S.J., Matrisian, L.M., and Parks, W.C. (1999). Regulation of intestinal alpha-defensin activation by the metalloproteinase matrilysin in innate host defense. *Science* *286*, 113-117.

Wilson, P.A., and Hemmati-Brivanlou, A. (1995). Induction of epidermis and inhibition of neural fate by Bmp-4. *Nature* *376*, 331-333.

Wong, V.W.Y., Stange, D.E., Page, M.E., Buczacki, S., Wabik, A., Itami, S., van de Wetering, M., Poulosom, R., Wright, N.A., Trotter, M.W.B., *et al.* (2012). Lrig1 controls intestinal stem-cell homeostasis by negative regulation of ErbB signalling. *Nat Cell Biol* *14*, 401-408.

Yamane, T., Kunisada, T., Tsukamoto, H., Yamazaki, H., Niwa, H., Takada, S., and Hayashi, S.I. (2001). Wnt signaling regulates hemopoiesis through stromal cells. *J Immunol* *167*, 765-772.

Yan, K.S., Chia, L.A., Li, X., Ootani, A., Su, J., Lee, J.Y., Su, N., Luo, Y., Heilshorn, S.C., Amieva, M.R., *et al.* (2012). The intestinal stem cell markers Bmi1 and Lgr5 identify two functionally distinct populations. *Proc Natl Acad Sci USA* *109*, 466-471.

Yu, J., Chia, J., Canning, C.A., Jones, C.M., Bard, F.A., and Virshup, D.M. (2014). WLS Retrograde Transport to the Endoplasmic Reticulum during Wnt Secretion. *Dev Cell* 29, 277-291.

Zeve, D., Seo, J., Suh, J.M., Stenesen, D., Tang, W., Berglund, E.D., Wan, Y., Williams, L.J., Lim, A., Martinez, M.J., *et al.* (2012). Wnt signaling activation in adipose progenitors promotes insulin-independent muscle glucose uptake. *Cell Metab* 15, 492-504.

Zhang, X., Abreu, J.G., Yokota, C., MacDonald, B.T., Singh, S., Coburn, K.L.A., Cheong, S.-M., Zhang, M.M., Ye, Q.-Z., Hang, H.C., *et al.* (2012). Tiki1 is required for head formation via Wnt cleavage-oxidation and inactivation. *Cell* 149, 1565-1577.

Zhao, C., Blum, J., Chen, A., Kwon, H.Y., Jung, S.H., Cook, J.M., Lagoo, A., and Reya, T. (2007). Loss of beta-catenin impairs the renewal of normal and CML stem cells in vivo. *Cancer Cell* 12, 528-541.

Zhou, W.-J., Geng, Z.H., Spence, J.R., and Geng, J.-G. (2013). Induction of intestinal stem cells by R-spondin 1 and Slit2 augments chemoradioprotection. *Nature* 501, 107-111.